INFORMATION TO USERS

This manuscript has been reproduced from the microfilm master. UMI films the text directly from the original or copy submitted. Thus, some thesis and dissertation copies are in typewriter face, while others may be from any type of computer printer.

The quality of this reproduction is dependent upon the quality of the copy submitted. Broken or indistinct print, colored or poor quality illustrations and photographs, print bleedthrough, substandard margins, and improper alignment can adversely affect reproduction.

In the unlikely event that the author did not send UMI a complete manuscript and there are missing pages, these will be noted. Also, if unauthorized copyright material had to be removed, a note will indicate the deletion.

Oversize materials (e.g., maps, drawings, charts) are reproduced by sectioning the original, beginning at the upper left-hand corner and continuing from left to right in equal sections with small overlaps.

Photographs included in the original manuscript have been reproduced xerographically in this copy. Higher quality 6" x 9" black and white photographic prints are available for any photographs or illustrations appearing in this copy for an additional charge. Contact UMI directly to order.

Bell & Howell Information and Learning
300 North Zeeb Road, Ann Arbor, MI 48106-1346 USA

UMI®
800-521-0600

Université d'Ottawa · University of Ottawa

Abstract

This thesis has been divided into three major sections. The first section deals with the preparation and characterization of silica-supported vanadium(V) complexes. The reactions of $O{=}VX_3$, X = Cl or O^iPr, with the surface of partially dehydroxylated silica gives a single well-defined surface complex, $\equiv SiOVOX_2$. These complexes have been characterized by ^{51}V magic angle spinning and ^{13}C cross-polarization magic angle spinning NMR spectroscopy and infrared spectroscopy. The incorporation of ^{18}O labels into specific positions of the silica-supported vanadium complexes has been achieved. When the hydroxyl groups are first exchanged with $H_2{}^{18}O$, the subsequent reaction with $O{=}VX_3$ gives exclusively $\equiv Si^{18}OV^{16}OX_2$. Reaction of $^{18}O{=}VCl_3$ with unlabelled silica gives only $\equiv Si^{16}OV^{18}OCl_2$. The surface complexes undergo clean ligand replacement without displacing or diluting the isotope labels. Other reactions are investigated which are analogous to molecular vanadium reactions and relevant to the understanding of mechanisms in heterogeneous catalysis.

The second section deals with a special type of reactivity of silica-supported vanadium(V) complexes. A nonhydrolytic low-temperature route to ternary V-Ti-Si catalysts has been developed. $Ti(O^iPr)_4$ migrates underneath the silica-supported vanadium overlayer to give a heterobinuclear complex containing one Ti per V, bound to the silica surface via Si-O-Ti linkages. When $Ti(O^iPr)_4$ reacts with the surface of partially dehydroxylated silica, a dinuclear species is

formed. Because of this reaction it was not possible to form the mixed Ti-V species by depositing the Ti first. However once a method was developed for the formation of mononuclear silica-supported titanium complexes, we demonstrate that indeed the heterobinuclear species can also be formed by the reaction of $O=V(O^iPr)_3$ with $\equiv SiOTi(O^iPr)_3$. Although there is precedence in the literature for nonhydrolytic condensation of metal chloride alkoxides, this is the first example of such a stoichiometric reaction on a surface.

The last part of this thesis deals with the study of silica-supported organovanadium species. The reaction of $V(CH_2SiMe_3)_4$ with the surface of partially dehydroxylated silica gives exclusively $(\equiv SiO)_2V(CH_2SiMe_3)_2$. This surface complex undergoes a surprisingly clean thermal transformation to generate a supported alkylidene complex, $(\equiv SiO)_2V=CHSiMe_3$, with concurrent liberation of $SiMe_4$. The reaction is quantitative and kinetically first order. The mechanism is believed to be a surface assisted α-H elimination. The unusual supported vanadium alkylidene reacts with olefins in the absence of alkylaluminum cocatalysts.

Acknowledgments

The completion of this work cannot be considered without thanking a number of people to whom I am very grateful. First, and foremost, I would like to thank Susannah Scott for giving me the opportunity to work in her lab for the purposes of this research. I would like to thank her not only for her guidance, patience and willingness to share her expertise throughout the course of my graduate work, but also for being a very understanding person.

I would like to thank everyone I had the pleasure of working with over the years, undergraduates, fellow graduate students and postdocs. There are far to many of you to mention but I would particularly like to thank my fellow graduate students, Marcel, Omar and Jamila, who have been with me for most of my time here at the University of Ottawa. You've all made life in the lab interesting to say the least.

I would like to thank the entire Chemistry Department support staff, paticularly my fellow Maritimers John Hopkins, Don Hopkins and Lee Sorensen. I would also like to thank Dr. Glenn Facey for his help with running the solid state NMR spectra.

Finally I would like to thank my friends and family. My colleagues Dave Molapo and Sham Syal, thanks for the workouts. I hope that your squash games improve with age. My family, Mom, Dad, Jill and Jamie, your support may have gone unthanked at times but it was never unnoticed. Last but certainly not least

I would like to thank my best friend for life, Susan Virdee, for being there for me whenever I needed and particularly for putting up with me during the writing of this thesis.

Table of Contents

List of Figures

Chapter 4

Page

Chapter 5

Page

Chapter 6

List of Schemes

List of Tables

Chapter 6

Page

Chapter 1

Introduction

1.1 Supported catalysts

Supported metal oxide catalysts are typically formed when one metal oxide is deposited on a second metal oxide (the support) possessing a high surface area. In many cases, the deposited metal oxide preferentially forms a metal oxide overlayer rather than a separate crystalline metal oxide phase. The surface metal oxide is usually the active catalytic component (e.g., vanadium oxide, rhenium oxide, chromium oxide) while the oxide support (e.g., silica, alumina, titania) provides high surface area, mechanical strength and thermal stability. Supported metal oxide catalysts find wide application in a large number of industries such as petroleum refining, chemical manufacturing and pollution control.

1.2 Vanadium in catalysis

The catalytic properties of vanadium oxide for the mild oxidation of hydrocarbons have been known since the 1960's.[1] The first reactions to be catalyzed industrially were the oxidation of *o*-xylene to phthalic anhydride[2] and benzene to maleic anhydride.[3] Although V_2O_5 itself was found to be active for several mild oxidations, it was soon recognized that the presence of other components improved its properties.

1.2.1 Silica-supported vanadium catalysts

Silica-supported vanadium oxide is used extensively as a catalyst in a large number of commercial applications, including oxidations of hydrocarbons,[4] sulfur dioxide[5] and carbon monoxide, as well as the selective catalytic reduction of NO_x by NH_3.[6] A considerable amount of literature exists on the subject of vanadium catalysts supported on different oxides including SiO_2, TiO_2, Al_2O_3 and others. This section will be restricted to silica-supported systems due to their relevance to this research interest. A subsequent section will deal with the mixed vanadium/titania/silica system.

The widespread use of silica as a carrier for metal oxides is partially due to the fact that it is generally considered to be an inert support: interaction with the immobilized species is weak.[7] In such cases, silica is acting mainly as a dispersant, without altering the activity of the deposited material. Given the amount of research dedicated to this subject, it is surprising that there are still a significant number of conflicting reports regarding the structure of silica-supported vanadium oxide catalysts.

One of the most influential parameters is whether or not water vapor is present.[8,9] Under ambient conditions, three major species have been proposed for silica-supported vanadium oxide catalysts: tetrahedral and octahedral dispersed vanadium species as well as crystalline V_2O_5. Under controlled (dry) atmosphere, only tetrahedral vanadia species were reported at below monolayer coverage, with crystalline V_2O_5 appearing at above

monolayer coverages. Tetrahedral vanadium species include the proposed tripodal silica-supported vanadium species,[10,11] **1**, as well as one and two dimensional chains.[8]

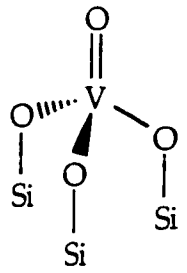

1

The ambiguity about the structure of the silica-supported vanadium oxide species arises from different methods of preparation. A variety of techniques have been utilized in attempts to form monolayers of supported vanadium, for example, chemical vapor deposition (CVD) of $VOCl_3$,[12] or vanadium alkoxides,[13,14] liquid phase deposition of the alkoxides[15] and ion exchange from aqueous vanadate solutions.[16] Although surface reactions between the vanadium-containing reagent and the grafting sites such as OH groups are important for control of the structure of supported vanadium oxide, there have been few reports about the elementary surface reactions which take place during the deposition process. Deposition is usually followed by calcination in air or O_2, and the exact nature of the processes occurring in the latter step are also not really understood.

Despite a paucity of experimental evidence, there has been much speculation on how the structure of supported catalysts affects their reactivity.

Over bulk vanadium oxide, oxygen transfer is proposed to occur from terminal V=O bonds and does not involve V-O-V units.[4] For instance, if the reaction of hydrocarbons with the silica-supported vanadium species involves the activation of the C-H bonds, then the mechanism of addition across V=O may be affected by the acidity of the hydrocarbon. Two possible modes of addition have been proposed, eq. 1.1 and 1.2.[4]

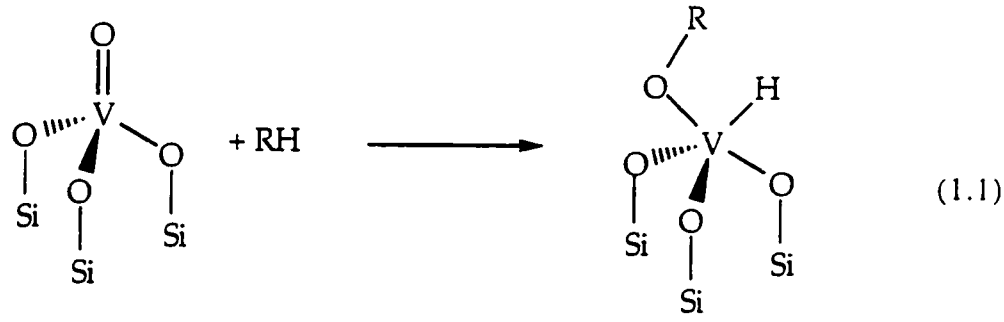

(1.1)

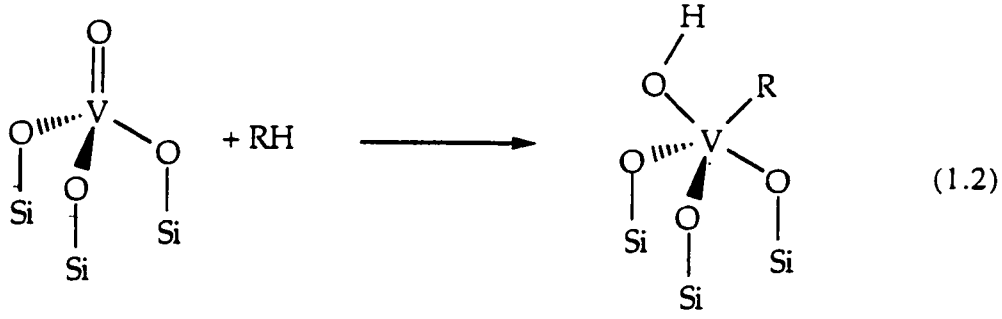

(1.2)

Some reactions are photochemically-induced. In the excited state, the polarization of the V=O bond is reversed, to $V^{+}=O^{-}$. Therefore, it is expected that hydrocarbons will bind differently depending on whether they are basic or acidic and whether they interact with the vanadyl in its ground state or its excited state. It has also been proposed that the presence of Si-O-V bonds

influences reactions, since silica-supported vanadium is more active than V_2O_5. It has also been postulated that addition of substrates may occur across a SiO-V bond. There are two possibilities for such an addition, eq 1.3 and 1.4.[4]

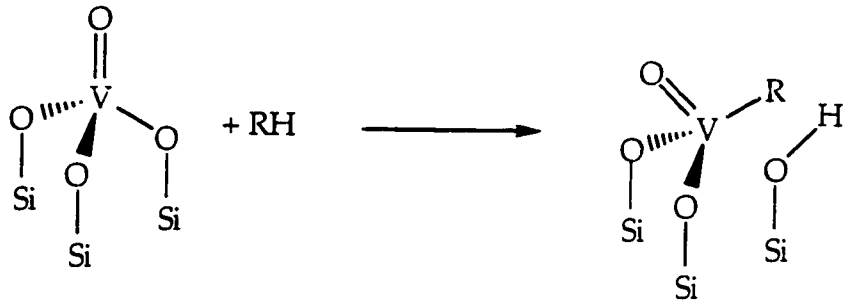

(1.3)

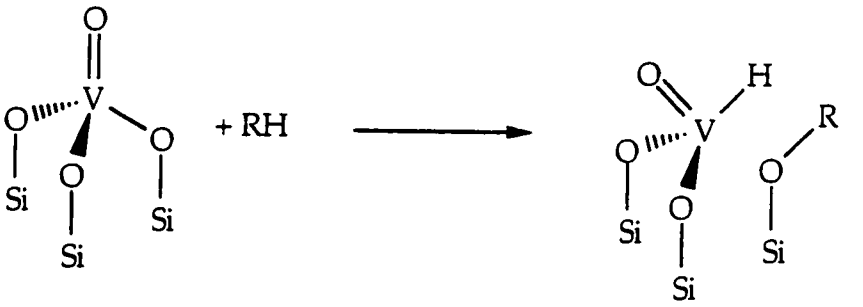

(1.4)

Raman spectroscopy has been used to support addition of ethanol and water accross SiO-V, however, it has been suggested that ethane adds accross V=O.[4]

Thus it has been proposed that the adsorption of molecules on vanadium oxide surfaces can result in several different intermediate structures, eq. 1.1-1.4. The important question is, does the structure of the supported catalyst affect the product distribution, *i.e.* is there a relationship between structure and selectivity? In cases where intermediates have been suggested, those containing V-O-C linkages, eq. 1.1, are proposed to lead to

selective oxidation products, whereas alkyl fragments bound to the vanadium through M-C linkages, eq. 1.2 and 1.3, are thought to yield carbon oxides.[4]

In spite of the importance of supported vanadia catalysts, many fundamental questions still have not been answered, for example, the significance of coverage, stability of the surface vanadia monolayer, and nature of the surface species after calcination.[17] Progress has been hampered by the use of oxide supports that contain significant amount of impurities, comparisons of results obtained under different conditions and the use of characterization techniques which are not always capable of providing the desired information.

1.2.2 Homogeneous catalysis by vanadium

Most research on homogeneous catalysis with vanadium has focused on the oxidation of organic substrates, particularly olefins, with alkylhydroperoxides. Many transition metal compounds in their highest oxidation states, particularly vanadium(V), molybdenum(VI), tungsten(VI) and titanium(IV), are known to catalyze homogeneous reactions of alkyl hydroperoxides with unsaturated molecules such as olefins.[18] Despite some similarities among the different catalyst systems, an inspection of the literature reveals that vanadium has found more synthetic applications in homogeneous catalytic oxidations than Ti(IV), W(VI), or even Mo(VI) which is the metal of choice for the Halcon process.[19] There is a large body of literature on these reactions because of the commercial importance of

epoxides. Vanadium compounds and complexes of a few other transition metal complexes can also act as effective catalysts in the homogeneous oxidation of organic substrates by hydrogen peroxide. The mechanism of catalysis shown in Scheme 1.1 has gained moderate acceptance in spite of many important unanswered questions.[20] Elucidating the mechanisms of catalytic processes, and clarification of the detailed structures of the active intermediates and their configurations in the transition states during substrate oxidation present challenging problems.

It is believed that the metal precursor binds the peroxide in an equilibrium process which lies largely to the right.[18] An intermediate is thus formed, in which n may be 1, 2, or even 3, where n is equal to the number of coordinated alkylperoxide ligands, eq. 1.5.

$$VO(OR)_3 \underset{ROH}{\overset{R'OOH}{\rightleftharpoons}} VO(OR)_{3-n}(OOR')_n \qquad (1.5)$$

Evidence for an intermediate was obtained by ^{51}V NMR.[18]

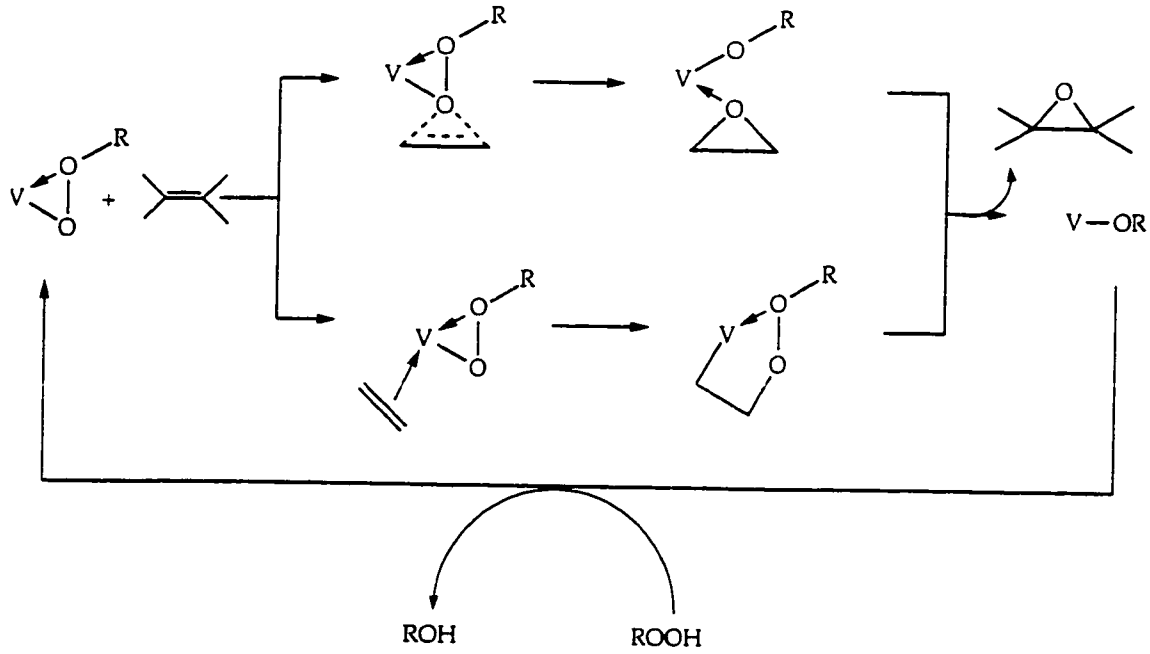

Scheme 1.1 Proposed catalytic cycle for the epoxidation of olefins by alkylhydroperoxides

One alkylperoxovanadium complex was characterized by X-Ray crystallography, Figure 1.1.[21] Unfortunately, this particular complex is inert in the epoxidation of olefins.

1.3 More complex vanadium oxide systems

Catalysts containing vanadia supported on titania have been a subject of considerable interest over the past two decades because of their successful application to the oxidation of aromatic compounds[22,23] and the selective catalytic reduction of NO_x by ammonia.

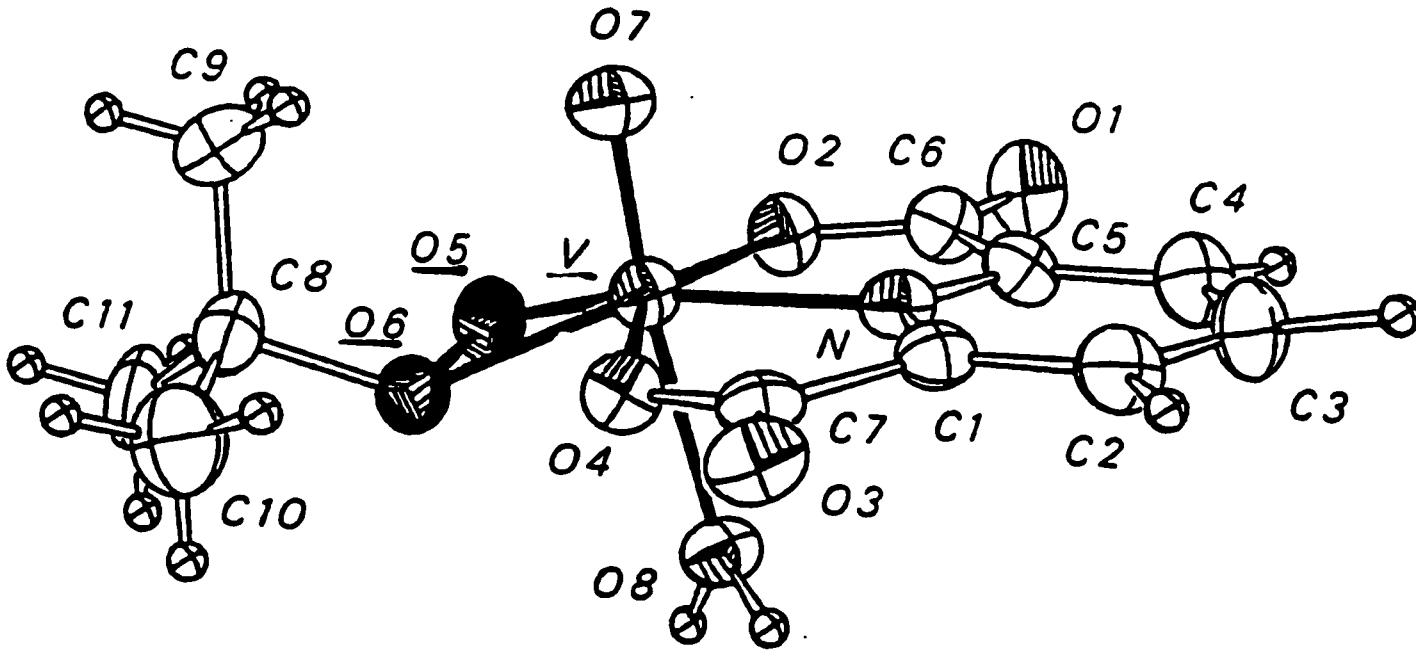

Figure 1.1 Crystal structure of an alkylperoxovanadium complex.[21]

The presence of supported vanadia induces conversion of TiO_2 from the anatase to the rutile phase at lower temperatures than for unmodified TiO_2.[24] This transformation negatively affects the activity and selectivity towards selective oxidation products. The moderate surface area and poor mechanical strength of V_2O_5/TiO_2 (anatase) and the inferior resistance to sintering of the catalyst are serious drawbacks.

The use of mixed TiO_2-SiO_2, instead of TiO_2 alone, as support for the vanadia phase is a very promising alternative because silica-supported titania is characterized by higher thermal stability, better mechanical properties and higher surface area compared to TiO_2 alone.[25] It has been shown that vanadium oxide species deposit almost exclusively on the titania support in the simultaneous presence of titania and silica.[26] Moreover, as the exposed titania support appears to be associated with non-selective oxidation products, vanadium loadings must be in the region of a monolayer or higher to ensure selectivity.

1.4 The surface chemistry of silica

Crystalline silica exists in nature primarily as α-quartz. Other stable polymorphs include β-cristobalite, HP-tridymite and β-quartz. Due to the hardness of α-quartz, 7 on the Mohs scale of 10, it is fairly resistant to mechanical alteration. Similarly, its low solubility in water preserves α-

quartz during chemical weathering. As a result, α-quartz is one of the most common minerals found in sedimentary rocks.[27]

Silica in its various crystalline and amorphous forms has an extremely wide spectrum of industrial applications. Its uses range from a simple raw material for glasses, ceramics and the production of silicon, to highly technical applications such as quartz oscillators and optical waveguides, as well as supports for a number of heterogeneous catalysts.

Silica is probably the best understood oxide due to its simple structure of SiO_4 tetrahedra. Its surface consists of Si-O-Si siloxane bridges of low reactivity and hydroxyl groups which are usually the reactive sites.[28] Furthermore, Lewis acid/base sites and Bronsted acid/base sites (other than the hydroxyl groups), which are found in most other oxides, are absent in silica. The silica used in this research is a pyrogenic or fumed silica, marketed by Degussa under the trade-name Aerosil™. It is prepared by the high temperature flame hydrolysis of $SiCl_4$, see Chapter 2. This is a non-porous silica with a surface area of 200 m^2/g.

On the surface of silica there are three types of hydroxyl groups, isolated, geminal and vicinal pairs. On fully hydrated silica, the total number of hydroxyl groups is 4.9/nm^2. This number decreases to 1.2-1.4/nm^2 if the silica is treated at 450°C under dynamic vacuum.[28]

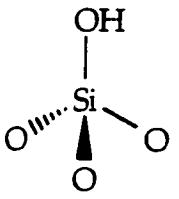

Isolated

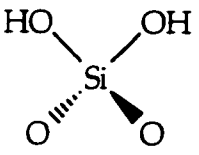

Geminal pair

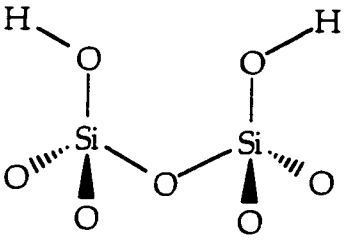

Vicinal pair

Upon heating, hydrogen-bonded pairs of hydroxyl groups condense to give siloxane bridges and liberate water, eq 1.6. This effect is shown in Figure 1.2.

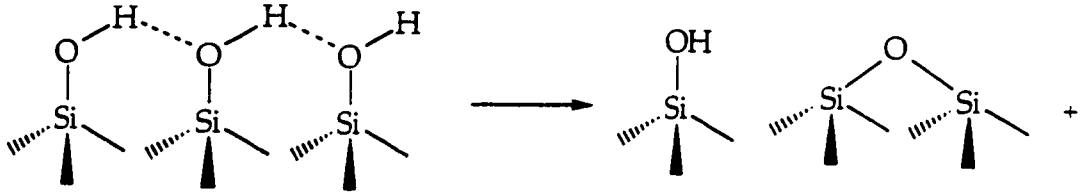

$+ H_2O$ (1.6)

It follows that the temperature of dehydroxylation of the silica controls the density of the hydroxyl groups on the surface.[28] It is important to note that, under moderate conditions (<500°C), vicinal and geminal pairs do not undergo internal condensation.

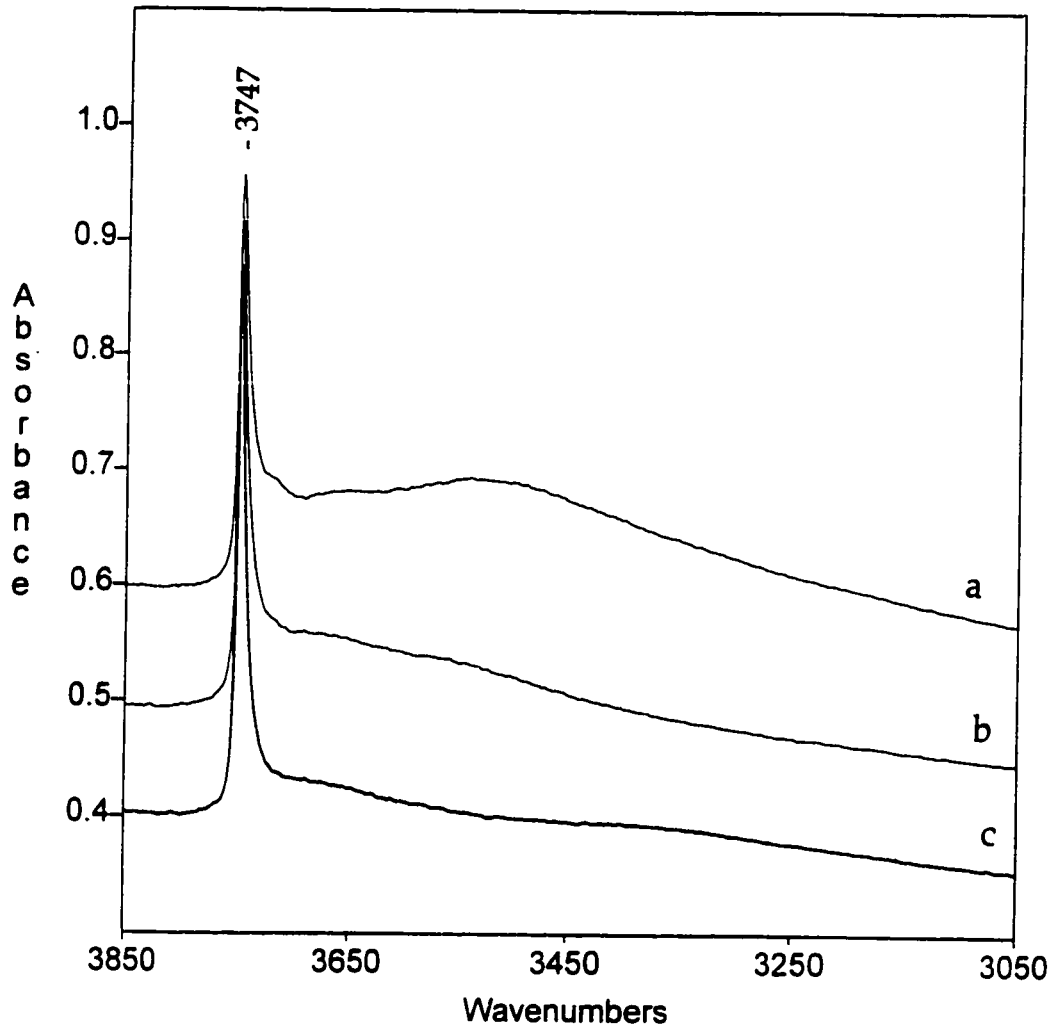

Figure 1.2 Infrared spectra of self-supporting disks of silica showing the effect of temperature on the hydroxyl group distribution. (a) Silica-25, (b) silica-200 and (c) silica-500, where the appended number indicates the temperature of activation in °C.

A number of studies have attempted to clarify the nature of the silica surface and several models have been proposed. Work on amorphous silica indicates that its structure most closely resembles that of β-cristobalite and similar crystalline phases.[29] In 1958, DeBoer and Vleekins proposed a model based on the (111) face of β-cristobalite.[30] On this surface, hydroxyl groups are arranged in a hexagonal array and separated by about 5Å which corresponds to a density of 4.55 OH per nm^2, close to the accepted value for various silicas of 4.9 OH per nm^2.

The mechanism of dehydration of such a surface was investigated in more depth by Hockey.[31] He postulated that the higher values of hydroxyl density on untreated silica are caused by lattice defects. The hydroxyl groups arising from such defects are close enough in proximity that silanol pairs might be expected to condense at relatively low temperatures resulting in the regular β-cristobalite surface.

The DeBoer-Vleekins model, in conjunction with the Hockey defect mechanism, has a number of difficulties. Some studies indicate that a significant number of hydroxyl groups occur in pairs even on surfaces heated above 450°C. This is inconsistent with the geometry of the (111) face of β-cristobalite. Furthermore, reducing the density of hydroxyl groups below the value of 4.55/nm^2 would be virtually impossible, according to the model, considering the strain that would be imposed on the lattice due to the distance between hydroxyl groups. In reality it is possible to have a silica

surface with a density of hydroxyl groups as low $1/nm^2$ without any appreciable change in the surface area.

A model that eliminates some of the inadequacies of the DeBoer-Vleekins model and takes into account the existence of paired hydroxyl groups is that of Peri and Hensley.[32] They describe the surface of untreated silica as similar to the (100) face of β-cristobalite, Figure 1.3a. Each surface silicon is connected to two geminal hydroxyl groups. Calculations based on this geometry gives rise to a density of hydroxyl groups equal to 8.0 per nm^2. According to Peri and Hensley, the process of dehydration involves random condensation along the rows of hydroxyl groups, Figure 1.3b. It is important to note that the Peri-Hensley model for dehydration only gives rise to paired hydroxyl groups, both geminal and vicinal. Although this surface is thermodynamically stable, with a surface hydroxyl density of $4.56/nm^2$, further condensation would have to involve vicinal pairs of hydroxyl groups. Formation of siloxanes from these pairs would be quite difficult and would be rather easy to rehydrate due to strain. The minimum hydroxyl density according to this model is 1.2 widely separated geminal pairs per nm^2. Unlike the DeBoer and Vleekins model, no clear mechanism for the formation of isolated single hydroxyl groups is suggested by the Peri-Hensley model.

Due to the shortcomings of models based on crystalline phases of silica, it is probably best to consider the surface of amorphous silica to be made up of a heterogeneous mixture of all these crystalline domains.

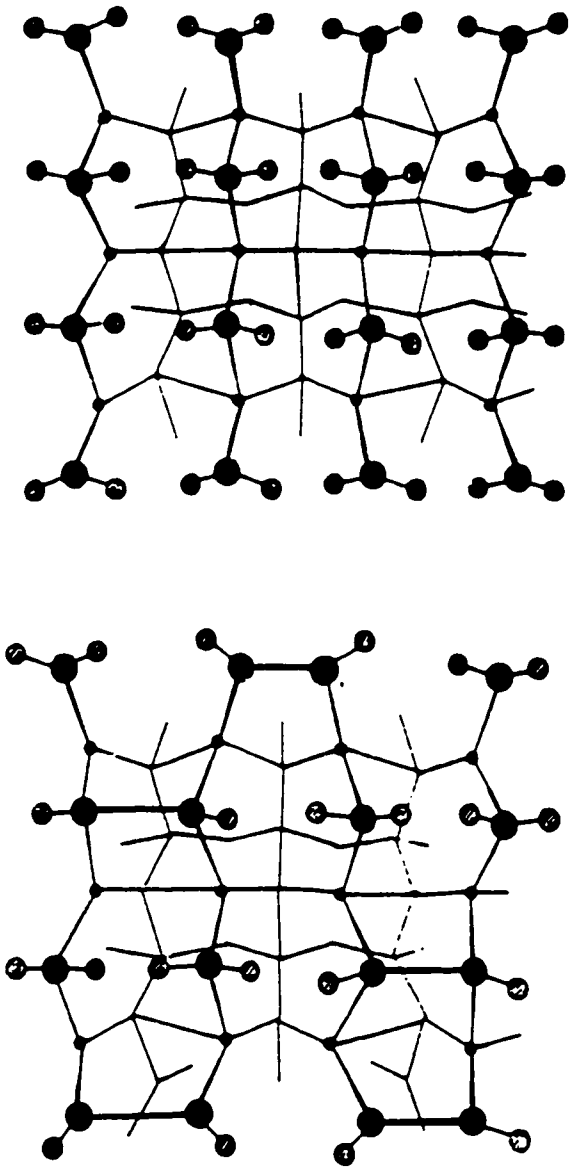

Figure 1.3 Surface geometry of β-cristobalite (100) face, (a) completely hydrated; (b) following partial dehydration. Large circles indicate surface silicon atoms, small circles indicate hydroxyl groups.[29]

1.5 Surface organometallic chemistry

Despite the impact organometallic chemistry has had on homogeneous catalysis, heterogeneous catalysis strongly dominates the industrial scene, accounting for 85% of all commercial catalytic processes.[33] Although heterogeneous catalysis, not without good reason, has advantages in application, homogeneous catalysis often permits a far more detailed mechanistic understanding of microscopic processes and catalytic mechanisms. It is sometimes possible to optimize homogeneous catalysts step-by-step for a particular problem. This is potentially a striking advantage over heterogeneous catalysis. The strengths and weaknesses of homogeneous and heterogeneous catalysis are shown in Table 1.1.[34]

The reaction of organometallic compounds, extended to inorganic and main group complexes, with the surfaces of oxides and metals along with their subsequent reactions is defined as the field of surface organometallic chemistry.[35] Organometallic complexes are chemically bound to the surface yet retain many features of their molecular structure. These surface organometallic complexes can therefore be considered to belong to both the molecular and the solid state and, in cases where they have been fully characterized, a picture of their reactivity can be constructed using molecular concepts.[36]

Surface organometallic chemistry attempts to bridge the two types of catalysis. Although superficially resembling heterogeneous catalysts, the relatively uniform structure, reactivity and distribution on the support of the

surface organometallic complexes make them essentially homogeneous in nature. Therefore it may be possible to obtain catalytically active materials which have the benefits of both homogeneous and heterogeneous catalysis.

Table 1.1 Comparison of homogeneous and heterogeneous catalysis.

	Homogeneous	Heterogeneous
Activity	high	variable
Selectivity	high	variable
Reaction conditions	moderate	harsh
Service life of catalysts	variable, usually short	long
Sensitivity towards catalyst poisons	low	high
Diffusion problems	none	may be important
Catalyst recycling	expensive	easy
Variation of steric and electronic properties	possible	not possible
Mechanistic understanding	accessible	difficult

1.6 References

(1) Courtine, P.; Bordes, E. *Appl. Catal. A: Gen.* **1997**, *157*, 45-65.

(2) Wainwright, M. S.; Foster, N. R. *Catal. Rev.* **1979**, *19*, 211.

(3) Seoane, J. L.; Boutry, P.; Montarnal, R. *J. Catal.* **1980**, *63*, 182-191.

(4) Oyama, S. T. *Res. Chem. Intermed.* **1991**, *15*, 165-182.

(5) Dobkina, E. I.; Petrovskaya, G. I.; Kuznetsova, S. M. *Russ. J. Appl. Chem.* **1996**, *69*, 835-838.

(6) Groeneveld, M. J.; Boxhoorn, G.; Kuipers, H. P. C. E.; van Grinsven, P. F. A.; Gierman, R.; Zuideveld, P. L. in *Proc. 9th Int. Congr. Catal.*, CIC: Calgary, 1988, pp 1743-1749.

(7) Schraml-Marth, M.; Wokaun, A. *J. Chem. Soc., Faraday Trans.* **1991**, *87*, 2635-2446.

(8) Van Der Voort, P.; White, M. G.; Mitchell, M. B.; Verberckmoes, A. A.; Vansant, E. F. *Spectrochim. Acta, Part A* **1997**, *53*, 2181-2187.

(9) Jehng, J.-M.; Deo, G.; Weckhuysen, B. M.; Wachs, I. E. *J. Mol. Catal. A: Chem.* **1996**, *110*, 41-54.

(10) Went, G. T.; Oyama, S. T.; Bell, A. T. *J. Phys. Chem.* **1990**, *94*, 4240-4248.

(11) Wachs, I. E. *J. Catal.* **1990**, *124*, 570-573.

(12) Bond, G. C.; Konig, P. *J. Catal.* **1982**, *77*, 309-315.

(13) Inumaru, K.; Okuhara, T.; Misono, M. *J. Phys. Chem.* **1991**, *95*, 4826-4832.

(14) Nickl, J.; Dutoit, D.; Baiker, A. *Appl. Catal.* **1993**, *98*, 173-193.

(15) Kijenski, J.; Baiker, A.; Glinski, M.; Dollenmeier, P.; Wokaun, A. *J. Catal.* **1986**, *101*, 1-11.

(16) Roozeboom, F.; Mittelmeijer-Hazeleger, M. C.; Moulijn, J. A.; Medema, J.; de Beer, V. H. J.; Gellings, P. J. *J. Phys. Chem.* **1980**, *84*, 2783-2791.

(17) Wachs, I. E.; Weckhuysen, B. M. *Appl. Catal. A: Gen.* **1997**, *157*, 67-90.

(18) Di Furia, F.; Modena, G.; Curci, R.; Bachofer, S. J.; Edwards, J. O.; Pomerantz, M. *J. Mol. Catal.* **1982**, *14*, 219-229.

(19) Conte, V.; Di Furia, F.; Licini, G. *Appl. Catal. A: Gen.* **1997**, *157*, 335-361.

(20) Conte, V.; Di Furia, F.; Moro, S. *J. Phys. Org. Chem.* **1996**, *9*, 329-336.

(21) Mimoun, H.; Chaumette, P.; Mignard, M.; Saussine, L. *Nouv. J. Chim.* **1983**, *7*, 467-475.

(22) Dias, C. R.; Portela, M. F.; Galan-Fereres, M.; Banares, M. A.; Granados, M. L.; Pena, M. A.; Fierro, J. L. G. *Catal. Lett.* **1997**, *43*, 117-121.

(23) Elguezabal, A. A.; Corberan, V. C. *Catal. Today* **1996**, *32*, 265-272.

(24) Vejux, A.; Courtine, P. *J. Solid State Chem.* **1978**, *23*, 93-103.

(25) Reichmann, M. G.; Bell, A. T. *Appl. Catal.* **1987**, *32*, 315-322.

(26) Jehng, J. M.; Wachs, I. E. *Catal. Lett.* **1992**, *13*, 9-13.

(27) Heaney, P. J.; Prewitt, C. T.; Gibbs, G. V. *Silica: Physical Behavior, Geochemistry and Materials Applications;*, Mineralogical Society of America: Washington, D. C, 1994.

(28) Morrow, B. A. *Stud. Surf. Sci. Catal.* **1990**, *57*, A161-A224.

(29) Sindorf, D. W.; Macial, G. E. *J. Am. Chem. Soc.* **1983**, *105*, 1487-1493.

(30) DeBoer, J. H.; Vleekins, J. M. *Proc. K. Ned. Akad. Wet., Ser. B: Palaentol., Geol., Phys., Chem.* **1958**, *B61*, 85-93.

(31) Hockey, J. A. *Chem. Ind.* **1965**, 57-63.

(32) Peri, J. B.; Hensley, A. L. *J. Phys. Chem.* **1968**, *72*, 2926-2933.

(33) Parshall, G. W.; Putscher, R. E. *J. Chem. Ed.* **1986**, *63*, 189-194.

(34) Nugent, W. A.; Mayer, J. M. *Metal Ligand Multiple Bonds*; ; Wiley: New York, 1988.

(35) Scott, S. L.; Basset, J.-M.; Niccolai, G. P.; Catherine C, S.; Candy, J.-P.; Lecuyer, C.; Quignard, F.; Choplin, A. *New J. Chem.* **1994**, *18*, 115-122.

(36) Scott, S.; Basset, J.-M. *J. Mol. Catal.* **1994**, *86*, 5-22.

CHAPTER 2

Experimental Techniques

2.1. Reagents

2.1.1. Silica

The silica used was Degussa Aerosil™-200. This high purity silica is nonporous and pyrogenic, meaning it is produced by the flame hydrolysis of $SiCl_4$, eq. 2.1 and 2.2,[1] and has a surface area of 200 m^2/g.

in a CH_4-O_2 flame:

$$SiCl_4 + O_2 \rightarrow SiO_2 + 2\,Cl_2 \qquad (2.1)$$

$$2\,H_2O + 2\,Cl_2 \rightarrow 4HCl + O_2 \qquad (2.2)$$

2.1.2. Vanadium and titanium molecular complexes

$VOCl_3$ (yellow liquid), $VO(O^iPr)_3$ (colorless liquid), VCl_4 (brown liquid), $TiCl_4$ (colorless liquid) and $Ti(O^iPr)_4$ (colorless liquid) were purchased from Aldrich and transferred under N_2 into glass reactors equipped with either high vacuum Teflon stopcocks (Young valves) or high vacuum stopcocks greased with the perfluorinated grease Krytox (Aldrich). The liquids were subjected to several freeze-pump-thaw cycles to remove dissolved gases, then distilled under vacuum to remove alcohol and HCl impurities.

$V(CH_2Si(CH_3)_3)_4$ (green solid) was synthesized from $VCl_3 \cdot 3THF$ (Aldrich) and $(CH_3)_3SiCH_2MgCl$, 1M in diethylether (Aldrich) and purified by sublimation.[2]

$V^{18}OCl_3$ (yellow liquid) was synthesized by reaction of VCl_3 (Aldrich) with $^{18}O_2$ (95% ^{18}O, Cambridge Isotopes) in a closed grease-free reactor at 250°C. VCl_3 was transferred under N_2 into the reactor, which was evacuated and then filled with 25-100 Torr $^{18}O_2$. As the VCl_3 was heated in a tube furnace, yellow $V^{18}OCl_3$ condensed on the inner walls of the reactor outside the heated region. The $V^{18}OCl_3$ was frozen in liquid N_2 while the remaining $^{18}O_2$ was evacuated. The product was then transferred to a grease-free glass bulb under vacuum via trap-to-trap distillation with liquid N_2. The product was characterized by its characteristic IR spectrum with peaks at 1042 cm^{-1}, $\nu(V=^{16}O)$, 996 cm^{-1}, $\nu(V=^{18}O)$, and 505 cm^{-1}, $\nu(V-Cl)$. The isotope enrichment was judged to be ca. 95% from the relative intensities of the $\nu(V=O)$ modes at 1042 ($V=^{16}O$) and 996 ($V=^{18}O$) cm^{-1} in the gas phase IR spectrum.

2.1.3. Gases

CD_2CD_2 (98% D), DCl (99% D), and $^{18}O_2$ (95% ^{18}O) (Cambridge Isotopes), NO, N_2O, CH_2CH_2 and HCl (Matheson Gas Products), CO, O_2 and H_2 (Air Products) and $C^{18}O$ (97.4% ^{18}O, MSD Isotopes) were either purchased in glass bulbs or transferred into glass bulbs prior to use. Known pressures of gases were transferred into the reactors via a high vacuum line equipped with a Baratron capacitance manometer. CD_2CD_2, CH_2CH_2, CO, N_2O and NO were passed through a trap containing BTS Deoxo Catalyst (Caledon Laboratories Ltd.) and 3Å molecular sieves (Aldrich) to remove any O_2 and H_2O present. The trap was first activated

by heating at 200 °C under a flow of H_2. O_2 was passed through a trap containing only 3Å molecular sieves to remove H_2O. HCl and DCl were used as received.

2.1.4. Liquids and solvents

The alcohols ^{i}PrOH and CH_2=$CHCH_2OH$ (Aldrich), and acetone were dried by stirring over CaH_2 (Aldrich) at room temperature, followed by distillation under N_2, and were stored in glass reactors over 3Å molecular sieves. ^{t}BuOH and neopentyl alcohol were also dried by stirring over CaH_2 (since both are solids at room temperature, they were heated to 5-10 °C above their respective melting points), followed by distillation under N_2 into glass reactors and stored over 3Å molecular sieves. Phenylisocyanate and p-tolylisocyanate (Aldrich) were dried by stirring over P_2O_5 under N_2 followed by vacuum distillation. Styrene was distilled under reduced pressure from CaH_2 and stored in a glass reactor over 3Å molecular sieves. ^{t}BuOOH (5-6 M in decane, Aldrich) was dried by stirring over $MgSO_4$ (Aldrich) and stored under N_2 over 3Å molecular sieves. Benzene-d_6 was distilled under N_2 over sodium/benzophenone and stored in a glass reactor over 3Å molecular sieves. D_2O, $H_2{}^{18}O$ (Cambridge Isotopes) were used as received and $(CD_3)_3COD$ (Aldrich) was dried by stirring over 3Å molecular sieves followed by trap-to-trap distillation and stored over 3Å molecular sieves. Before use, each liquid reagent was subjected to three freeze-pump-thaw cycles, then introduced into the reactor via vapor phase transfer through a high vacuum manifold.

All solvents for synthesis, including diethylether, THF, pentane, hexane, octane and toluene, were distilled immediately prior to use over sodium/benzophenone or sodium-potassium alloy/ benzophenone.

2.2 Preparation of surface vanadium and titanium complexes

2.2.1 Pretreatment of silica

A standard pretreatment procedure was followed in order to ensure reproducibility. In all reactions, silica-500 (the number indicating the temperature, in °C, of pretreatment) was prepared by first calcining, to remove adsorbed hydrocarbons, in 200 Torr O_2 at 500°C for 2 hours, followed by partial dehydroxylation at 500°C for at least 3 hours under dynamic vacuum ($<10^{-4}$ Torr). To prepare silica-200 and silica-25, the calcination step was omitted. The silica was simply heated to the appropriate temperature for 3 hours under dynamic vacuum. The temperature of dehydroxylation controls the density of hydroxyl groups on the surface. (see section 1.4)

2.2.1.1 Deuteration of silica

Deuterated silica was prepared by two different methods: exchange with D_2O or DCl. In the first (more time consuming) method, the silica is treated with four to six cycles of D_2O vapor at 450°C for 3 hours alternating with evacuation. For silica-500, the pellet was then heated under dynamic vacuum at 500°C for an additional 2 hours. For silica-200, after the final cycle, more D_2O was added, the temperature was lowered to 150°C and the silica was left for 16 hours to become

rehydrated. The sample was then evacuated and the temperature raised to 200°C for 2 to 3 hours. This method gave >90% deuteration of the surface hydroxyl groups, appearing as ν(O-D) at 2762 cm^{-1}. The extent of deuteration was judged by the relative decrease in intensity of the ν(O-H) vibration at 3747 cm^{-1}. In the second method, three to four cycles of 20 Torr DCl followed by dynamic vacuum at room temperature also gave >90% deuteration. Silica is not chlorinated by DCl at room temperature.[3]

2.2.1.2 ^{18}O-labelling of silica

^{18}O-labelled silica was prepared in the following manner: the silica pellet was first dehydroxylated at 500°C followed by four to six cycles of $H_2{}^{18}O$ vapor/vacuum at 400°C. After the final cycle, the temperature was raised to 500°C and the sample was evacuated at that temperature for one hour. The isotope enrichment was estimated at >80% from the intensity ratio ν(^{16}O-H)/ν(^{18}O-H) at 3747 and 3736 cm^{-1}, respectively, in the IR transmission spectra of self-supporting disks. This method of isotopic enrichment is a modified version of a literature method.[4]

2.2.2 Breakseal techniques

Whereas $TiCl_4$, VCl_4 and $VOCl_3$ are sufficiently volatile to be transferred into reactors via the vapor phase, all other reagents had to be introduced using breakseal techniques. A breakseal reactor was prepared, Figure 2.1, and leak-tested on a high vacuum line. Liquid reagents were syringed into the breakseal reactor

under flowing N_2. Products were then frozen in liquid N_2 while the reactor was evacuated. Reagents were then subjected to three freeze-pump-thaw cycles on a high vacuum line, to remove dissolved gases. With the product still frozen in liquid N_2, the breakseal was sealed off from the rest of the reactor at the restriction with a torch, leaving the metal complex sealed inside the breakseal under static vacuum.

Products which could not be transferred by syringe were sublimed into the breakseal under vacuum through a glass "U" tube. The freeze-pump-thaw cycles were generally omitted in these cases, since the products were solids.

A hammer, usually a piece of iron sealed inside a glass tube, was placed in the open end of the breakseal. A restriction was created in the glass to facilitate sealing off the breakseal after reaction. The open end of the breakseal was then sealed onto the reactors as shown in Figures 2.3 and 2.5.

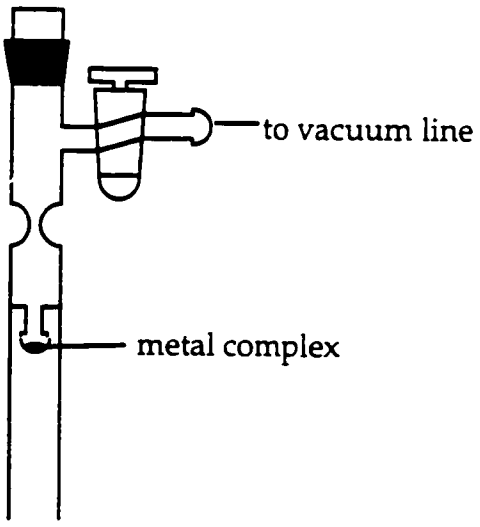

Figure 2.1 Schematic of a breakseal reactor

2.2.3 Grafting of metal complexes

After pretreatment and cooling of the oxide surfaces, the oxides were exposed to the vanadium and titanium precursors by one of two methods. An excess of one of the volatile precursors ($VOCl_3$, $TiCl_4$ or VCl_4) was introduced into a reactor via vapor phase transfer on a high vacuum line. Following 15-30 minutes of reaction, the reactor was evacuated to remove the excess metal reagent as well as volatile products formed in the reaction with the surface, leaving only chemisorbed species in the reactor.

All other precursors were introduced into reactors using breakseals. After pretreatment and cooling to room temperature of the oxide surfaces, the breakseal containing the precursor was broken using a hammer, Figures 2.3 and 2.5. The thermal treatment area of the reactor was placed into liquid N_2 and the metal complexes were sublimed from the breakseal to the cold trap for 1 to 16 hours (depending on volatility). At this time, the reactor was removed from liquid N_2 and allowed to stand at room temperature until the reaction was complete, from 1 to 12 hours depending on the volatility of the metal complex. Excess reagent and reaction products were then desorbed to the breakseal sidearm using a liquid N_2 cold trap. Desorption generally required several hours, after which time the breakseal was flame-sealed at the restriction, isolating the oxide-supported metal complex for subsequent manipulation.

2.3 Characterization of supported metal complexes

2.3.1 Infrared spectroscopy

Infrared experiments were performed in high-vacuum *in situ* IR cells (volume ca. 300 mL), Figure 2.3, equipped with either KCl or ZnSe windows. Transmission spectra were recorded on a dry-air purged Mattson Research Series FTIR equipped with DTGS detector. For both background and sample spectra, 32 scans were recorded at a resolution of 2 cm^{-1}.

2.3.1.1 Infrared spectroscopy of self-supporting disks

In self-supporting disk experiments, silica was pressed (125 kg/cm^2) into pellets 1.6 cm in diameter containing 2-10 mg of silica per cm^2. The pellets were placed in a sample holder inside an *in situ* infrared cell, Figure 2.3.

The silica was prepared by moving the sample holder to the thermal treatment area of the cell, where calcination and dehydroxylation take place. After cooling to room temperature and recording spectra of both the silica pellet, Figure 2.2a, and windows, a metal complex was introduced into the cell as described above.

Sample scans, taken at each stage of reaction, were obtained by sliding the sample holder into the IR portion of the cell and aligning the pellet perpendicular to the IR beam of the spectrometer. Spectra of gas phase products were obtained by sliding the sample holder out of the IR portion of the cell leaving only the KCl or ZnSe windows in the beam.

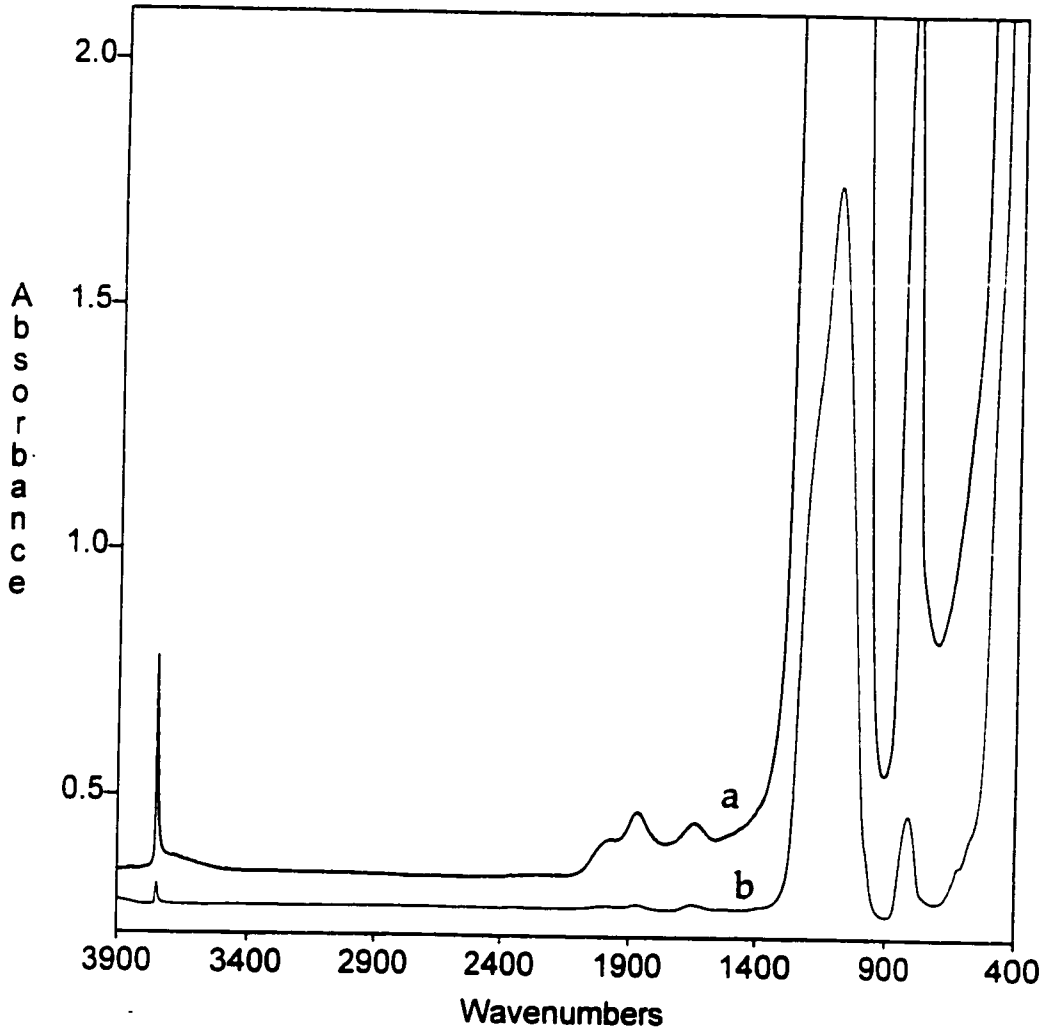

Figure 2.2 Transmission infrared spectra of silica-500. (a) Self-supporting disk; (b) thin film supported on a ZnSe IR window.

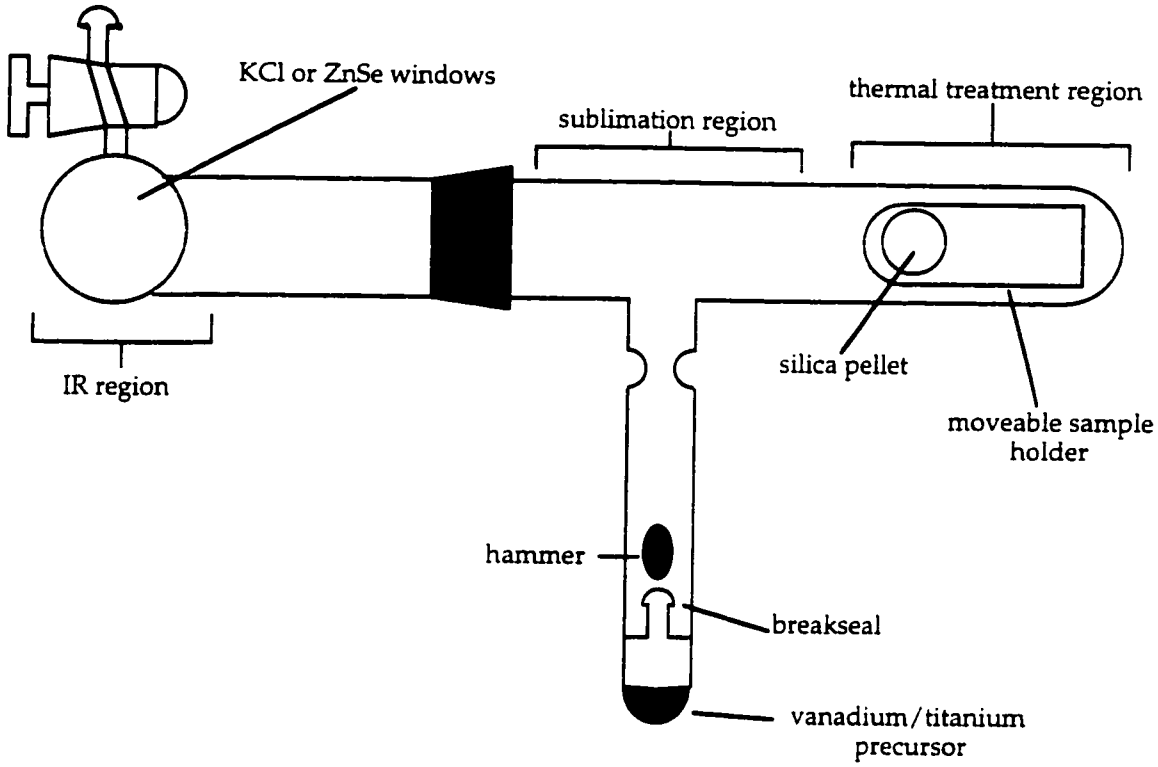

Figure 2.3 Schematic of an *in situ* infrared cell (side view)

2.3.1.2 Infrared spectroscopy of thin silica films

Thin film experiments were performed in a specially-designed IR cell. The cell was modified to contain a sample holder that holds a 25 mm ZnSe disk and which slides end to end without being able to rotate, so that the ZnSe disk is always parallel to the IR windows of the cell. Furthermore, all reagents, including $VOCl_3$ and $TiCl_4$, were introduced via breakseals. Silica was spread in a thin film onto the ZnSe disk (0.1-0.5 mg silica/cm^2) and placed inside the

modified IR cell, Figure 2.2b. Thermal pretreatment was carried out in the usual manner but at 450°C rather then 500°C because of the thermal limitations of the ZnSe disk. After cooling, the IR cell was placed inside the spectrometer and the silica film was alligned in the IR beam. Once alligned, neither the silica film nor the IR cell were moved for the remainder of the experiment to ensure accurate spectral subtraction. Otherwise the same experimental conditions were used as for self-supporting disks (e.g., resolution, number of scans).

2.3.2 Solid state NMR spectroscopy

Supported vanadium complexes for NMR experiments were prepared in Schlenk type reactors equipped with a high vacuum stopcock and one or more 5 mm Pyrex NMR tube glass blown on at right angles to the main body of the reactor, Figure 2.5. NMR experiments used compacted silica rather than pellets. The silica was prepared by first pressing it into a thick pellet of 50-100 mg, followed by grinding in a mortar. After preparation of the silica-supported vanadium complexes in the manner previously described, samples were transferred *in vacuo* into the NMR tubes and sealed off at 25-30 mm lengths with a torch, to give tubes containing approximately 20 mg of sample. ^{51}V MAS (magic angle spinning) NMR, frequency 52.6 MHz, and ^{13}C CP-MAS (cross polarization magic angle spinning) NMR, frequency 50.32 MHz, were recorded on a Bruker ASX-200 spectrometer. The ^{51}V NMR spectra were collected using a 4.8 μs 90° pulse. The relaxation delay was 0.2 s. The samples were spun at 3000-4000 Hz and the spin rate was varied in order to identify spinning side bands, Figure 2.4.

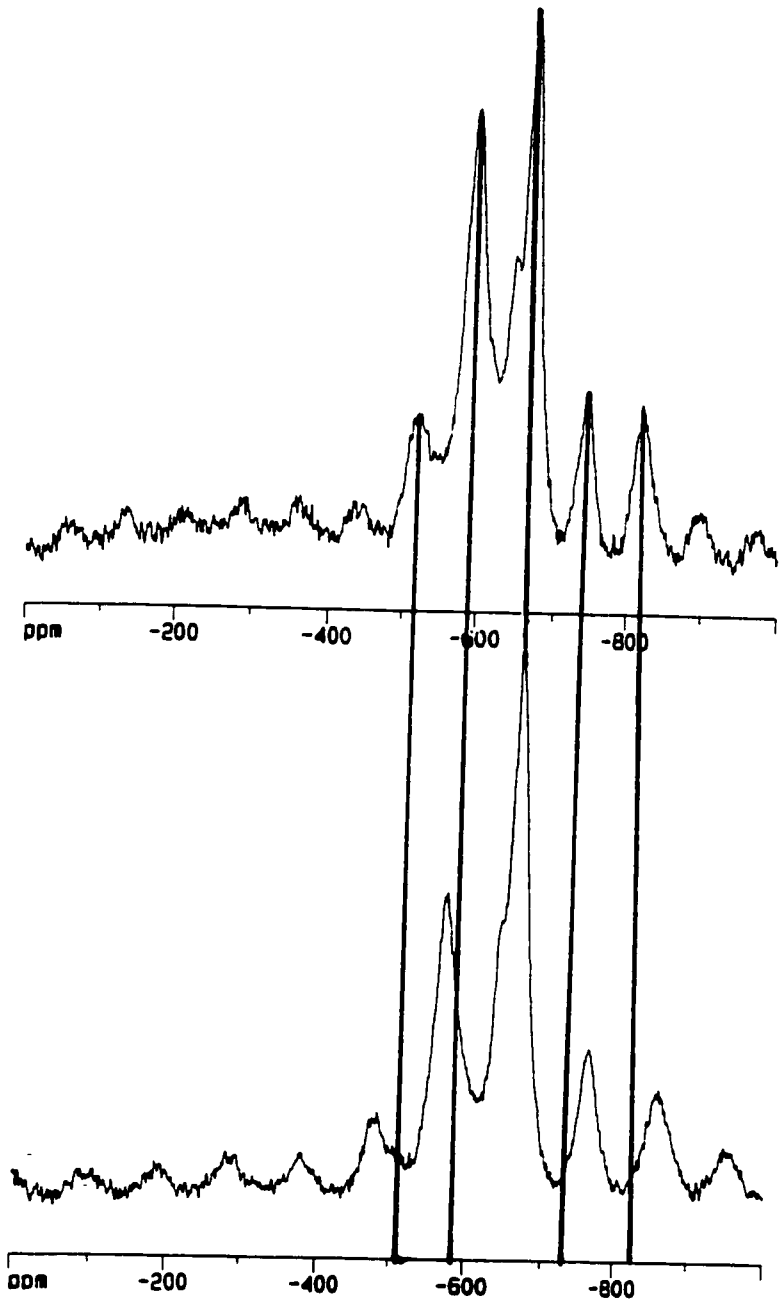

Figure 2.4 ^{51}V MAS NMR spectra of $\equiv SiOVO(O^iPr)_2$ (a) spinning at 3000 Hz; (b) spinning at 4000 Hz

Line shape analysis to determine true chemical shifts was not attempted; values reported are peak maxima. The ^{13}C CP-MAS NMR spectra were collected using a 4 μs 90° proton pulse with a contact time of 1000 μs. The relaxation delay was 2 s. All ^{51}V spectra were baseline corrected with a spline fit.

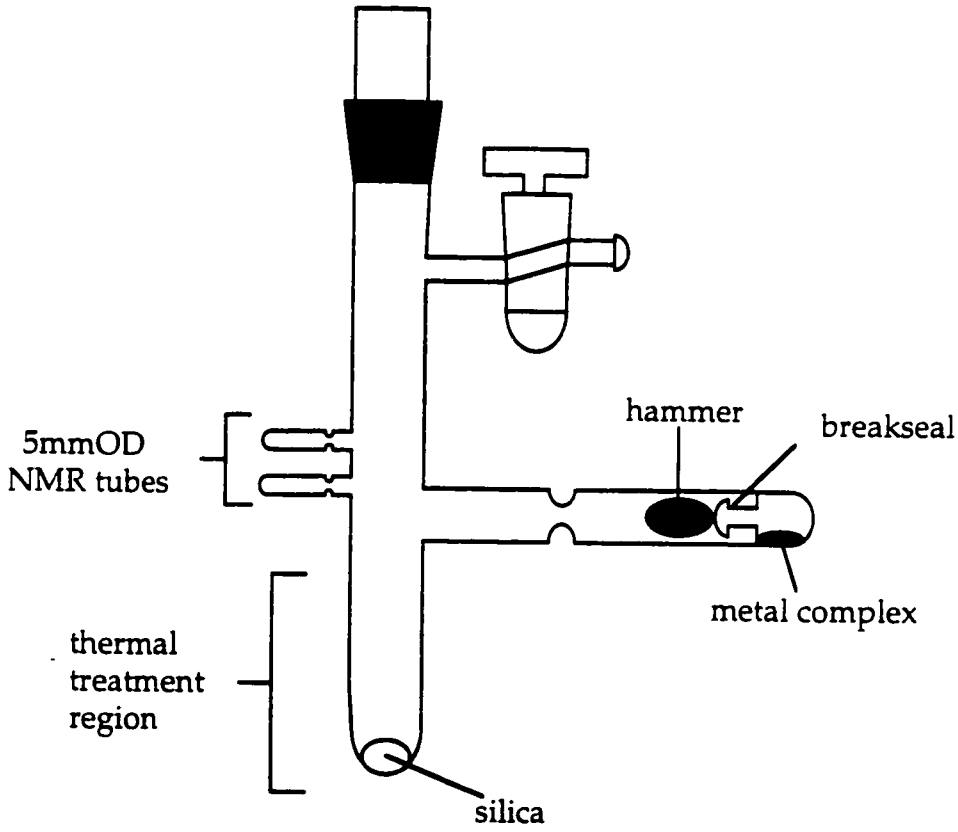

Figure 2.5 Schematic of a NMR reactor

2.3.3 Diffuse reflectance UV-visible spectroscopy

Samples for diffuse reflectance UV-visible spectroscopy were prepared in the same manner as the solid-state NMR samples, however, instead of being transferred into NMR tubes, the samples were transferred into 2 x 5 mm rectangular quartz tubing and sealed off with a torch above a graded seal. Diffuse reflectance UV-vis spectra were recorded on a Varian Cary 1E spectrophotometer equipped with an integrating sphere diffuse reflectance attachment, and referenced to Spectralon.

2.3.4 Elemental analyses

At the end of each experiment, the vanadium was extracted from the silica in order to determine the amount that had been chemisorbed. The vanadium was quantitatively extracted by stirring each modified silica sample in 1 M H_2SO_4 to give solutions containing ca. 0.1 mg V/mL. These solutions were treated with 30% aqueous H_2O_2 (0.3 mL/mL sample solution) to form the strongly absorbing red-brown peroxovanadium complex.[5] Spectra were recorded in quartz cuvettes with a 1 cm path length and referenced to a H_2SO_4/H_2O_2 solution containing approximately the same amount of H_2O_2 per mL sample solution as the vanadium samples. The spectra were recorded on a Varian Cary 1E spectrophotometer. The absorbance at 462 nm was converted to vanadium concentration by comparison to a calibration curve prepared under the same conditions using ammonium vanadate, Figure 2.6.

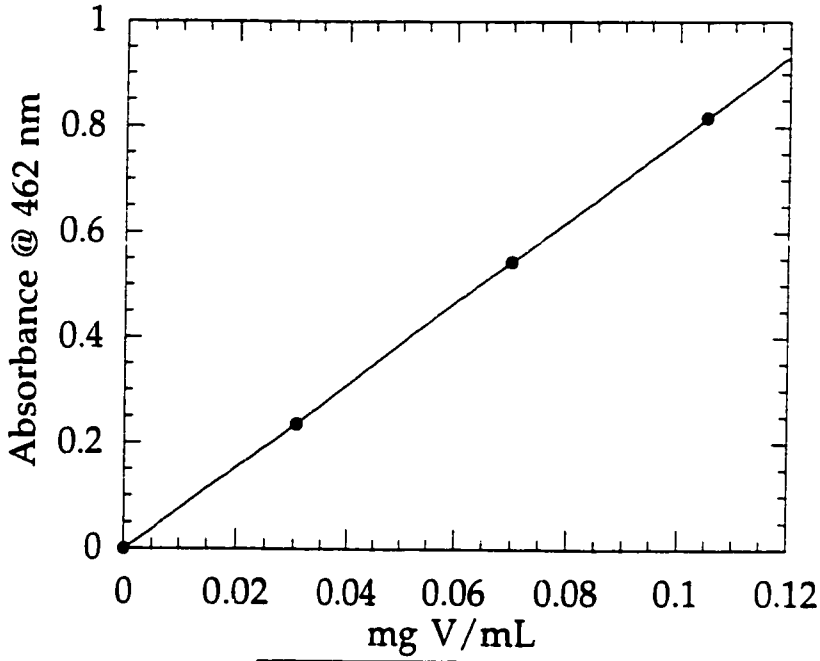

y = m1 + m2 * M0		
	Value	Error
m1	-0.0013273	0.0013396
m2	7.7888	0.020636
Chisq	5.3639e-06	NA
R	0.99999	NA

Figure 2.6 Calibration curve for vanadium alone

2.3.4.1 Simultaneous analysis of vanadium and titanium

For silica samples containing both vanadium and titanium, the metals loading was also determined by quantitative extraction. The method used for extraction was a modified version of that given for the analysis of titanium.[6] Metals were extracted by boiling the modified silica samples in 1.8 M H_2SO_4 for 1 hour, followed by addition of 0.1 mL of 30% H_2O_2 and dilution to 25 mL with 1.8 M H_2SO_4. This forms titanium and vanadium peroxo complexes with λ_{max} at 405 and 462 nm, respectively. The absorbance at each wavelength was measured, and the concentration of each metal calculated by solving simultaneously two equations with two unknowns, assuming that the complexes are non-interacting and their absorbances additive (observing Beer's Law). To calculate the amount of each metal present, calibration curves were prepared for each metal at the two different wavelengths. Calibration curves for vanadium (from ammonium vanadate) and titanium (from titanium standard atomic absorption solution (Aldrich), consisting of 1000 μg/mL of Ti in water) were prepared at both wavelengths, Figures 2.7 and 2.8. Therefore calibration curves for vanadium were prepared at 462 nm, where the vanadium peroxo complex has its λ_{max}, as well as at 405 nm, where the titanium peroxo complex has its λ_{max}. Likewise, calibration curves for titanium were prepared at each of the two wavelengths. Spectra were recorded on the Varian Cary 1E spectrometer and referenced to a mixture of 1.8 M H_2SO_4/30% H_2O_2.

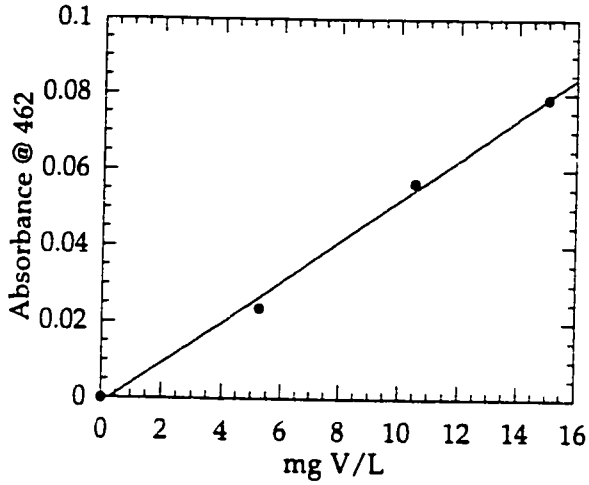

y = m1 + m2 * M0		
	Value	Error
m1	-0.0014025	0.0022887
m2	0.005346	0.00023984
Chisq	1.4603e-05	NA
R	0.99799	NA

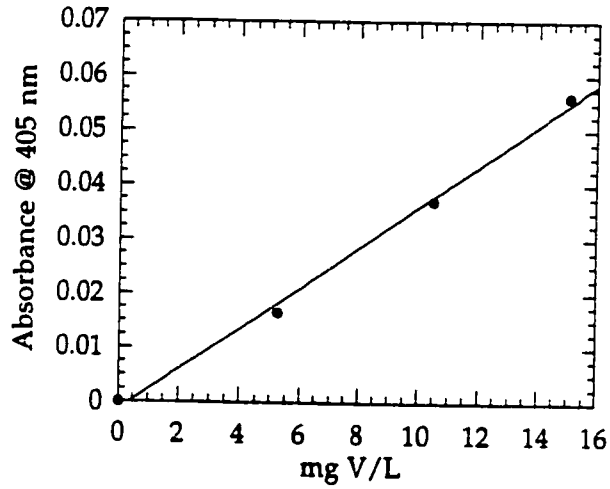

y = m1 + m2 * M0		
	Value	Error
m1	-0.0014587	0.0016762
m2	0.0037467	0.00017565
Chisq	7.8322e-06	NA
R	0.99781	NA

Figure 2.7 Calibration curves for vanadium in the presence of titanium

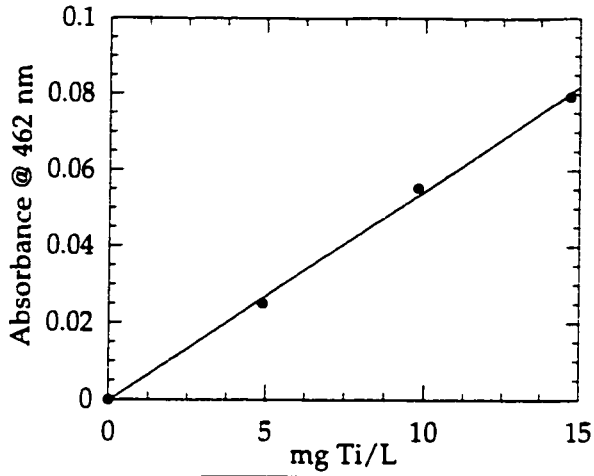

y = m1 + m2 * M0		
	Value	Error
m1	-0.000267	0.0014989
m2	0.0054771	0.00016351
Chisq	6.419e-06	NA
R	0.99911	NA

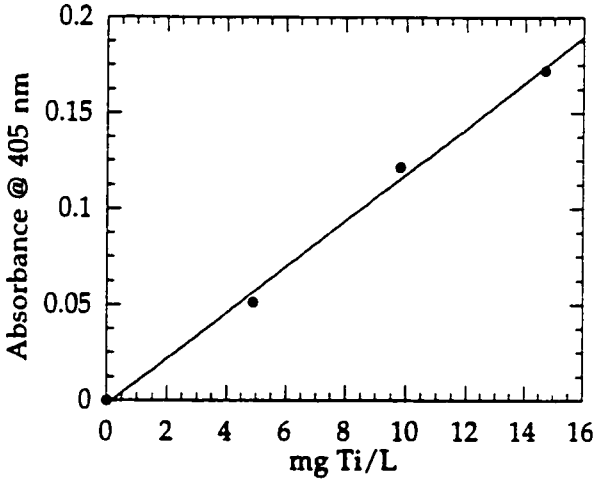

y = m1 + m2 * M0		
	Value	Error
m1	-0.00182	0.0050812
m2	0.011976	0.00055429
Chisq	7.3768e-05	NA
R	0.99786	NA

Figure 2.8 Calibration curves for titanium in the presence of vanadium

Each calibration curve was fitted using the equation for a straight line. The two equations for absorbance at 405 nm and the two for absorbance at 462 nm were then added, resulting in the following equations, where concentration of the metals is in mg/L:

$$Abs_{405} = -3.28x10^{-3} + 3.78x10^{-3}[V] + 1.20x10^{-2}[Ti] \quad (2.3)$$

$$Abs_{462} = -1.67x10^{-3} + 5.35x10^{-3}[V] + 5.48x10^{-3}[Ti] \quad (2.4)$$

The absorbance of a single solution was measured at the two wavelengths and the two equations are solved for [V] and [Ti]. To test the accuracy of this method, samples were also analyzed by traditional ICP, where the entire sample, including the silica, is dissolved in HF followed by analysis (France) and by direct introduction of the solid into the plasma (using the method of N. da Silva, Carleton University). Table 2.1 shows a comparison of the results. The extraction and traditional ICP results were very comparable, generally within 5% which is within experimental error. The direct introduction of the solid into the plasma gave results which far less accurate than the other two.

Table 2.1 Comparison of different methods for simultaneous analysis of vanadium and titanium on silica.

	Method					
	extraction		ICP		ICP (solids)	
sample	% V	% Ti	% V	% Ti	% V	% Ti
1	2.10		2.20			
2	1.95	1.88	2.10	1.95		
3	1.90				2.76	
4	1.75	1.70			3.31	2.66

2.3.5 Magnetic measurements

The pretreatment of silica and the preparation of silica-supported vanadium species were performed as described above, except that the samples were prepared in a special reactor made partially of quartz, Figure 2.9. The main part of the reactor consists of a 7 mm OD/5 mm ID quartz tube approximately 75 cm in length. At one end of the tube, a 7 mm OD piece of quartz rod, 10 cm long, is attached. At mid-length of the reactor, above a quartz-pyrex graded seal, there are three attachments: a breakseal containing the molecular vanadium complex, a high vacuum stopcock and a tube in which the pretreatment of the silica can take place. The final component of the reactor consists of a 5 mm OD solid quartz rod approximately 25 cm long. At the end of this quartz rod there is a bulb filled with iron so that the rod can be held in place with a magnet. The rod was placed inside

the reactor and the pretreatment and modification of the silica surface was performed as described previously. Once all manipulations were complete, approximately 40 mg of the modified silica was transferred to the bottom of the reactor, where the main tube is sealed to the quartz rod, and the smaller movable quartz rod was lowered down on top of the modified silica The sample was then sealed off with a flame 10 cm above the silica leaving the sample sealed under vacuum between two solid pieces of quartz.

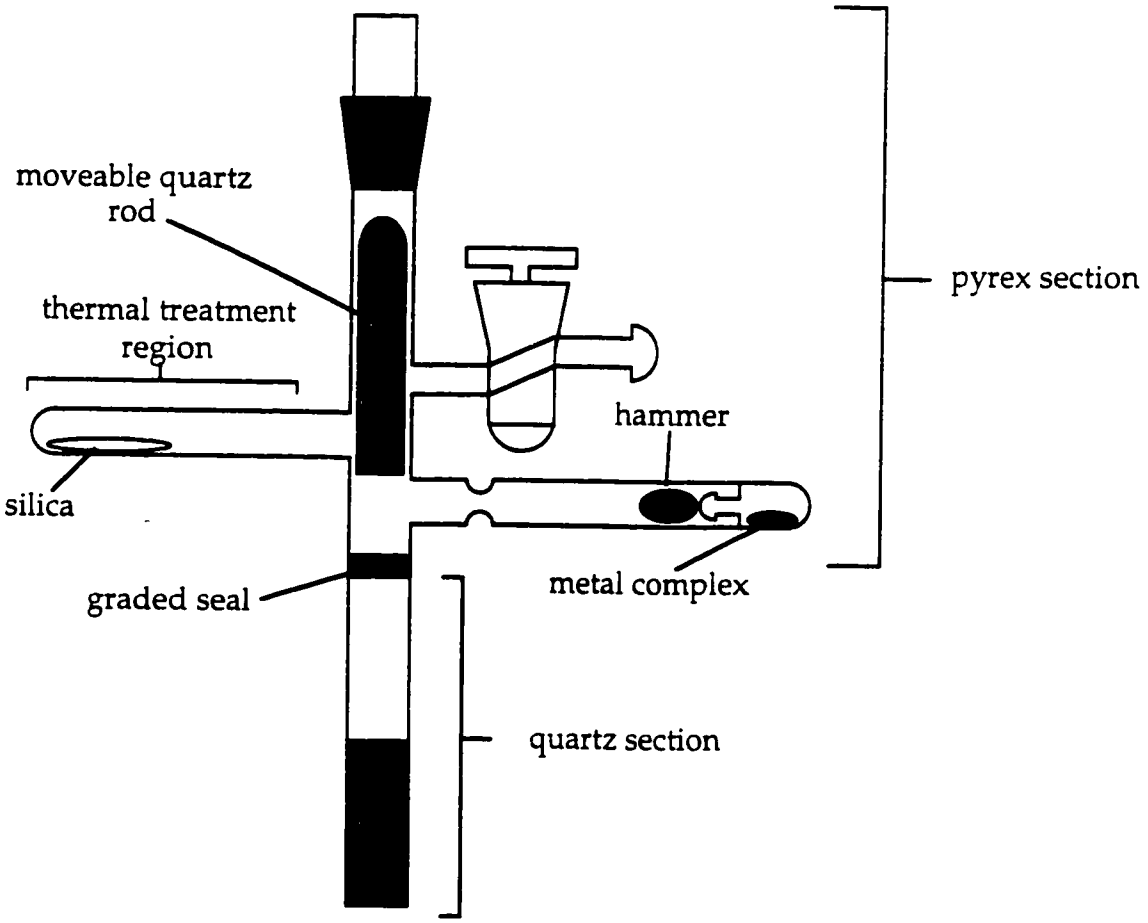

Figure 2.9 Schematic of the magnetic susceptibility reactor

Susceptibility was measured as a function of temperature on a SQUID magnetometer at Quantum Design in San Diego California. The instrument operates at 5 T using a 3 cm Reciprocating Sample Option scan at 1 Hz with iterative regression, 10 cycles per measurement and 5 measurements per average.

Paramagnetic moments are not measured directly. The magnetic susceptibility is first determined and the magnetic moment can be calculated from this. When a substance is placed in a magnetic field:

$$B = H + 4\pi I \qquad (2.5)$$

where H is the magnitude of the magnetic field, B is the flux within the substance, and I is the intensity of magnetixation

The magnetic permeability is defined by the ratio B/H, eq. 2.6, where k is the magnetic susceptibility per unit volume.

$$B/H = 1 + 4\pi k \qquad (2.6)$$

Magnetic susceptibilities are usually reported on the basis of weight rather than volume, eq. 2.7 and 2.8.

$$\chi = k/d \qquad (2.7)$$

$$M * \chi = \chi_M \qquad (2.8)$$

where d is the density in g/cm^3, M is the molecular weight, χ is the gram susceptibility, and χ_M = molar susceptibility

For an ideal paramagnet,

$$\chi_M^{corr} = C/T \qquad (2.9)$$

where C is the Curie constant, T is the absolute temperature, and χ_M^{corr} is the molar susceptibility after a diamagnetic correction

According to classical statistical mechanics, the Curie constant can be expressed as:

$$C = N\mu^2/3k \qquad (2.10)$$

where N is Avogadro's number, k is Boltzmann's constant, and μ is the magnetic moment per molecule (in BM)

Therefore

$$\chi_M^{corr} = N\mu^2/3kT \qquad (2.11)$$

$$\mu = (3k/N)^{1/2}(\chi_M^{corr}T)^{1/2} \qquad (2.12)$$

$$\mu = 2.84(C)^{1/2} \qquad (2.13)$$

To calculate the magnetic moment per metal atom, C must be obtained.[7] The value of C is extracted from the curve fit of the plot of susceptibility versus temperature (i.e., figure 6.5). C is then corrected for amount of vanadium present, since the vanadium makes up only 2 wt.% of the material analyzed, and for the field strength, eq. 2.14.

$$C = (m1)(m_{wt})/(mass)(field) \qquad (2.14)$$

where m1 is the constant from the non linear curve fit of susceptibility versus temperature, field is the field strength, m_{wt} is the molar mass of the metal atom/mass of metal in sample, and mass is the mass of modified silica

The effective magnetic moment per metal atom is then obtained from eq. 2.13.

2.4 Analysis of volatile reaction products

Gases were analyzed qualitatively by GC and GC-MS. GC analyses of volatile products were performed on a Hewlett-Packard 5710A gas chromatograph with variable temperature oven control, equipped with a 2 m 1/4" stainless steel column packed with Porasil, and a FID detector. For C_1-C_3 hydrocarbons, gas mixtures were injected with the oven at room temperature, whereas all other injections were done at 85-150°C depending on the boiling point of the product being analyzed. Retention times were confirmed with standards injected under the same experimental conditions.

Further analyses of volatile products, particularly analysis of the isotope enrichment of tetramethylsilane obtained in the acid protonolysis of $(\equiv SiO)_2V(CH_2SiMe_3)_2$ and $(\equiv SiO)_2V{=}CHSiMe_3$ by DCl, were performed by GC/MS. Analyses were performed on a HP 5890 Series II gas chromatograph with a Kratos mass selective detector using Concept 1H and a J & W, DBI column (30 m long, i.d. 0.2 mm, film thickness 0.33 μm).

2.5 Quantification of volatile reaction products

2.5.1 High vacuum techniques

All experiments other than synthesis of organometallic complexes were performed on high vacuum systems. The vacuum system consists of a main vacuum manifold and a gas manifold, each equipped with a Baratron capacitance manometer, attached to a mercury diffusion pump backed by an Edwards RV3 rotary vane pump, for an absolute line pressure of $\leq 10^{-4}$ Torr. A liquid N_2 trap was placed between the main vacuum manifold and the mercury diffusion pump. There are three high vacuum stopcocks attached to the vacuum manifold, each fitted with spherical joints to which reactors can be attached.

2.5.2 IR quantification

To quantify products of surface reactions, for example the amount of protonated ligand released upon grafting of a metal complex onto silica, the IR spectrum of the product was compared to an IR calibration curve.

Each calibration curve was prepared by measuring the gas phase IR absorbance (peak intensity) as a function of pressure. All products were transferred into glass reactors equipped with high vacuum stopcocks. These reactors were connected to an empty gas phase IR cell via the high vacuum line through a modified "T" joint which was directly attached to a "4-decade" Baratron capacitance manometer, either 10 or 1000 Torr full scale depending on the pressure range required. A known pressure of the gas was introduced into the IR cell and the IR spectrum was recorded at resolution of 2 cm^{-1} and this operation was repeated at several different pressures. Calibration curves were prepared for HCl, 2-propanol, tetramethylsilane, CO_2 and ^tBuOH, figures 2.10a-e.

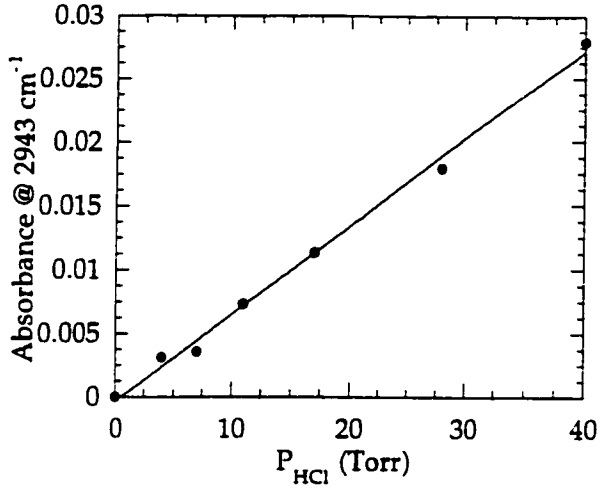

y = m1 + m2*M0		
	Value	Error
m1	-0.00032808	0.00045847
m2	0.00068745	2.2686e-05
Chisq	3.1481e-06	NA
R	0.99729	NA

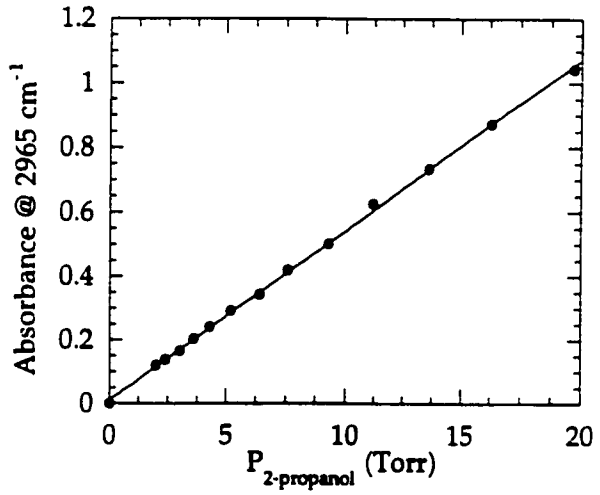

y = m1 + m2 * M0		
	Value	Error
m1	0.011393	0.0038394
m2	0.052994	0.00041018
Chisq	0.00089869	NA
R	0.99964	NA

Figure 2.10 Calibration curve for (a) HCl; (b) 2-propanol

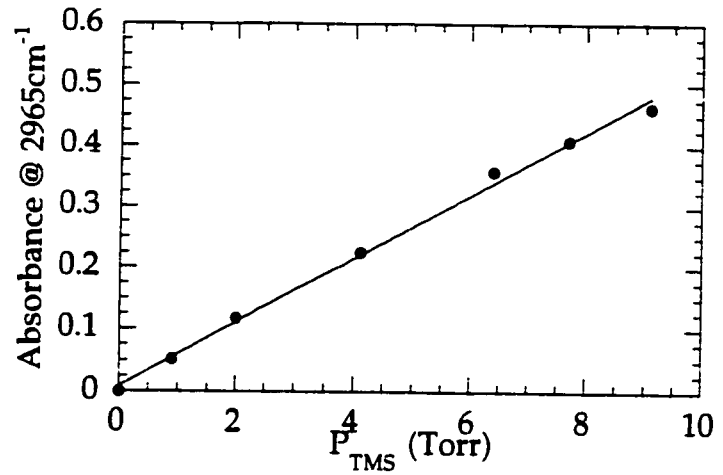

c

y = m1 + m2 * M0		
	Value	Error
m1	0.0089591	0.0077417
m2	0.051823	0.0014317
Chisq	0.00076239	NA
R	0.9981	NA

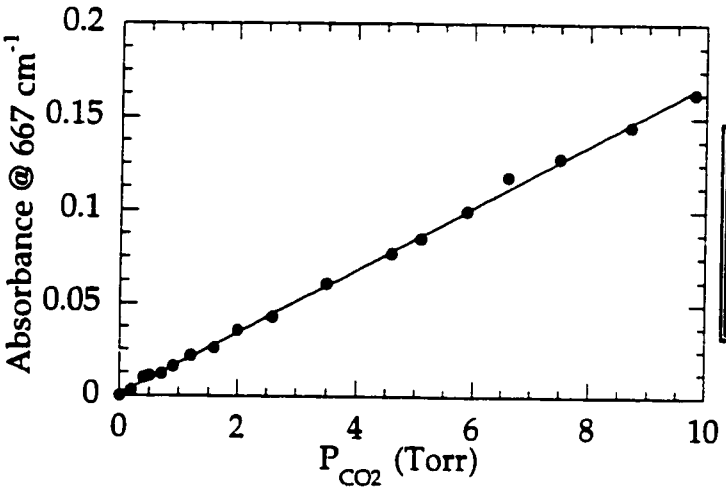

d

y = m1 + m2 * M0		
	Value	Error
m1	0.001182	0.00076845
m2	0.016743	0.00016675
Chisq	7.5673e-05	NA
R	0.99921	NA

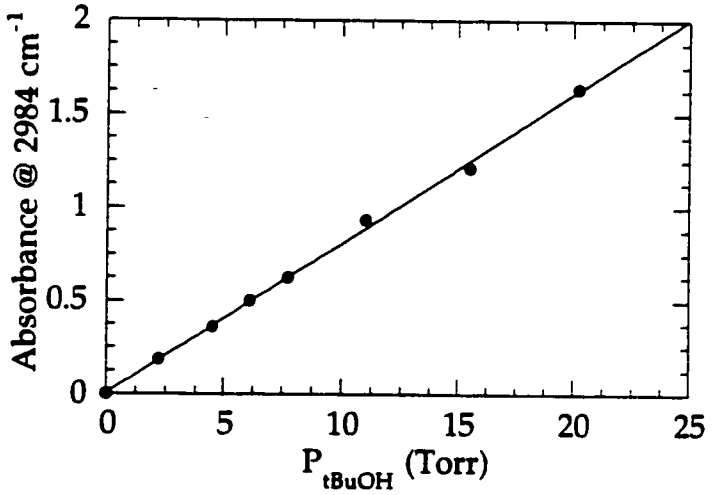

e

y = m1 + m2*M0		
	Value	Error
m1	0.0074569	0.014327
m2	0.080244	0.0013571
Chisq	0.0036059	NA
R	0.99914	NA

Figure 2.10 Calibration curve for (c) tetramethylsilane; (d) CO_2; (e) ^tBuOH

2.6 References

(1) Heaney, P. J.; Prewitt, C. T.; Gibbs, G. V. *Silica: Physical Behavior, Geochemistry and Materials Applications*; Mineralogical Society of America: Washington, D. C, 1994.

(2) Razuvaev, G. A.; Latyaeva, V. N.; Vyshinskaya, L. I.; Drobotenko, V. V. *J. Organomet. Chem.* **1981**, *208*, 169-182.

(3) Haukka, S.; Lakomaa, E. L.; Root, A. *J. Phys. Chem.* **1993**, *97*, 5085-5094.

(4) Morrow, B. A.; Devi, A. *Can. J. Chem.* **1970**, *48*, 2454-2456.

(5) Vogel, A. J. *A Textbook of Quantitative Inorganic Analysis*; Longman: London, 1961.

(6) Haukka, S.; Saastamoinen, A. *Analyst* **1992**, *117*, 1381-1384.

(7) Wold, A.; Dwight, K. *Solid State Chemistry*; Chapman Hall: London, 1993.

Chapter 3

Synthesis of Silica-supported Vanadium(V) Complexes

3.1 Introduction

Vanadium-containing solid catalysts are widely used for the partial oxidation of hydrocarbons,[1-3] oxidation of SO_2 and selective catalytic reduction (SCR) of NO_x.[4] The atomic level structure of these materials has been studied by vibrational spectroscopy,[5,6] ^{51}V solid state NMR,[7] EXAFS/XANES[8] and interpreted by comparison to molecular model compounds.[9,10] Three types of vanadium species have been identified on oxide surfaces: monomeric pseudo-tetrahedral complexes, 2-D oxo bridged chains and bulk crystallites of V_2O_5.[11] The reactivity of these mixed oxide catalysts containing vanadium is highly dependent on the metal-support interaction and seems to be enhanced when vanadium is dispersed as a monolayer on the oxide support.[12]

Oxygen labelling has been used in the study of mechanisms of heterogeneous oxidation over mixed metal oxides. For example, by rehydration of Mo/SiO_2 with $H_2{}^{18}O$, both basal and terminal oxygen atoms were exchanged and vibrational assignments were based on the magnitude of the observed isotope shifts.[13] Labelling of bulk MoO_3 was achieved by reduction followed by reoxidation in the presence of $^{18}O_2$, and was used to identify the active sites for reoxidation.[14] Similarly, V-P-O catalysts for the conversion of n-butane to maleic anhydride were enriched using $^{18}O_2$ to determine the location of active oxygen for combustion and selective

oxidation.[15] However, in all of these systems, it was not possible to incorporate the isotope label exclusively in a specific coordination site on the catalyst surface.

Our approach, using volatile molecular precursors to graft vanadium, makes it possible to synthesize surface species whose composition is very uniform within a given sample. The homogeneous nature of the vanadium environment makes it amenable to study using spectroscopy. Furthermore, it allows us to incorporate ^{18}O atoms into specific coordination sites.

In this chapter we describe the preparation and characterization of well-defined silica-supported vanadium(V) complexes of the type $\equiv SiOVOX_2$ and their ^{18}O labelling.

3.2 Stoichiometry of the reaction of $O=VX_3$ with silica

The temperature at which silica is heated determines the density of surface hydroxyl groups. Fully hydroxylated silica contains approximately 4.9 OH/nm^2,[16] while silicas which have been partially dehydroxylated at 200 and 500°C have 2.6 and 1.2 OH/nm^2, respectively.[17] These silicas will be referred to as silica-25, silica-200 and silica-500, respectively, where the appended number indicates the temperature at which the silica was treated in vacuum before reaction with the vanadium complexes.

When $O=VX_3$ (X is O^iPr or Cl) vapor at room temperature contacts the surface hydroxyl groups of silica, a chemical reaction takes place in which

adsorbed vanadium species are formed with concurrent liberation of protonated ligands as HX, equation 3.1.

$$n \equiv SiOH + O{=}VX_3 \rightarrow (\equiv SiO)_n V(O)X_{3-n} + n\ HX \qquad (3.1)$$

After desorption of unreacted $O{=}VX_3$, the amount of chemisorbed vanadium was determined by extraction. The value of n was evaluated by determining the amount of 2-propanol or HCl liberated by quantitative gas phase IR spectroscopy (neither 2-propanol nor HCl react significantly with silica at room temperature). The value of n was then confirmed by quantifying the 2-propanol or HCl liberated upon hydrolysis of the chemisorbed vanadium complexes. The surface complexes are extremely sensitive to water vapour. In addition to quantitative release of HX, the addition of water leads to dramatic color changes from virtually colorless to red and eventually to yellow-green. In all cases, we found n=1. The results are summarized in Table 3.1 for silicas activated at various temperatures.

Our results indicate that the maximum amount of chemisorbed vanadium is nearly equal to the initial quantity of surface hydroxyl groups, which, naturally, decreases as the dehydroxylation temperature increases.

Table 3.1. Stoichiometry of the room temperature reaction of $O=VX_3$ with SiO_2

Dehydroxylation temperature of silica	X	weight % chemisorbed vanadium[a]	V grafted per ≡SiOH[b]	HX liberated per grafted V	
				during grafting[c]	after grafting[d]
500	O^iPr	2.2	0.99	0.96	1.8
500	Cl	2.2	0.92	1.1	2.0
200	O^iPr	4.2	0.98	0.97	1.9
200	Cl	4.3	0.96	0.97	1.9
25	O^iPr	7.6	0.96	0.94	1.8
25	Cl	7.4	0.94	0.95	1.9

[a] ± 0.1, based on the average of 3-15 independent experiments.

[b] Ratio of the amount of chemisorbed V to the hydroxyl content of unmodified silica at each dehydroxylation temperature (4.9, 2.6 and 1.2 OH/nm^2 for silica-25, -200 and -500 respectively).[16,17]

[c] Ratio of the amount of HX liberated during grafting of $O=VX_3$ on silica to the amount of chemisorbed vanadium.

[d] Ratio of the amount of HX liberated by hydrolysis of surface complexes to the amount of chemisorbed vanadium.

The stoichiometry of equation 3.1 is independent of dehydroxylation temperature of silica over the range 25-500°C. The value n=1.0 is an average value. However, since physisorbed $O{=}VX_3$ was desorbed from the silica surface before analysis, we can exclude significant contributions from unreacted $O{=}VX_3$, and consequently also the disubstituted species $(\equiv SiO)_2V(O)X$. Thus the molecular complexes $O{=}VCl_3$ and $O{=}V(O^iPr)_3$ react at room temperature with only one ≡SiOH regardless of the density of surface hydroxyl groups. The grafting reactions are formulated as:

$$\equiv SiOH + O{=}V(O^iPr)_3 \rightarrow \equiv SiOVO(O^iPr)_2 + {}^iPrOH \qquad (3.2)$$

$$\equiv SiOH + O{=}VCl_3 \rightarrow \equiv SiOVOCl_2 + HCl \qquad (3.3)$$

The absence of $(\equiv SiO)_2VOX$ among the products can be rationalized from the kinetics of reactions of $O{=}VCl_3$ with a large excess of alcohol.[18,19] The second ligand substitution is always much slower than the first. During the grafting reaction on silica, which takes place in the presence of a large excess of $O{=}VX_3$, even adjacent hydroxyl groups are likely to react with two different molecules of $O{=}VX_3$.

Equations 3.2 and 3.3 confirm the stoichiometry previously inferred for the reaction of $O{=}VCl_3$[20] and $O{=}V(OR)_3$[21,22] with oxide surfaces, based on a comparison of the amount of grafted vanadium to the hydroxyl content. In another study, the reaction of $O{=}V(OEt)_3$ with silica-250 and silica-500 was

reported to yield a mixture of mono and disubstituted surface vanadium complexes at 150°C.[23] However, it has also been reported that the reaction of $O=V(O^tBu)_3$ with the surface of silica-200 and silica-500 yield uniquely $\equiv SiOV(O)(O^tBu)_2$. In all these studies, the surface complexes were subsequently hydrolyzed[20] and/or annealed[20,23] to remove the ligands. In our experience, subjecting the surface complexes $\equiv SiOVO(O^iPr)_2$ and $\equiv SiOVOCl_2$ to temperatures above 75°C results in a dramatic color change from colorless to purple, possibly due to reduction of vanadium.[22,24]

3.3 Solid-state NMR characterization

Whereas determinations of the stoichiometry of grafting reactions by the methods described in section 3.2 gives only an *average* degree of ligand substitution in surface complexes, it is in principle possible by NMR spectroscopy to analyze the *distribution* of surface vanadium species. As discussed later, Chapter 4, this approach proved useful in studies of their reactivity.

The ^{51}V MAS NMR spectrum of the product of reaction of $O=V(O^iPr)_3$ with silica-500 is shown in Figure 3.1. A single broad resonance at -650 ppm was identified as the true peak maximum; all other bands are spinning side bands whose position shifted when the spin rate was varied. The resonance at -650 ppm is assigned to the monosubstituted vanadium complex, $\equiv SiOVO(O^iPr)_2$.

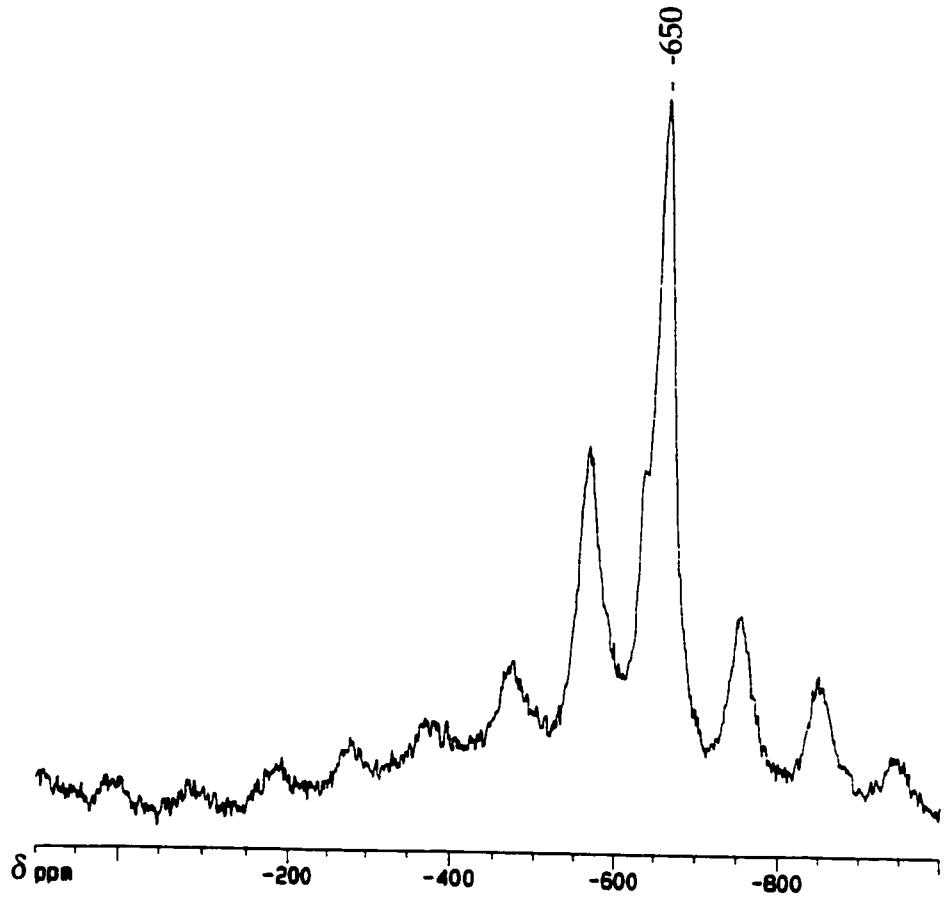

Figure 3.1 ^{51}V MAS NMR spectrum of ≡SiOVO(O^iPr)$_2$, spin rate 4000 Hz

However, the difference in chemical shift between ≡SiOV(O)(O^iPr)$_2$ and the starting material O=V(O^iPr)$_3$, at -630 ppm, is only 20 ppm. Given the peak width in Figure 3.1 of ca. 80 ppm, and the likelihood that other species such as (≡SiO)$_2$VO(O^iPr) will have similar chemical shifts, we cannot confidently distinguish between different possible surface complexes in this spectrum. On silica-200 and silica-25, the products of reaction of O=V(O^iPr)$_3$ with ≡SiOH gave spectra identical to the one shown in Figure 3.1. The ^{13}C CP-MAS NMR spectrum of ≡SiOV(O)(O^iPr)$_2$ on silica-500 contains a band at 84.3 ppm, assigned to the methylene carbon, and another sigmal at 24.5 ppm, assigned to the methyl carbons of the isopropoxo ligands, Figure 3.2.

The ^{51}V MAS NMR spectrum of the product of reaction of O=VCl_3 with silica-500 is shown in Figure 3.3. Only one resonance was observed at -293 ppm, assigned to ≡SiOVOCl_2. In samples where unreacted O=VCl_3 was not desorbed from the silica, physisorbed O=VCl_3 was also observed as a signal at 0 ppm. In molecular chemistry, each substitution of one chloro ligand of O=VCl_3 by an alkoxo ligand results in a large upfield shift of the ^{51}V resonance, attributed to the substitution of a purely σ-donating ligand by a σ,π-donating ligand.[10,25] By comparison to the chemical shifts of mixed alkoxochlorovanadium(V) complexes, Table 3.2, it appears that a similar effect derives from the substitution of chloro ligands by "siloxo" ligands derived from the silica surface.

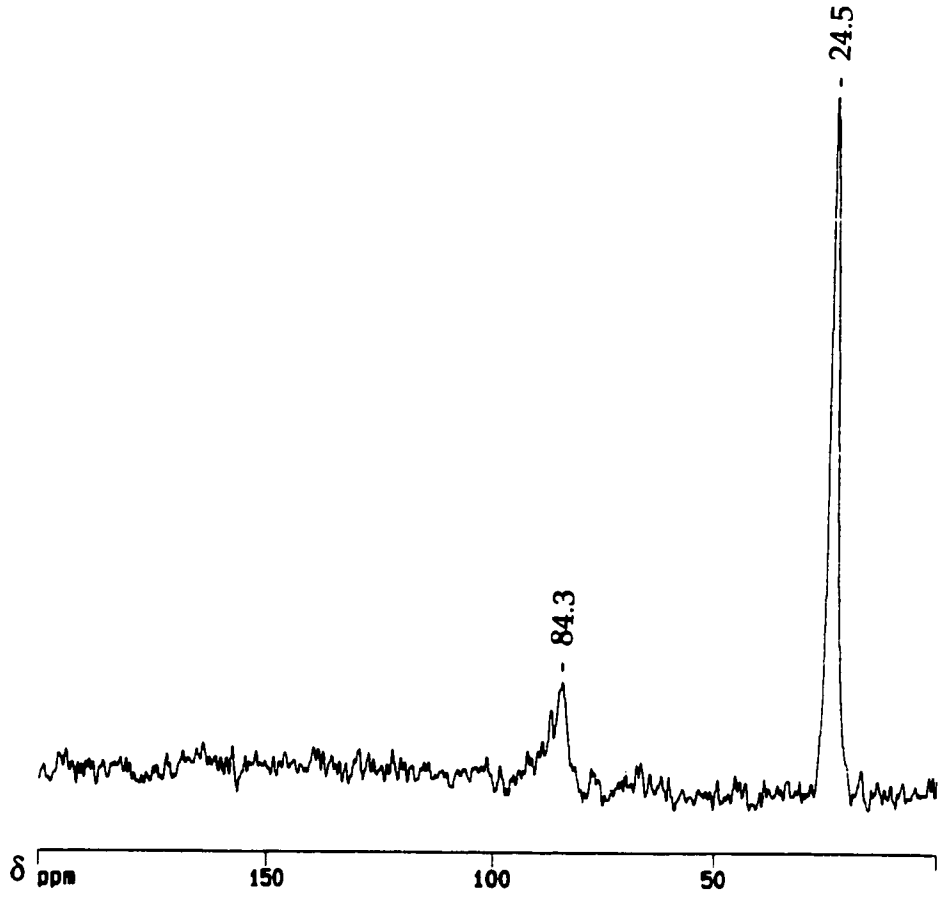

Figure 3.2 ^{13}C CP-MAS NMR spectrum of ≡SiOVO(O^iPr)$_2$, spin rate 4000 Hz

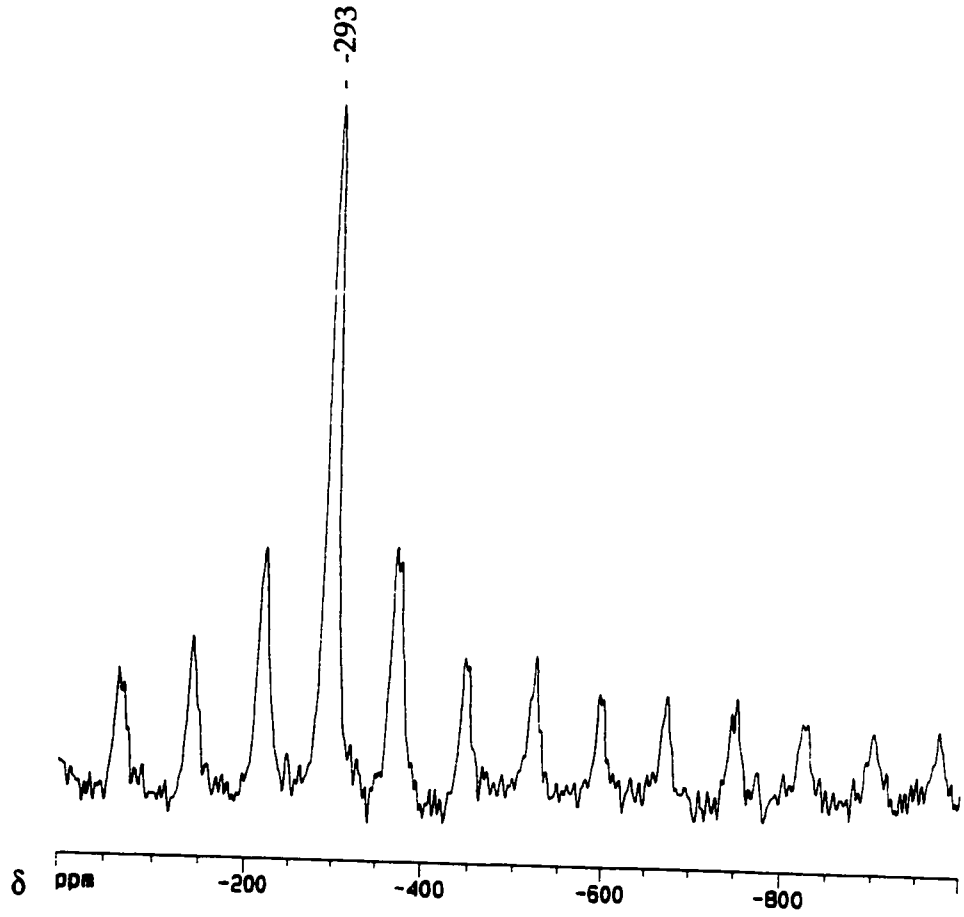

Figure 3.3 ^{51}V MAS NMR spectrum of ≡SiOVOCl$_2$, spin rate 4000 Hz

The ca. 300 ppm ^{51}V upfield shift for $\equiv SiOVOCl_2$ relative to $O=VCl_3$ is consistent with the substitution of a single chloro ligand by an oxygen donor ligand during grafting. We predict that disubstituted $(\equiv SiO)_2VOCl$ should have a ^{51}V chemical shift of ca. -500 ppm. Since no peaks in this region were observed, we conclude that species other than $\equiv SiOVOCl_2$ are not present in significant amounts on the silica surface.[26] However, the presence of intense spinning side bands makes it difficult to exclude the possibility of a small amount (< 5%) of the disubstituted product on the surface.

Table 3.2. ^{51}V NMR data for molecular and analogous surface complexes

Molecular complex	Chemical shift, (ppm)	Analogous surface complex	Peak maximum, (ppm[a])
$VOCl_3$	0		
$VO(O^tBu)Cl_2$	-325[25]	$\equiv SiOVOCl_2$	-293 (55)
$VO(O^tBu)_2Cl$	-537[25]	$\equiv SiOVOCl(O^tBu)$	-548 (75)
$VO(O^iPr)_3$	-630	$\equiv SiOVO(O^iPr)_2$	-650 (70)
$VO(O^tBu)_3$	-670[25]		

[a] FWHM peak widths are given in ppm in parentheses.

Similar spectra were obtained for ≡SiOVOCl$_2$ supported on silica-200 and silica-25. Therefore, both quantitative analyses (Table 3.1) and ^{51}V NMR spectra support our conclusion that a single surface species, (≡SiO)VOX$_2$, is formed in these reactions.

3.4 Infrared Characterization

The infrared spectrum of a thin self-supporting disk of silica-500 shows an intense band at 3747 cm^{-1}, Figure 3.4a, which is assigned to the O-H stretching vibration of non-interacting hydroxyl groups on the silica surface.[17] The broad bands at 1977, 1868 and 1647 cm^{-1} are overtones and combinations of the intense Si-O-Si fundamental modes which render the silica virtually opaque below 1200 cm^{-1}, although there are two "windows" of partial transparency from 1000 to 850 cm^{-1} and from 750 to 600 cm^{-1}. By using a very thin film of silica spread on an infrared transparent disk of ZnSe, it is possible, using careful spectral subtraction, to discern bands in the semi-opaque regions.[17]

3.4.1 The region 4000-1200 cm^{-1}

Admission of O=V(O^{i}Pr)$_3$ vapor at room temperature to the *in situ* IR cell, Figure 2.1 (Chapter 2), containing a self supporting disk of silica, led to immediate spectral changes. The band at 3747 cm^{-1} due to surface silanols almost completely disappeared, and 2-propanol was detected by its gas phase

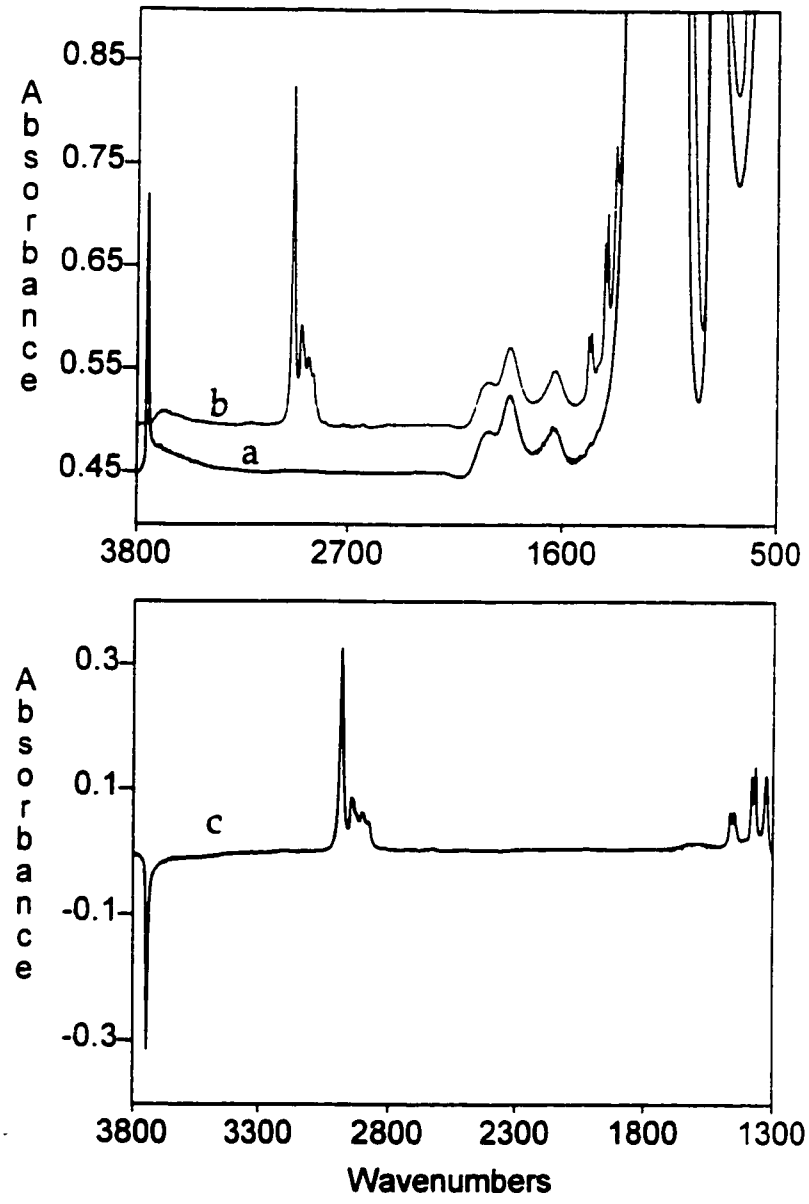

Figure 3.4 Transmission infrared spectra of a self-supporting disk: (a) silica-500; (b) ≡SiOVO(O^iPr)$_2$; (c) difference spectrum, obtained by subtraction (a) from (b).

IR spectrum and GC retention time. After prolonged desorption of volatiles to a liquid N_2 trap, the IR spectrum shown in Figure 3.4b was recorded.

New bands in the ν(C-H) region were observed at 2975, 2930 and 2883 cm^{-1}, assigned to vibrations of the isopropyl groups, Table 3.3. The CH_3 deformation modes appear as in-phase and out-of-phase doublets at 1464 and 1451 cm^{-1} (δ_{as}) and 1379 and 1365 cm^{-1} (δ_s). The O-C(H) deformation at 1327 cm^{-1} is the lowest frequency band visible before the intense absorption of SiO_2 saturates the spectrum. These observations are consistent with the formation of $\equiv SiOV(O)(O^iPr)_2$ according to equation 3.2. By spectral subtraction, a very weak band can be seen at 2020 cm^{-1}, Figure 3.5a. This band is likely the first overtone of a ν(V=O) fundamental (see below).

The reaction, under similar conditions, of $O=VCl_3$ with silica also causes the near total disappearance of surface hydroxyl groups, accompanied by the appearance of HCl in the gas phase. After evacuation, no new strong bands were apparent in the IR spectrum of the silica disk in the region above 1200 cm^{-1}. The expected ν(V=O) mode of $\equiv SiOVOCl_2$ is expected to be masked by the intense absorbance of the silica below 1200 cm^{-1}. Spectral subtraction reveals a weak band at 2069 cm^{-1}, assigned to 2ν(V=O), Figure 3.5b.

3.4.2 The region 1000-850 cm^{-1}

Bands in the region 1100 to 900 cm^{-1} are generally assigned to the stretching vibrations of terminal V=O bonds, whose frequencies are sensitive

Table 3.3. Infrared bands (cm^{-1}) of molecular complexes and analogous surface complexes

$VOCl_3$	$\equiv SiOVOCl_2$	$VOCl_2(O^iPr)$[28]	$\equiv SiOVOCl(O^tBu)$	$VOCl(O^iPr)_2$ [28]	$\equiv SiOVO(O^iPr)_2$	Assignment
		2990	2983	2980	2975	$\nu_{as}(CH_3)$
		2942		2935	2930	$\nu(CH)$
		2886	2875	2899	2899	$\nu_s(CH_3)$
2084	2069		2038		2020	$2\nu(V=O)$
		1457, 1471	1473, 1460	1451, 1465	1452, 1464	$\delta_{as}(CH_3)$
		1376, 1391	1369, 1345	1368, 1383	1366, 1379	$\delta_s(CH_3)$
		1328		1335	1326	$\delta(CH\text{-}O)$
		1137		1119		$\nu(C\text{-}O)$
1043	1043	1029 (cis)		1015 (C_s)	1012	$\nu(V=O)$
	960		960		960	$\nu(V\text{-}O\text{-}Si)$

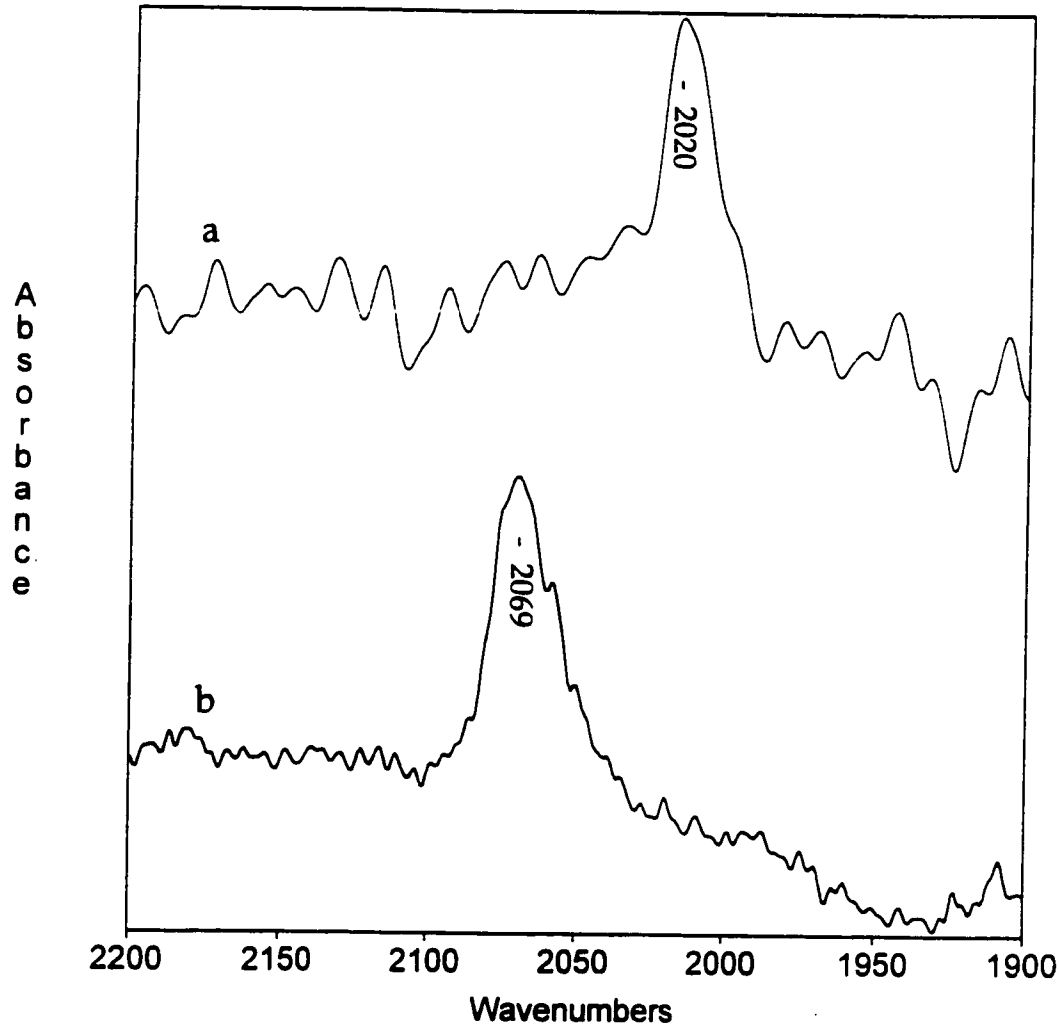

Figure 3.5 Difference infrared spectra of the ν(V=O) overtone region of a self-supporting disk of silica-500; (a) ≡SiOVO(O^iPr)$_2$, (b) ≡SiOVOCl_2.

to the degree of hydration of the surface.[5,27] However, interpretation of vibrational spectra in this region is complicated for several reasons. First, other vibrations such as ν(V-O-Si) modes and ν(V-O-V) modes of polymeric species are expected at similar frequencies. Second, oxides such as silica are only partially transparant to IR radiation in this region. Raman spectroscopy has been used to complement infrared spectroscopy of surface species since the oxides themselves are not strong Raman scatterers, however, Raman intensities of surface bound species are weak and vibrations of bonds with partial ionic character are usually not observed.[11]

In the spectral window region between 1000 and 850 cm^{-1}, the reaction of $O=V(O^iPr)_3$ with a self supporting disk of silica-500 gives rise to two new bands at 980 and 960 cm^{-1}, which can be seen clearly after subtraction of the silica background spectrum, Figure 3.6a. Just above 980 cm^{-1}, a negative feature is assigned to the disappearance of the ν(Si-O) mode of ≡SiOH,[17] which decreases in intensity relative to the spectrum of the unmodified silica surface during the reaction with $O=VX_3$ which consumes the surface hydroxyl groups. No bands can be observed from 1000-1200 cm^{-1} due to the intense absorption of silica. The reaction of $O=VCl_3$ with silica-500 to give $\equiv SiOVOCl_2$ also yields a broad band centered at 958 cm^{-1}, Figure 3.6b, but there is no band at 980 cm^{-1}. Only the negative feature caused by the disappearance of surface hydroxyl groups is seen.

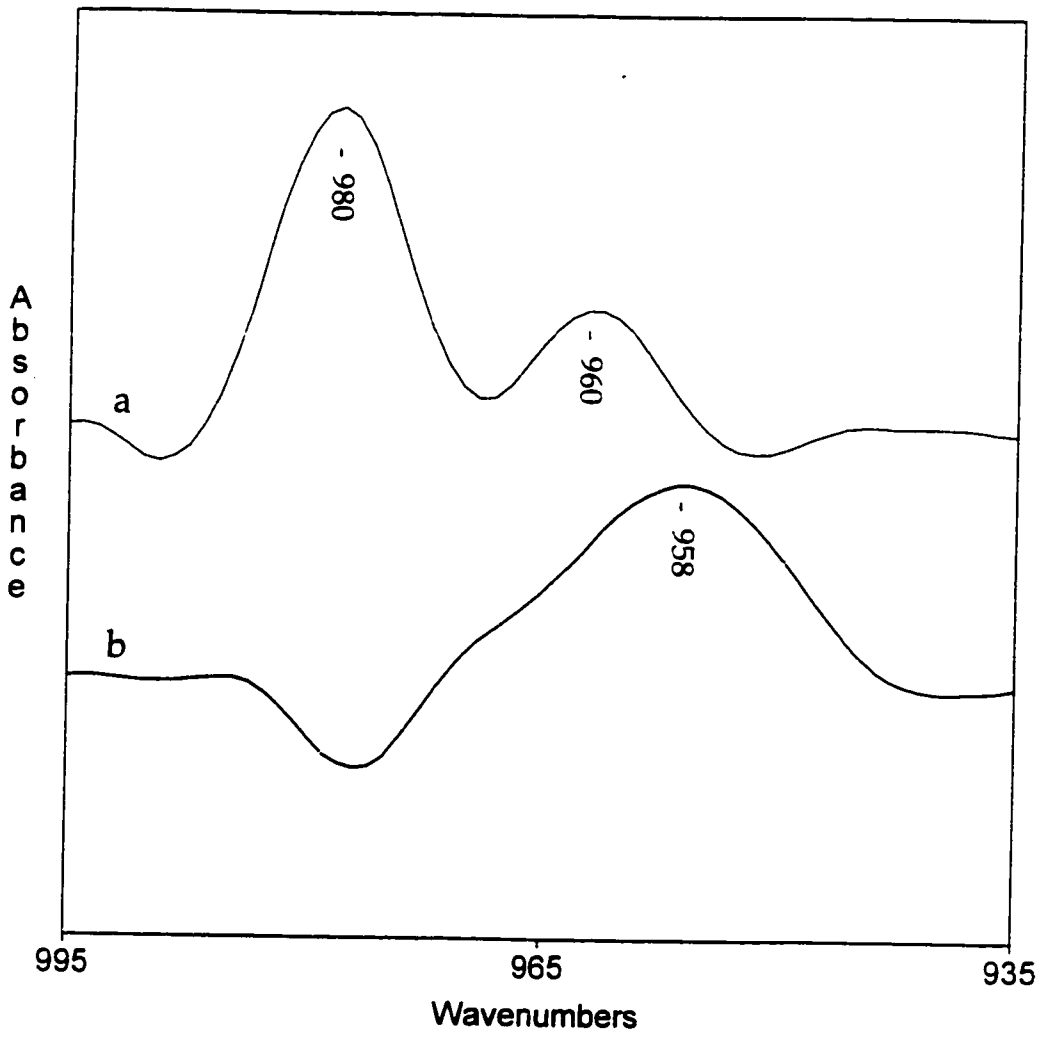

Figure 3.6 Difference infrared spectra of the spectral "window" region of a self-supporting disk of silica-500; (a) ≡SiOVO(O^iPr)$_2$, (b) ≡SiOVOCl_2.

The band at ca. 960 cm^{-1}, which is observed in both spectra, is assigned (see section 3.5.2) to the ν(Si-O) vibration of the SiOV unit which both ≡SiOVO(O^iPr)$_2$ and ≡SiOVOCl_2 must have in common, by comparison to the frequency of the ν(Ti-O-Si) mode of oxide-supported titanium complexes, at 960 cm^{-1}.[28] The band at 980 cm^{-1} could be assigned to the ν(V=O) mode of ≡SiOVO(O^iPr)$_2$, however, the overtone region shows a band at 2020 cm^{-1}, Figure 3.5a, which is more than twice the fundamental frequency of the 980 cm^{-1} band. The latter is therefore probably a vibration of the isopropyl ligands.[29] The expected ν(V=O) modes of ≡SiOVO(O^iPr)$_2$ and ≡SiOVCl_2 are completely masked by the intense absorbance of the silica above 1000 cm^{-1}. For more complete vibrational information in this region, we were obliged to use the thin film technique, described below.

3.4.3 The region 1200-1000 cm^{-1}

For reasons described above, this spectral region is inaccessible using self-supporting disks of silica. However, the thin film technique, used in conjunction with careful spectral subtraction, renders this region partially transparent.[17] Thin film spectra of ≡SiOVO(O^iPr)$_2$ and ≡SiOVCl_2 on silica-450 each contain the band at ca. 960 cm^{-1} previously observed on self-supporting disks, and the negative feature near 980 cm^{-1} due to disappearance of the (≡Si-OH) mode.

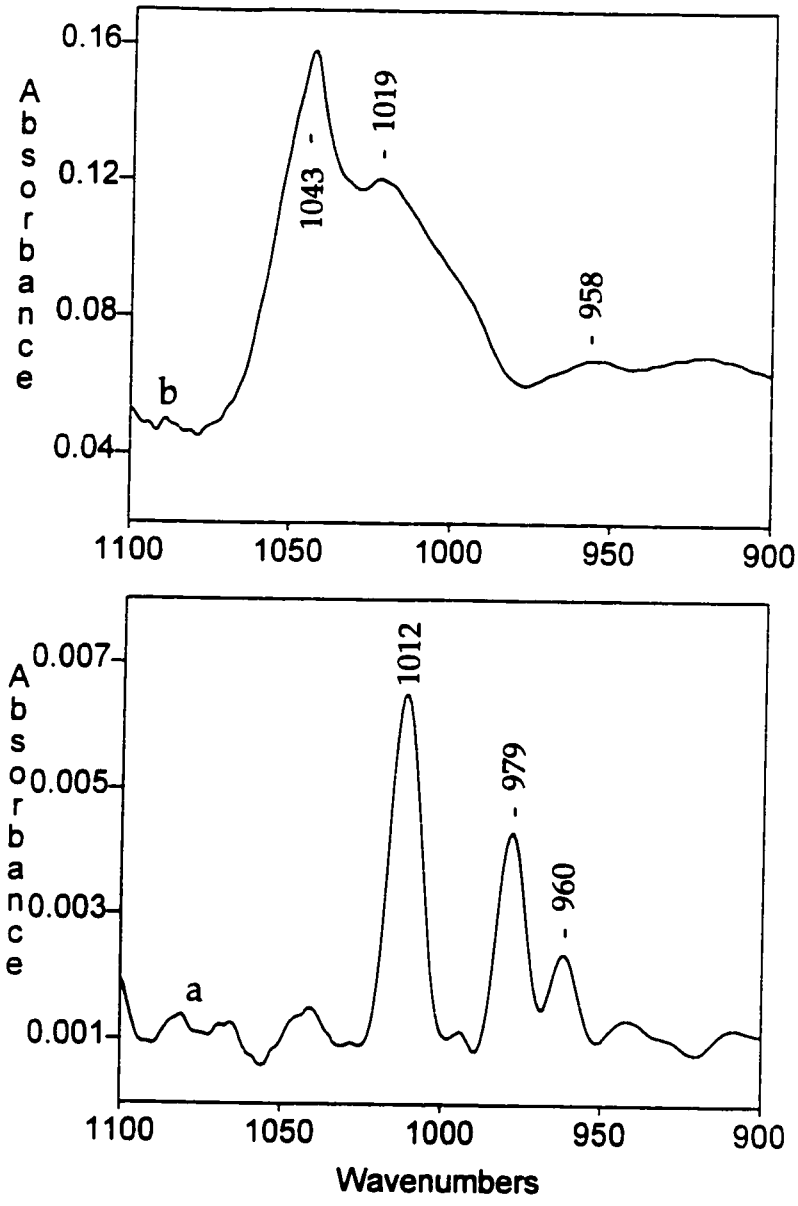

Figure 3.7 Transmission infrared spectra of silica-450 thin films: (a) difference spectrum of ≡SiOVO(O^{i}Pr)$_2$; (b) difference spectrum of ≡SiOVOCl$_2$.

Two additional bands are observed in each spectrum: for ≡SiOVO(O^{i}Pr)$_2$, they appear at 1012 and 979 cm^{-1}, Figure 3.7a, while for ≡SiOVOCl$_2$, they appear at 1043 and 1019 cm^{-1}, Figure 3.7b. The observation of two bands in the region of terminal ν(V=O) vibrations could be interpreted as evidence for a dioxo species. Although a species (≡SiO)VO$_2$ would have such a spectrum, its V=O modes should be significantly lower in frequency than those observed here.[30] Furthermore, its existence is not consistent with the retention of two V-X bonds, as shown by ^{51}V NMR spectroscopy and quantitative analysis.

A second possible explanation for the presence of two ν(V=O) bands is the existence of rotational isomers:

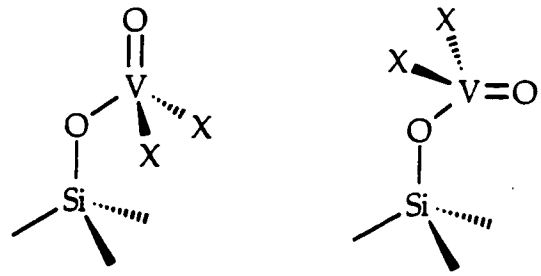

trans cis

The molecular mixed chloroalkoxovanadium(V) complexes have been reported to exhibit this kind of isomerism in their infrared spectra.[31] However, if this explanation is correct, it is curious that only one overtone 2ν(V=O) is observed in the spectra of our surface species. Other possible

explanations for the second band include an artifact of spectral subtraction or a silica surface mode.

3.5 ^{18}O-labelling of ≡SiOVOX$_2$

To further elucidate the assignment of bands in this spectral region, we performed several isotope labelling experiments. Our approach, using molecular precursors to graft vanadium to silica, allows specific oxygen atoms of the surface species to be labelled.

3.5.1 Reaction of V^{18}OCl$_3$ with silica

The reaction of V^{18}OCl$_3$ with silica-500 causes the 2ν(V=O) overtone to appear at 1970 cm^{-1}, Figure 3.8, while the position of the ν(V-O-Si) mode at 959 cm^{-1} remains unchanged relative to the unlabelled surface species, Figure 3.6b. These observations are consistent with the formation of ≡SiOV^{18}OCl$_2$, where only the terminal oxygen of the surface complex is labelled, as in equation 3.4.

$$\equiv SiOH + V^{18}OCl_3 \rightarrow \equiv SiOV^{18}OCl_2 + HCl \qquad (3.4)$$

The isotope shift of the overtone frequency, 98 cm^{-1}, is approximately double the shift expected for the fundamental mode. By comparison, the ^{16}O-^{18}O isotope shift for VOCl$_{3(g)}$ is 46 cm^{-1}.

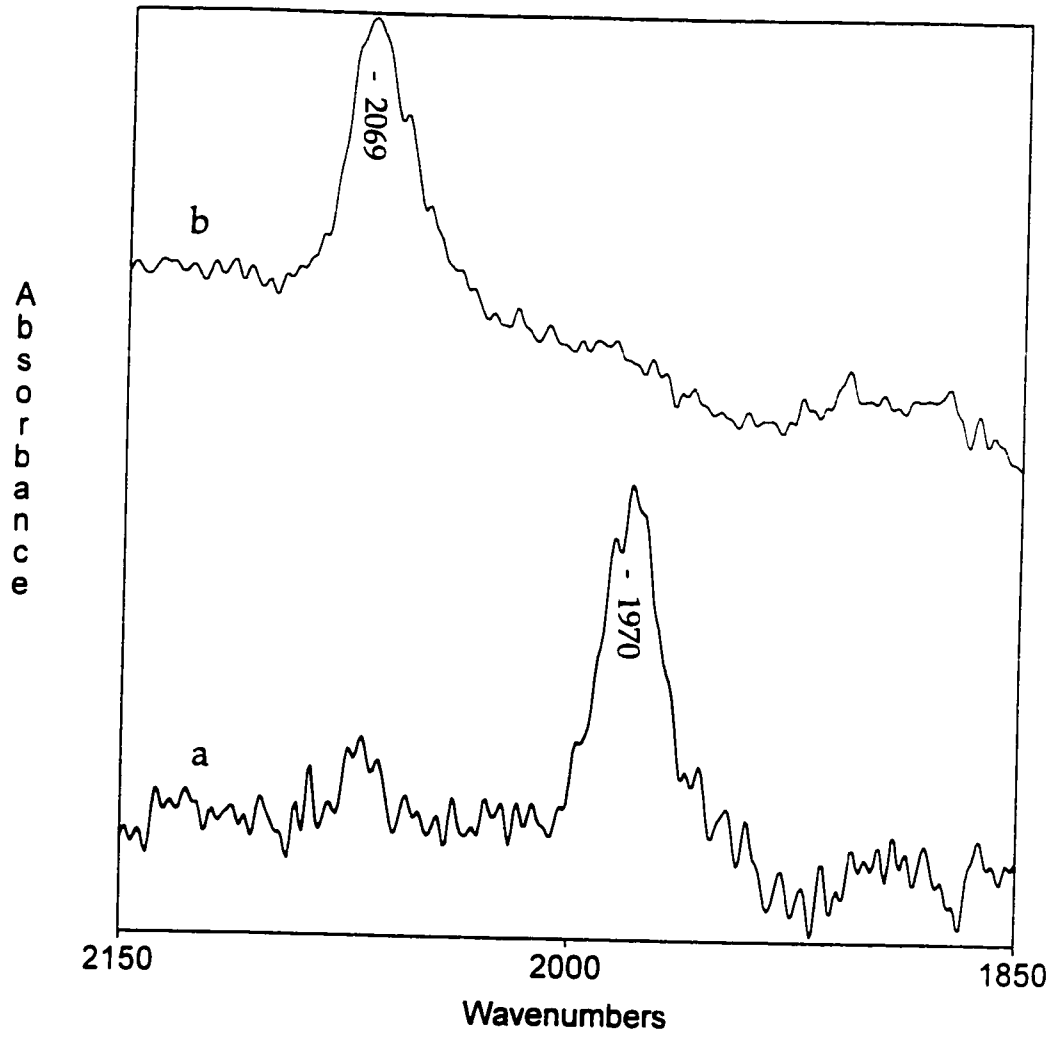

Figure 3.8 Difference infrared spectra of the ν(V=O) overtone region of a self-supporting disk of silica-500: (a) ≡SiOV^{18}OCl$_2$, (b) ≡SiOVOCl$_2$.

The ν(V=O) fundamental and overtone of $V^{16}OCl_3$ at 1042 and 2077 cm^{-1} shift to 996 and 1984 cm^{-1}, respectively in $V^{18}OCl_3$. The predicted isotope shift for a V=O harmonic oscillator, based on a reduced masses calculation, is 45 cm^{-1}.

3.5.2 ^{18}O-labelling of the silica surface

Whereas the O-H stretching mode on unlabelled silica occurs at 3747 cm^{-1}, Figure 3.4a, when the oxygens of the hydroxyl groups are labelled with ^{18}O, the O-H stretching mode is observed at 3727 cm^{-1}, Figure 3.9.

The IR spectrum of the product of the reaction of $\equiv Si^{18}OH$ with $V^{16}OCl_3$ contains a weak band at 2068 cm^{-1}, previously observed in the reaction with unlabelled silica, and a medium-intensity band at 929 cm^{-1}, Figure 3.10. The latter is assigned to ν(V-^{18}O-Si), due to the formation of $\equiv Si^{18}OVOCl_2$, equation 3.5.

$$\equiv Si^{18}OH + VOCl_3 \rightarrow \equiv Si^{18}OVOCl_2 + HCl \qquad (3.5)$$

The isotope shift of the ν(V-O-Si) vibration due to ^{18}O substitution in the basal position is therefore 30 cm^{-1} (from 959 to 929 cm^{-1}), which is significantly less than the shift observed for the terminal oxo ligand (98/2 cm^{-1}, section 3.5.1). A similar analysis of the magnitudes of isotope shifts was used to assign stretching modes of terminal and bridging oxygens in oxide-supported molybdenum catalysts prepared by a traditional impregnation route.[13]

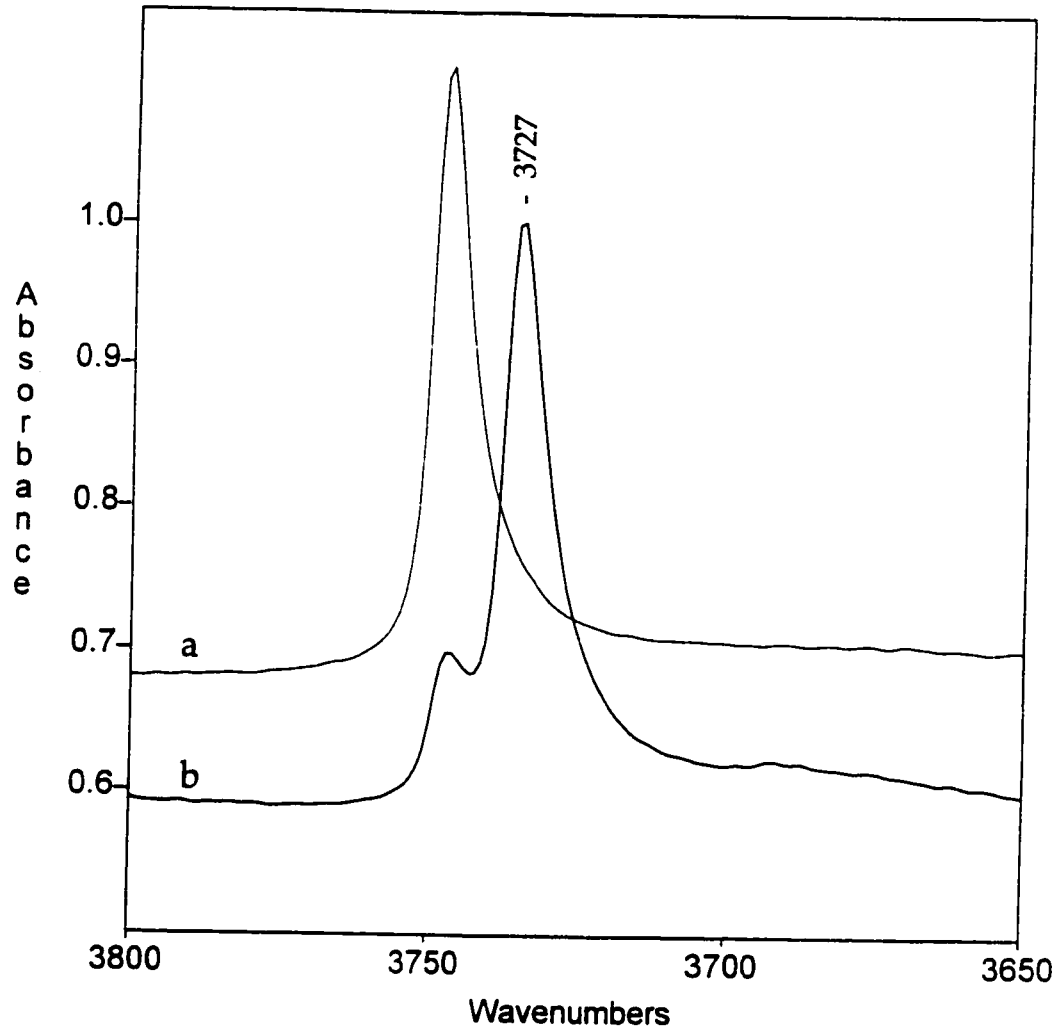

Figure 3.9 Transmission infrared spectra of the hydroxyl region of a self-supporting disk of silica-500; (a) unenriched; (b) ^{18}O enriched.

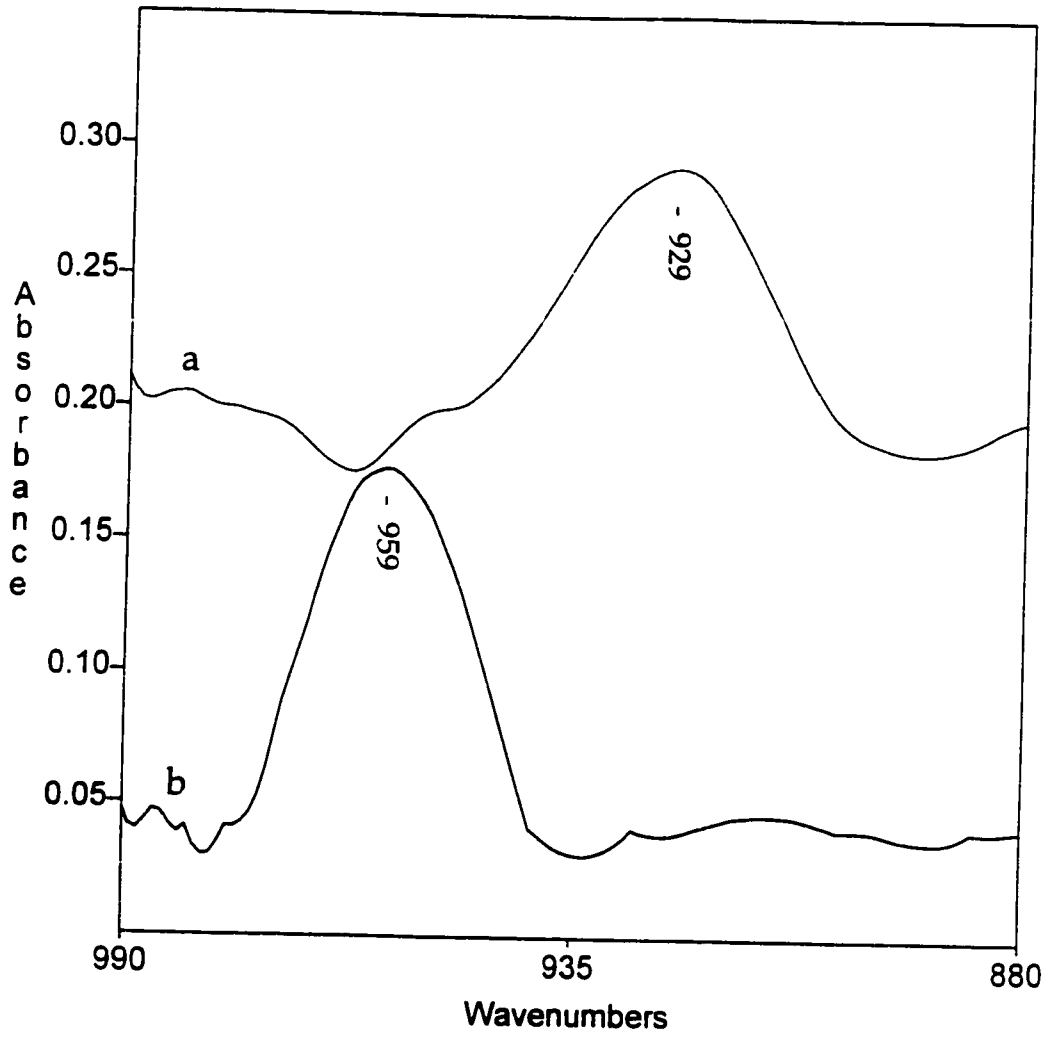

Figure 3.10 Difference infrared spectra of the spectral "window" region of a self-supporting disk of silica-500; (a) $\equiv Si^{18}OVOCl_2$, (b) $\equiv SiOVOCl_2$.

The absence of a shifted overtone mode for $\equiv Si^{18}OVOCl_2$ demonstrates that ^{18}O is not exchanged between the basal and terminal positions in the surface complex, during grafting.

The doubly-labelled surface complex $\equiv Si^{18}OV^{18}OCl_2$ was prepared by the reaction of $V^{18}OCl_3$ with an ^{18}O-exchanged silica thin film. Consistent with the observations on self-supporting disks, the ν(V=O) fundamental shifts by 43 cm^{-1} from 1043 cm^{-1} to 1000 cm^{-1}, as expected for the stretching mode of a terminal oxo ligand, while the ν(V-O-Si) mode shifts only 30 cm^{-1}, from 959 to 929 cm^{-1}. The IR frequencies of the selectively labelled complexes are summarized in Table 3.4.

3.6 Conclusions

The room temperature reactions of the molecular precursors $O=VX_3$ with the partially dehydroxylated surface of silica give a single chemisorbed product, $\equiv SiOVOX_2$, regardless of the density of surface hydroxyl groups. Our characterization of these materials by IR and ^{51}V MAS NMR demonstrates how these two techniques provide complementary information about the coordination sphere and electronic structure of surface species.

Table 3.4 Infrared frequency assignments (cm^{-1}) for silica-supported vanadium(V) chloro complexes

Surface complex	$\nu(V=O)^{a,b}$	$2\nu(V=O)^{b}$	$\nu(V-O-Si)$
$\equiv SiOVOCl_2$	1043	2068	959
$\equiv SiOV^{18}OCl_2$	994 (998)	1970 (1978)	959
$\equiv Si^{18}OVOCl_2$		2068	929
$\equiv Si^{18}OV^{18}OCl_2$	1000 (998)	1970 (1978)	929

[a] Observed only by the thin film technique, due to the strong absorbance of silica in this region.

[b] Values in parentheses are calculated frequencies, using isotope shifts from spectra of unlabelled $\equiv SiOVOCl_2$ for reduced masses calculations.

The NMR spectra show that the chemical shift is determined by the number of chlorine versus oxygen donor ligands in the first coordination sphere of vanadium. However, infrared spectroscopy shows that the replacement of a chloro ligand by a siloxo ligand has little effect on the frequency of $\nu(V=O)$. This finding suggests that the electron-withdrawing properties of the silica surface are similar to that of chloride.

Furthermore, using our technique of molecular precursors and gas-solid reactions, we have developed methods to prepare silica-supported vanadium complexes with ^{18}O isotope labels in nonequivalent ligand sites. There is no exchange or dilution of labels during grafting. This property can and will be exploited in Chapter 4 in our study of the mechanisms of surface reactions, for example, oxygen transfer, since we can follow the paths of individual ligands through stoichiometric and catalytic reaction cycles.

3.7 References

(1) Bond, G. C.; Tahir, S. F. *Appl. Catal.* **1991**, *71*, 1.

(2) Cullis, C. F.; Hucknall, D. J. In *Specialist Periodical Reports-Catalysis*; Royal Society of Chemistry: London, 1982; Vol. 5, p 273.

(3) Wainwright, M. S.; Foster, N. R. *Catal. Rev.* **1979**, *19*, 211.

(4) Bosch, H.; Janssen, F. *Catal. Today* **1988**, *2*, 369.

(5) Wachs, I. E. *J. Catal.* **1990**, *124*, 570-573.

(6) Busca, G. *Langmuir* **1986**, *2*, 577-582.

(7) Eckert, H.; Wachs, I. E. *J. Phys. Chem.* **1989**, *93*, 6796-6805.

(8) Tanaka, T.; Yamashita, H.; Tsuchitani, R.; Funabiki, T.; Yoshida, S. *J. Chem. Soc., Farad. Trans. I* **1988**, *84*, 2987.

(9) Das, N.; Eckert, H.; Hu, H.; Wachs, I.; Walzer, J.; Feher, F. *J. Phys. Chem.* **1993**, *97*, 8240-8243.

(10) Feher, F.; Walzer, J. *Inorg. Chem.* **1991**, *30*, 1689-1694.

(11) Went, G.; Oyama, T.; Bell, A. *J. Phys. Chem.* **1990**, *94*, 4240-4246.

(12) Oyama, S. T. *Res. Chem. Intermed.* **1991**, *15*, 165-182.

(13) Cornac, M.; Janin, A.; Lavalley, J. C. *Polyhedron* **1986**, *5*, 183-186.

(14) Ono, T.; Numata, H.; Ogata, N. *J. Mol. Catal. A: Chem.* **1996**, *105*, 31-37.

(15) Schrader, G. L.; Moser, T. P.; Lashier, M. E. In *Proc. 9th Int. Cong. Catal.*; CIC: Calgary, 1988, pp 1624-1631.

(16) Zhuravlev, L. T. *Langmuir* **1987**, *3*, 316.

(17) Morrow, B. A. *Stud. Surf. Sci. Catal.* **1990**, *57*, A161-A224.

(18) Mittal, R. K.; Mehrotra, R. C. *Z. Anorg. Allg. Chem.* **1964**, *332*, 189-196.

(19) Funk, H.; Weiss, W.; Zeising, M. *Z. Anorg. Allg. Chem.* **1958**, *296*, 36-45.

(20) Hanke, W.; Bienert, R.; Jerschkewitz, H.-G. *Z. Anorg. Allg. Chem.* **1975**, *414*, 109-129.

(21) Kijenski, J.; Baiker, A.; Glinski, M.; Dollenmeier, P.; Wokaun, A. *J. Catal.* **1986**, *101*, 1-11.

(22) Schraml-Marth, M.; Wokaun, A. *J. Chem. Soc., Faraday Trans.* **1991**, *87*, 2635-2446.

(23) Inumaru, K.; Okuhara, T.; Misono, M. *J. Phys. Chem.* **1991**, *95*, 4826-4832.

(24) Busca, G.; Centi, G.; Marchetti, L.; Trifiro, F. *Langmuir* **1986**, *2*, 568-577.

(25) Devore, D.; Lichtenhan, J.; Takusagawa, F.; Maatta, E. *J. Am. Chem. Soc.* **1987**, *109*, 7408-7416.

(26) Pauling, H.; Andrews, D. A.; Hindley, N. C. *Helv. Chim. Acta* **1976**, *59*, 1233-1243.

(27) Busca, G.; Lavalley, J.-C. *Spectrochim. Acta* **1986**, *42A*, 443-445.

(28) Smirnov, K. S.; van der Graaf, B. *Micropor. Mater.* **1996**, *7*, 133-138.

(29) Sheppard, N.; Simpson, D. M. *Quart. Rev. Chem. Soc.* **1953**, *7*, 19-55.

(30) Griffith, W. P.; Lesniak, P. J. B. *J. Chem. Soc. A* **1969**, 1066-1071.

(31) Witke, K.; Lachowicz, A.; Brüser, W.; Zeigan, D. *Z. Anorg. Allg. Chem.* **1980**, *465*, 193-203.

Chapter 4

Reactivity of Silica-supported Vanadium Complexes

4.1 Introduction

In homogeneous and heterogeneous catalysis by vanadium complexes, substrate binding by ligand substitution at vanadium is often suggested to precede oxidation. For example, the high selectivity of vanadium-containing catalysts for the epoxidation of allylic alcohols by *tert*-butyl hydroperoxide has been attributed to binding of the alcohol to vanadium.[1] Similarly, the activation of peroxide by vanadium has been attributed to the formation of mono- and diperoxovanadium(V) complexes.[2,3] However, although in molecular chemistry examples of vanadium peroxo complexes and other presumed catalytic intermediates have been isolated, the nature of the active site on heterogenous catalysts is much less well-understood. It has been proposed that both terminal oxygen and basal oxygens take part in oxidation reactions.[4]

Using the methods described in Chapter 3, we have prepared well-defined silica-supported vanadium complexes. In this chapter, we investigate their reactivity towards alcohols, alkyl hydroperoxides and other small molecules under stoichiometric and catalytic conditions. Our objective is to investigate whether the terminal or the basal oxygens, or both, take part in oxygen transfer reactions.

4.2 Reactions with alcohols

4.2.1 Reaction with allyl alcohol

In the presence of excess allyl alcohol, ≡SiOVO(O^{i}Pr)$_2$ undergoes ligand substitution of the isopropoxo ligands, eq 4.1.

$$\equiv SiOVO(O^iPr)_2 + n\ CH_2{=}CHCH_2OH \rightarrow$$

$$\equiv SiOVO(O^iPr)_{2-n}(OCH_2CH{=}CH_2)_n + n\ ^iPrOH \qquad (4.1)$$

$$n = 0, 1, 2$$

In the infrared spectrum of a silica disk of ≡SiOVO(O^{i}Pr)$_2$ treated at room temperature with excess allyl alcohol vapour then evacuated, new bands were observed at 3088, 3022 and 1643 cm^{-1}, assigned to the ν(C-H) and ν(C=C) vibrations of the allyl groups. These bands are stable under dynamic vacuum and indicate the presence of chemisorbed $CH_2{=}CHCH_2O$- groups. In the ^{13}C CP-MAS NMR spectrum, new resonances are observed at 64.7 (OCH_2), 113.9 (CH_2) and 136.4 (CH) ppm, Figure 4.1, in addition to resonances at 24 and 84.8 ppm previously assigned to isopropyl groups, Chapter 3. Therefore we conclude that the substitution reaction shown in equation 4.1 is an equilibrium where the extent of displacement of the isopropoxo ligands depends on the amount of allyl alcohol present. Not much useful information was obtained from the ^{51}V NMR spectrum since, as

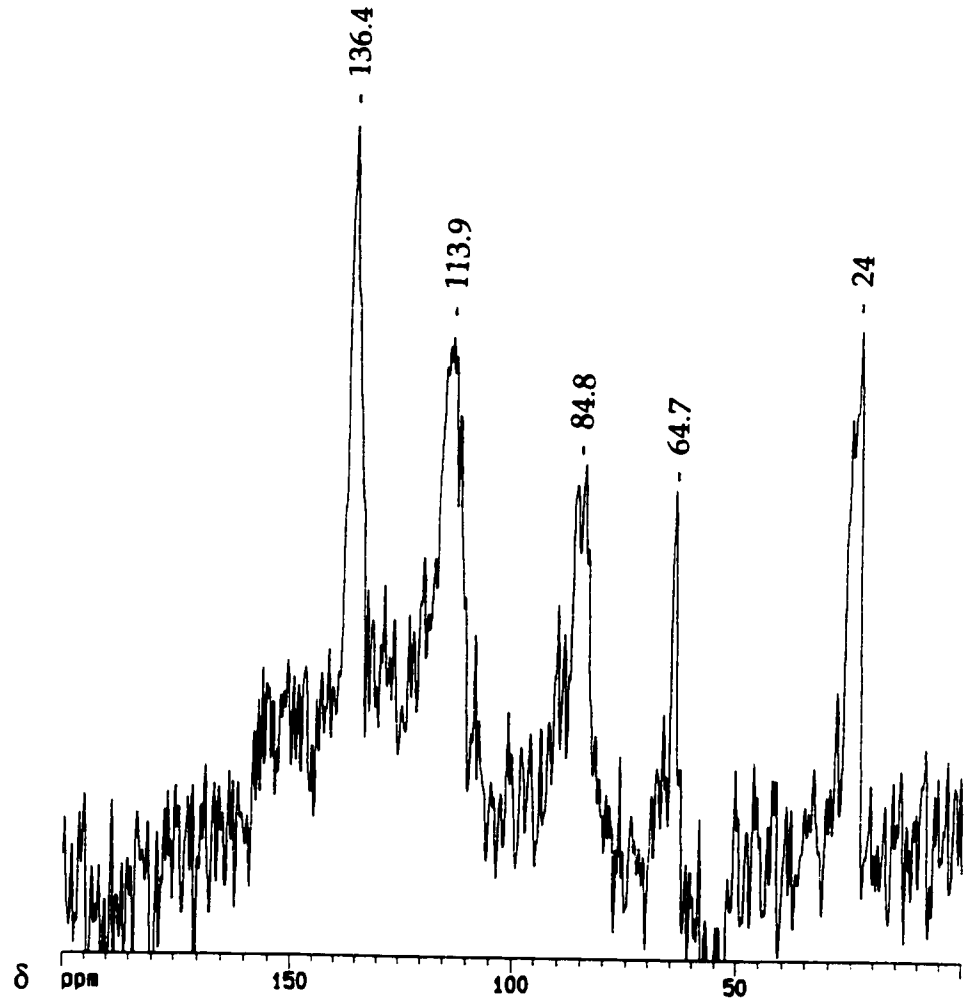

Figure 4.1 ^{13}C CP-MAS NMR spectrum of the product of reaction between $\equiv SiOVO(O^iPr)_2$ and $CH_2=CHCH_2OH$, spin rate 4000 Hz

described earlier (Chapter 3) substitution of isopropoxo and/or "siloxo" ligands by other oxygen donor ligands does not lead to a large change in the chemical shift. However, the ^{51}V NMR spectrum does show that the vanadium is still chemisorbed (not mobile), therefore excess alcohol does not cleave the Si-O-V unit. This result is expected based on the relative acidity of ≡SiOH versus ROH. This reaction will be discussed in more detail in the context of reactions of silica-supported vanadium complexes with *tert*-butyl hydroperoxide.

4.2.2 Reaction with ^{t}BuOH

The reaction of ≡SiOVO(O^iPr)$_2$ with ^{t}BuOH gave a similar result to the reaction with allyl alcohol. Peaks characteristic of ^{t}BuO groups were observed in the IR, 2980 and 2931 cm^{-1} ($\nu(CH_3)$), 1468 and 1460 cm^{-1} (δ_{as}), 1384 and 1368 cm^{-1} (δ_s) and 968 cm^{-1} (ρCH_3) as well as in the ^{13}C CP-MAS spectrum, Figure 4.2. As before, the ^{51}V NMR spectrum indicates that the Si-O-V unit was not cleaved but did not reveal the degree of ^{t}BuO/^{i}PrO ligand exchange. Therefore we decided to study the reactivity of ≡SiOVOCl_2 towards alcohols, since in these reactions, the displacement of chloro by alkoxo ligands should be more readily observed by spectroscopic techniques.

The reaction of ≡SiOVOCl_2 with excess *tert*-butyl alcohol liberates HCl and leads to the coordination of *tert*-butoxo groups, equation 4.2.

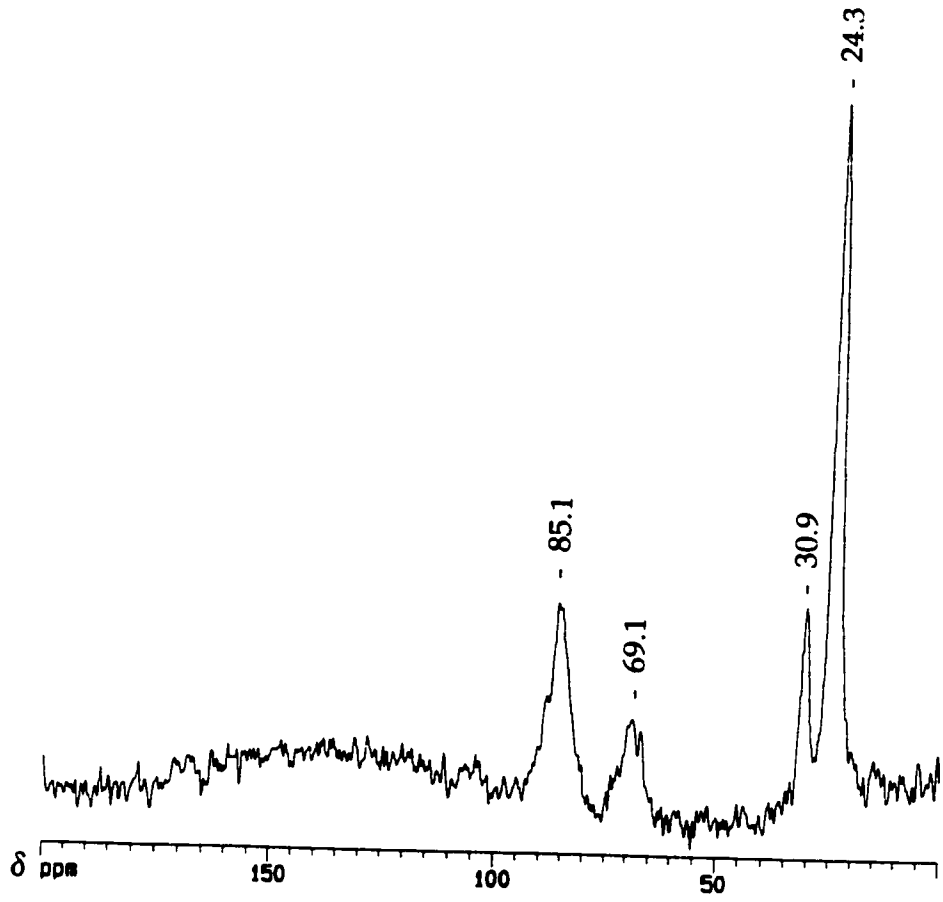

Figure 4.2 ^{13}C CP-MAS NMR spectrum of the product of reaction between $\equiv SiOVO(O^iPr)_2$ and ^tBuOH, spin rate 4000 Hz

$$\equiv SiOVOCl_2 + n\ {}^tBuOH \rightarrow \equiv SiOVOCl_{2-n}(O^tBu)_n + n\ HCl \qquad (4.2)$$

At room temperature the value of n was determined to be 0.95 by quantification of the amount of HCl liberated in the reaction by gas phase IR spectroscopy. The infrared spectrum of the surface species after reaction and evacuation of volatiles shows vibrations characteristic of *tert*-butyl groups, Table 3.3. A band at 960 cm^{-1}, assigned to the ν(V-O-Si) vibration of $\equiv SiOVOCl_2$, was still present in the product spectrum. No terminal V=O stretches were visible; however, the overtone 2ν(V=O) shifted from 2070 cm^{-1} to 2038 cm^{-1}, Figure 4.3. This is taken as evidence that the product of equation 4.2 does not have the composition $\equiv SiOVO(O^tBu)_2$ analogous to $\equiv SiOVO(O^iPr)_2$, since substitution of both chloro ligands by *tert*-butoxo groups is expected to lead to a ν(V=O) frequency near 1012 cm^{-1}, and a first overtone 2ν(V=O) near 2020 cm^{-1} (Chapter 3). Furthermore, the reaction of $\equiv SiOV^{18}OCl_2$ with ^tBuOH causes the overtone to shift from 1970 cm^{-1} to 1941 cm^{-1}, Figure 4.4. Exchange of terminal and basal oxygens can be ruled out, since there is no shift of the ν(V-O-Si) mode and only one 2ν(V=O) overtone was detected.

The formation of a mixed *tert*-butoxochloro surface species, $\equiv SiOVOCl(O^tBu)$, was confirmed by ^{51}V MAS NMR. The spectrum shows a

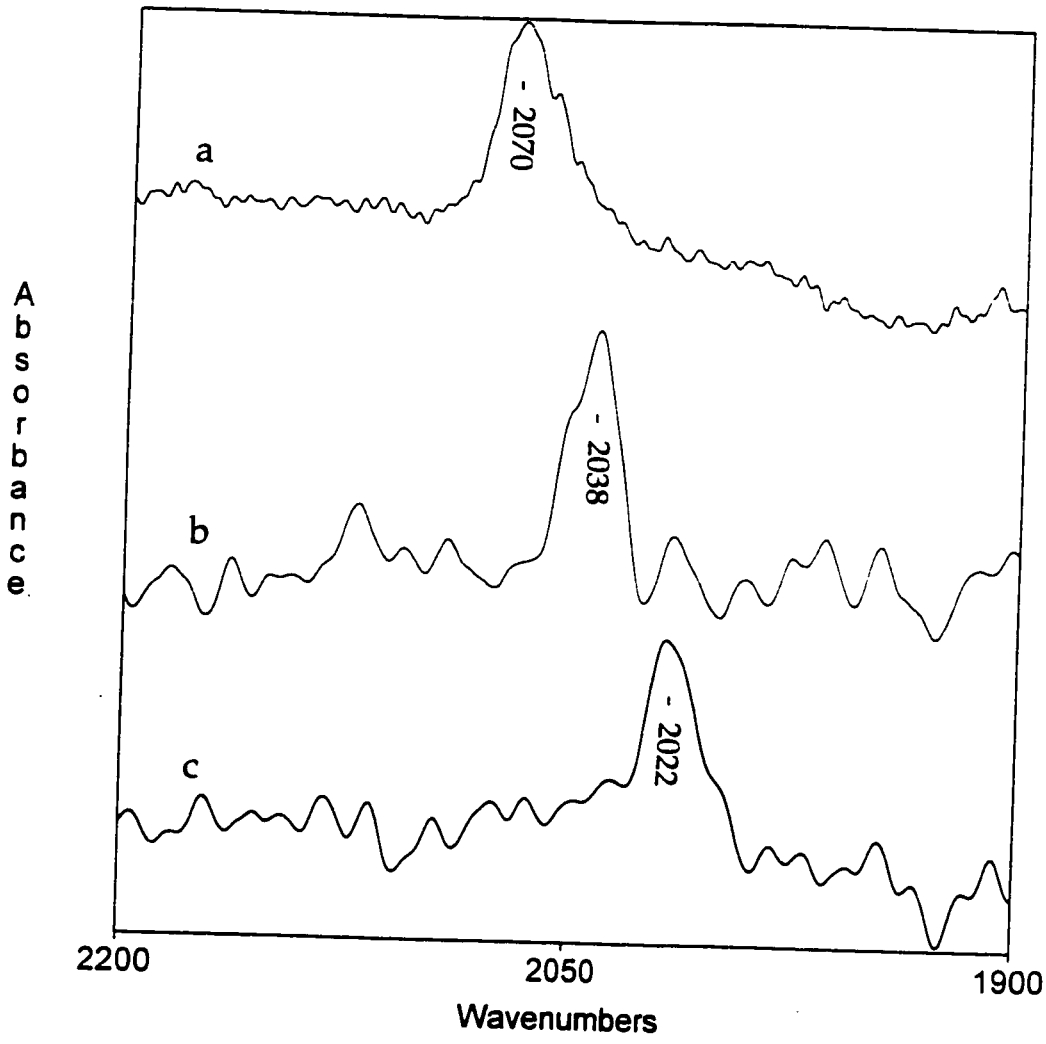

Figure 4.3 Difference infrared spectra of the 2 ν(V=O) region of a self-supporting disk of silica-500: (a) ≡SiOVOCl$_2$, (b) ≡SiOVOCl(O^{t}Bu), (c) ≡SiOVO(O^{t}Bu)$_2$.

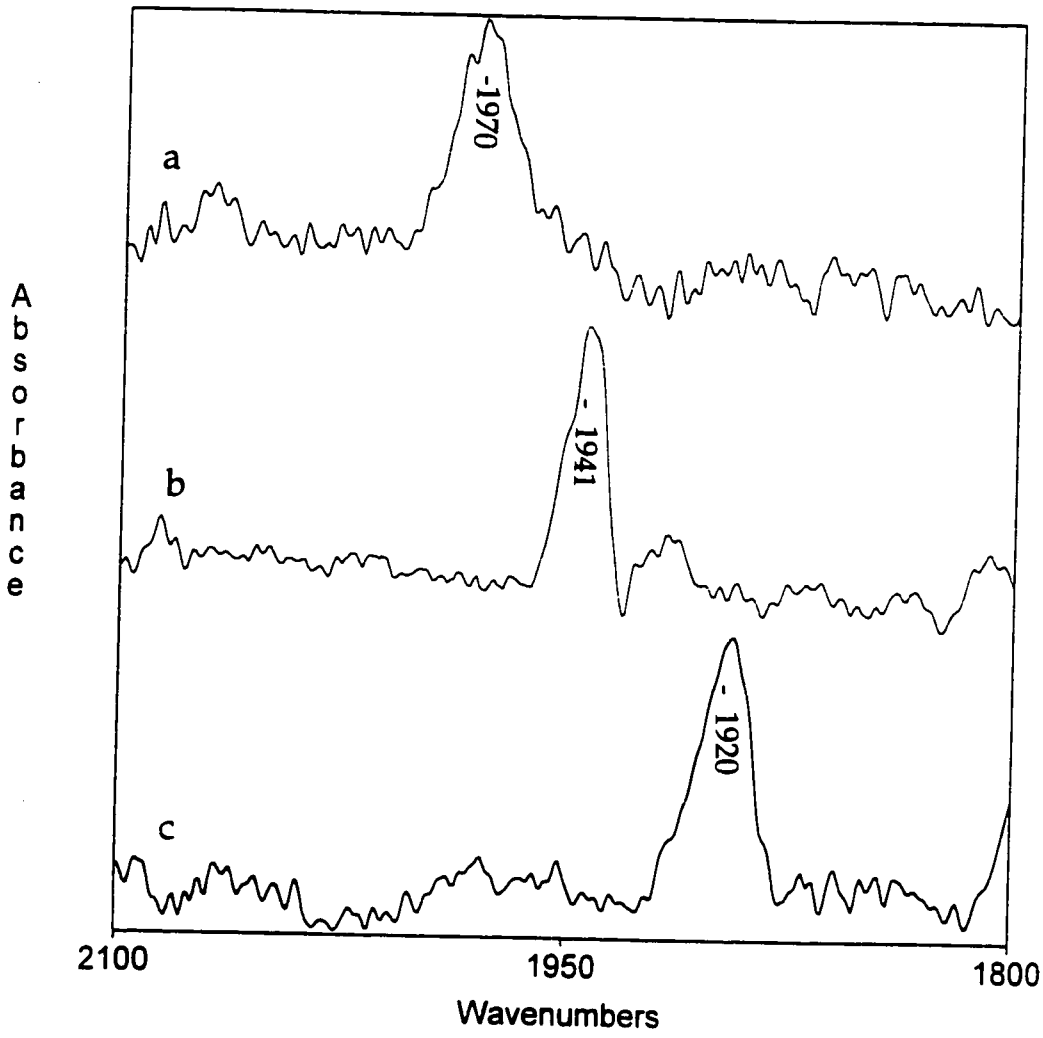

Figure 4.4 Difference infrared spectra of ν(V=O) overtone region of a self-supporting disk of silica-500: (a) ≡SiOV^{18}OCl$_2$, (b) ≡SiOV^{18}OCl(O^{t}Bu), (c) ≡SiOV^{18}O(O^{t}Bu)$_2$.

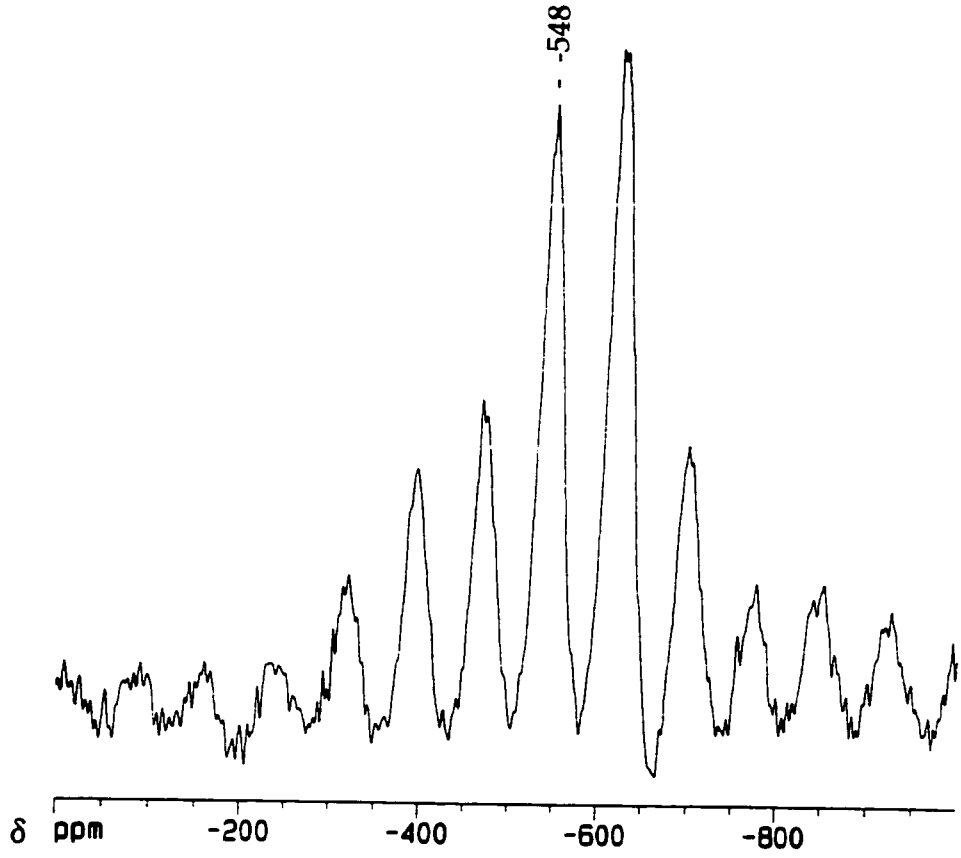

Figure 4.5 ^{51}V MAS NMR spectrum of ≡SiOVOCl(O^{t}Bu), spin rate 4000 Hz

single resonance at -548 ppm, Figure 4.5. Its chemical shift is in the region where monochlorobis(alkoxo)vanadium(V) molecular complexes appear, Table 3.2. The ^{13}C CP-MAS NMR spectrum revealed a single resonance at 29.5 ppm for the tert-butyl methyl groups; no signal for the quaternary carbon was observed. Partial substitution of the chloro ligands of $\equiv SiOVOCl_2$ is consistent with reports on the reactivity of $O=VCl_3$ with alcohols in which mixed chloroalkoxo complexes are formed.[5] Complete substitution does not occur even in the presence of a large excess of alcohol.[6]

The second chloride substitution can be effected by heating $\equiv SiOVOCl(O^tBu)$ to 60°C in the presence of excess *tert*-butyl alcohol vapour, eq. 4.3.

$$\equiv SiOVOCl(O^tBu) + {}^tBuOH \rightarrow \equiv SiOVO(O^tBu)_2 + HCl \qquad (4.3)$$

The product has $2\nu(V=^{16}O)$ at 2022 cm^{-1}, Figure 4.3, as expected from Table 3.2.

The observed isotope shift, $\Delta 2\nu(V=O)$, for $\equiv SiOV^{18}O(O^tBu)_2$ is 102 cm^{-1} to 1920 cm^{-1}, Figure 4.5. Ligand exchange reactions are depicted in Scheme 4.1.

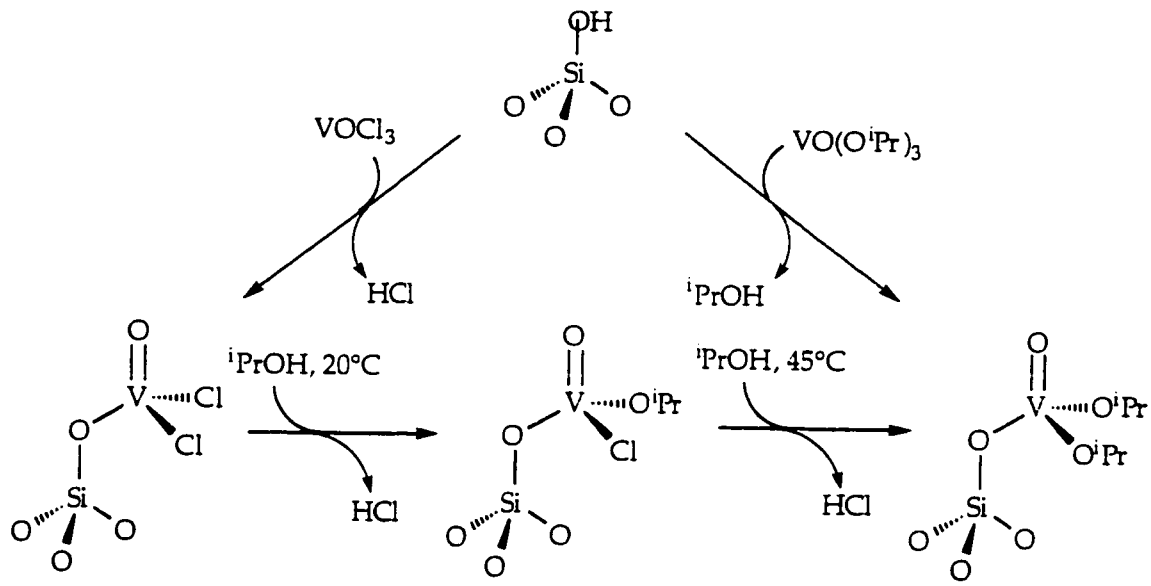

2ν(V=^{16}O) 2070	2038	2022
2ν(V=^{18}O) 1970	1941	1920

Scheme 4.1 Formation of silica-supported vanadium(V) complexes

4.2.3 Reaction with phenol

To attempt to substitute both chlorides on vanadium at once, we decided to attempt the exchange reaction with a more acidic alcohol than ^{t}BuOH, namely phenol. The addition of freshly distilled phenol to ≡SiOVOCl$_2$ led to immediate changes. The pellet changed from colorless to black and became completely opaque to visible light. By IR, the overtone vibration 2ν(V=O) disappeared and new bands appeared in the aromatic ν(CH) and ν(C=C) ring vibration regions. Furthermore, the peak in the ^{51}V NMR for ≡SiOVOCl$_2$ at -293 ppm disappeared indicating probable reduction of the vanadium.

We postulate that the result is probably the oxidative coupling of phenol, based on its solution chemistry. The oxidative coupling reaction is believed to occur by a rearrangement in a complex containing phenoxide residues and at least one metal center. Evidence in support of the existence of vanadium phenoxides has been previously reported,[7] unfortunately, our results are not sufficient to formulate a definitive mechanism for the oxidation of phenols. A possible mechanism may involve concerted coupling and electron transfer, Scheme 4.2.

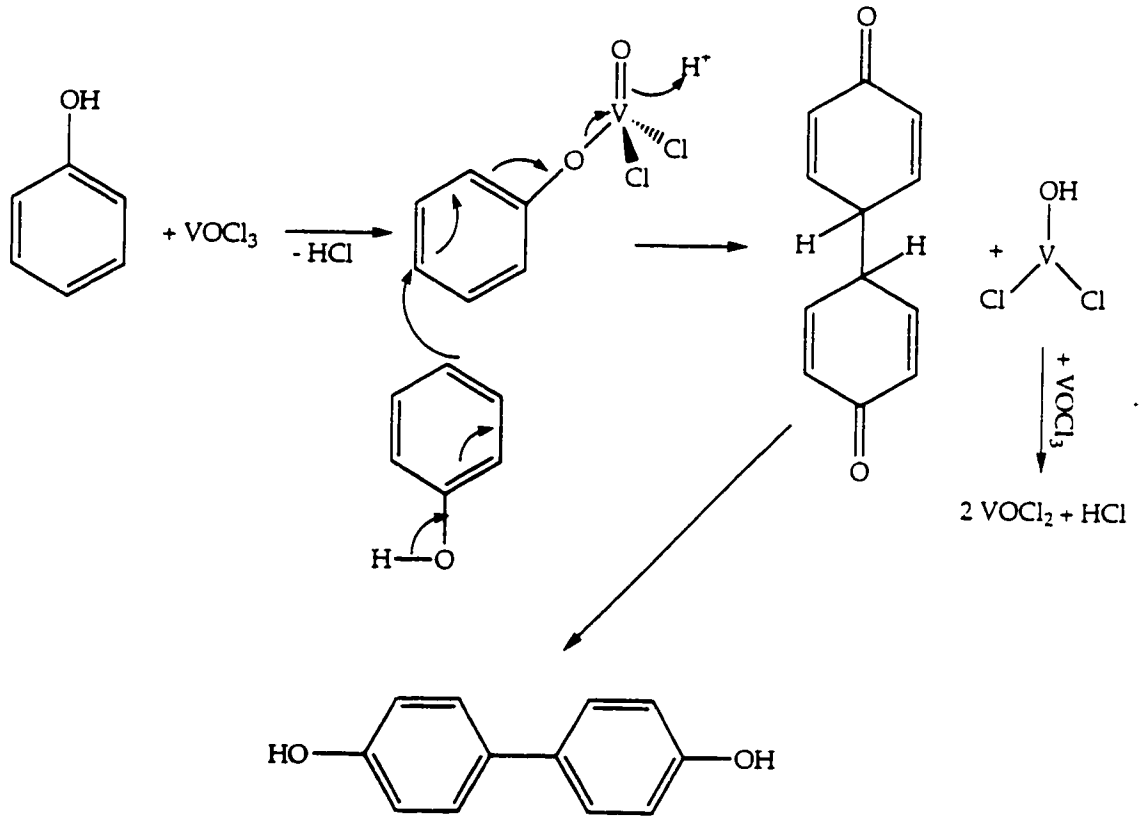

Scheme 4.2 Possible mechanism for the oxidative coupling of phenol

4.2.4 Rearrangement of α-acetylenic alcohol

α,β-Unsaturated carbonyl compounds are important intermediates in the manufacture of fragrances and vitamins. They have been obtained by reactions of α-acetylenic alcohols in the *Meyer-Schuster* and *Rupe* rearrangements, eq 4.5, which have been the subjects of a large number of reviews with some contradictory reports.[8-10]

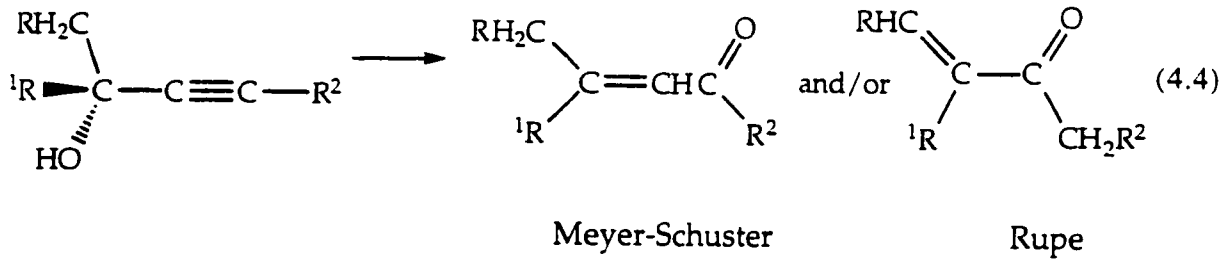

(4.4)

Meyer-Schuster Rupe

Isomerization of these alcohols is catalyzed by oxo-metal complexes, vanadate esters, $VO(OR)_3$, being particularly efficient, as depicted in Scheme 4.3.[9] We decided to test the reactivity of our silica-supported vanadium(V) complexes towards an α,β-unsaturated alcohol. Our method of preparing our silica-supported complexes and our site-specific oxygen-18 labelling capabilities should make it possible to see how the vanadium interacts with the alcohol.

We first attempted the reaction of 2-methyl-3-butyne-2-ol with $\equiv SiOVO(O^iPr)_2$.

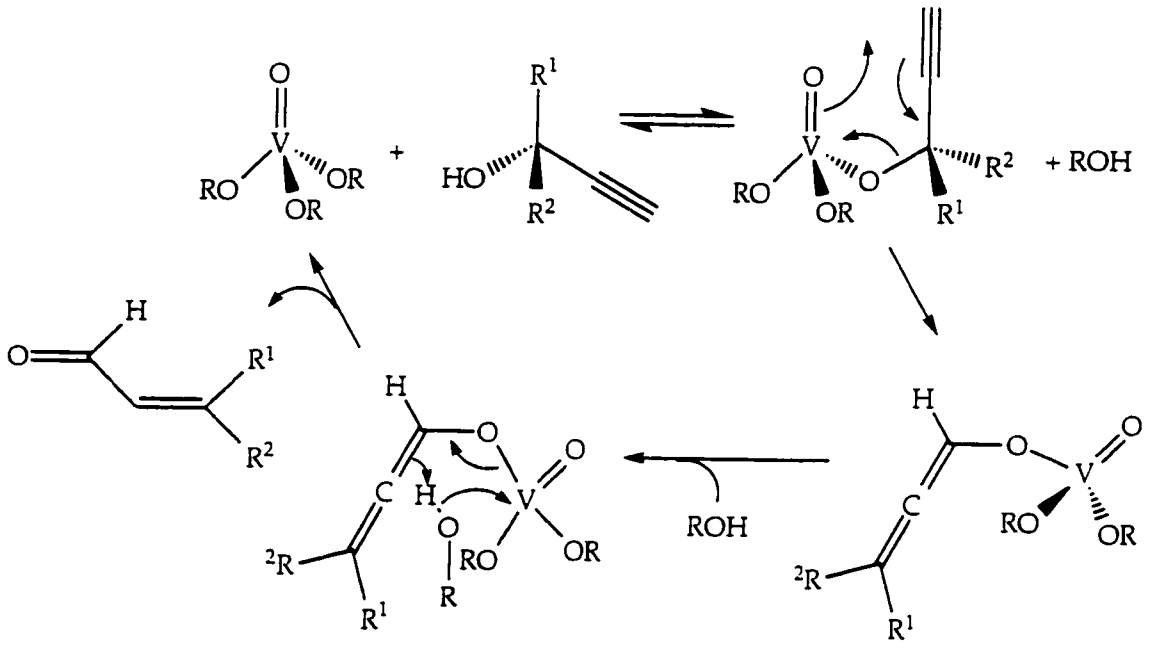

Scheme 4.3 Proposed mechanism for the rearrangement of acetylenic alcohols by vanadate esters.

Introduction of 2-methyl-3-butyne-2-ol to an IR cell containing a pellet of ≡SiOVO(O^iPr)$_2$ led to immediate changes in the infrared spectrum. New bands appeared at 3323 cm^{-1}, (ν(≡CH)), and 1470-1380 cm^{-1}, (δ(CH_3)), and the bands due to ν(CH) in the region 2985-2875 cm^{-1} shifted slightly. GC analysis of the gas phase showed only 2 compounds: 2-propanol and 2-methyl-3-butyne-2-ol. There was no evidence for a rearranged product. The pellet was then heated to 80°C for 2 hours.

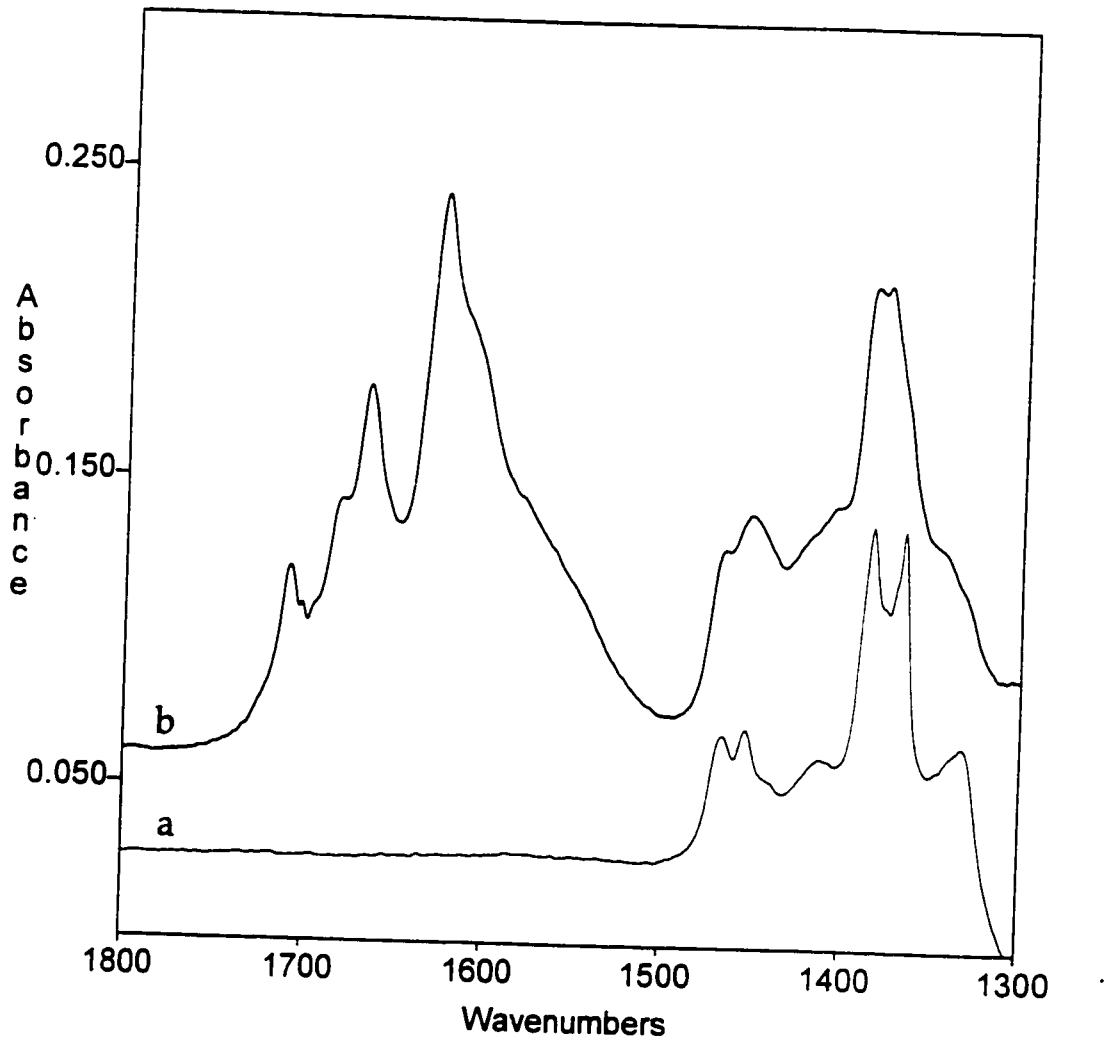

Figure 4.6 Difference infrared spectra of a self-supporting disk of (a) ≡SiOVO(O^iPr)$_2$; (b) after treatment with 2-methyl-3-butyne-2-ol at 80°C for two hours.

The resulting spectrum, Figure 4.6, shows 4 new bands, at 1709, 1682, 1665 and 1626 cm^{-1}, in the carbonyl stretching region. GC analysis of the gas phase showed a new product in trace amounts. It was suggested that there was not enough alcohol in the cell in order to liberate the new species from the surface, therefore, a large excess of 2-propanol was introduced into the IR cell. Upon condensation of all volatiles from the cell, the resulting IR spectrum was the same as that of $\equiv SiOVO(O^iPr)_2$. The IR spectrum of the volatile components contained 3 bands in the ca. 1710-1690 cm^{-1} region, however, upon GC analysis the only products identified were 2-propanol and 2-methyl-3-butyne-2-ol, and one other peak which could not be identified by GC .

The experiment was repeated using $\equiv SiOVOCl_2$. Interestingly, if the surface species $\equiv SiOVOCl_2$ was first reacted with ^iPrOH to give $\equiv SiOVO(O^iPr)_2$, followed by addition of 2-methyl-3-butyne-2-ol, the result was the same as described above. However, if 2-methyl-3-butyne-2-ol was added directly to $\equiv SiOVOCl_2$, the result was rather different. The presence of 2-methyl-3-butyne-2-ol vapour did not cause the liberation of HCl, however, upon condensing all volatiles from the cell, bands characteristic of 2-methyl-3-butyne-2-ol remained on the surface. The overtone, 2ν(V=O), at 2070 cm^{-1} was no longer visible. Upon heating at 60°C, two new bands appeared in the IR spectrum at 1620 and 1582 cm^{-1}, Figure 4.7, which increased in intensity with time. After heating for 16 hours a third small band appeared at 1763 cm^{-1}.

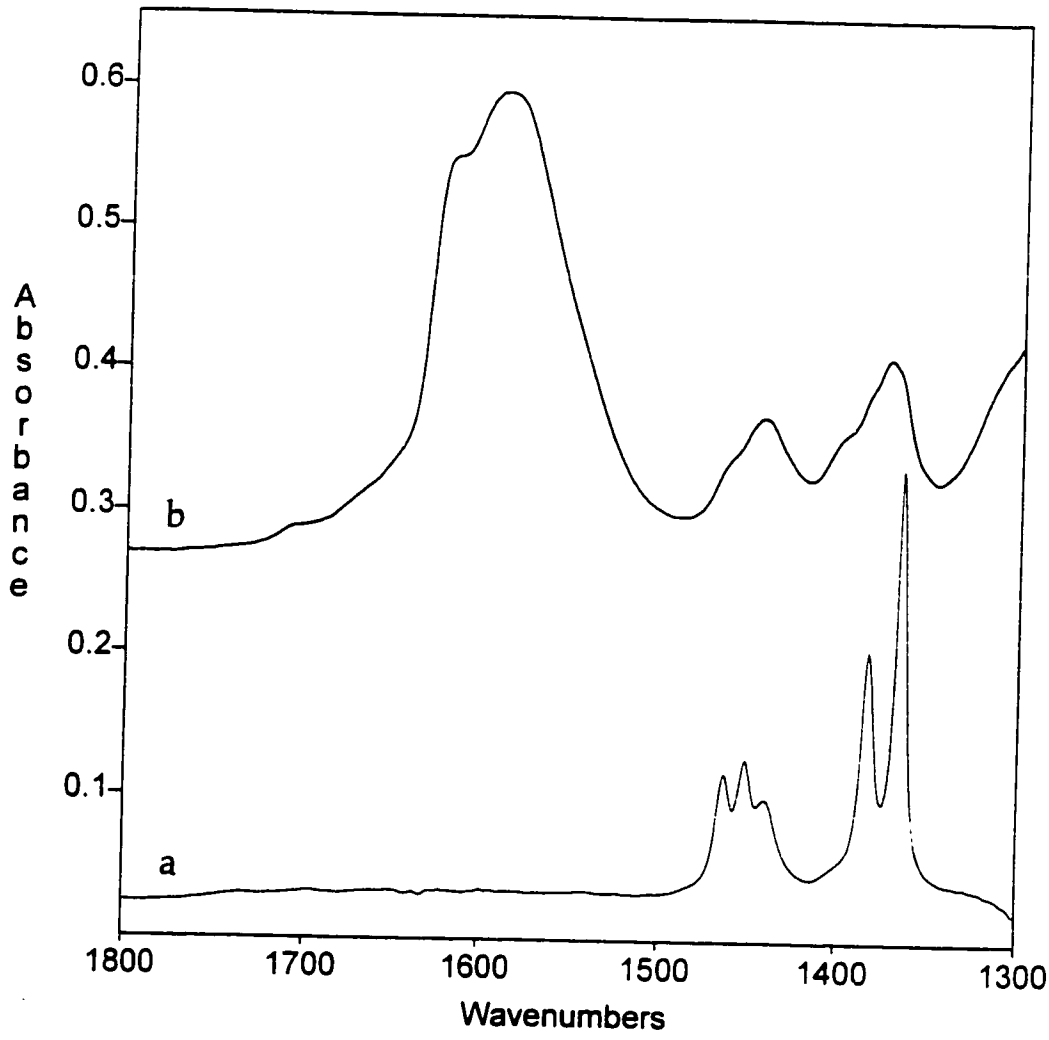

Figure 4.7 Difference infrared spectra of a self-supporting disk of ≡SiOVOCl$_2$ after treatment with 2-methyl-3-butyne-2-ol (a) at 25 °C; (b) at 60°C.

Subsequent reaction with 2-propanol resulted in a large decrease in the intensity of the bands at 1620 and 1582 cm^{-1} with liberation of a product with an IR band at 1622 cm^{-1} which again could not be identified by GC.

Since the rearrangement was neither as clean nor as efficient as we had hoped, we decided to investigate whether the reaction that was taking place at least involved the terminal V=O, which we could investigate by preparing $\equiv SiOV^{18}OCl_2$. Earlier we stated that the reaction of $\equiv SiOVO(O^iPr)_2$ with 2-methyl-3-butyne-2-ol resulted in the liberation of volatiles containing peaks in the IR spectrum at 1708, 1702 and 1696 cm^{-1}. If these bands are C=O modes, we predicted (using a reduced mass calculation) that the $C=^{18}O$ modes should appear at 1651, 1645 and 1640 cm^{-1}. The reaction of $\equiv SiOV^{18}O(O^iPr)_2$, 50% enriched in ^{18}O, with 2-methyl-3-butyne-2-ol again resulted in the liberation of 2-propanol and the chemisorption of some acetylenic alcohol. Upon heating and cleavage with excess 2-propanol, volatiles were liberated with bands in the ca. 1710-1690 cm^{-1} region with no peaks in the 1650-1640 cm^{-1} region.

We conclude that the accepted mechanism[8] for the rearrangement of acetylenic alcohols by $VO(OR)_3$ complexes has either been previously misinterpreted or the presence of the silica surface impedes the reaction in some way. It is possible that the fact that the vanadium is bound to the surface does not allow for rearrangement of the alcohol upon chemisorption.

4.3 Oxygen transfer reactions of silica-supported vanadium complexes

4.3.1 Reaction of isocyanates with surface complexes

The reaction of $\equiv SiOVOCl_2$ with a stoichiometric amount of ArNCO (Ar is phenyl or *p*-tolyl) at room temperature causes an immediate color change from colorless to purple and is accompanied by the liberation of CO_2, detected in the gas phase by its characteristic IR deformation mode at 667 cm^{-1}. These observations are consistent with the formation of a surface vanadium imido complex, $\equiv SiOV(NAr)Cl_2$, eq. 4.5, which has precedent in the chemistry of molecular transition metal complexes[11] and silica-supported metal oxo species.[12,13]

$$\equiv SiOVOCl_2 + ArNCO \rightarrow \equiv SiOV(NAr)Cl_2 + CO_2 \qquad (4.5)$$

The diffuse reflectance UV-vis spectrum of $\equiv SiOV(NAr)Cl_2$ consists of a broad band at 570 nm, Figure 4.8, compared to the spectrum of the purple molecular analogue $V(NC_6H_4CH_3)Cl_3$ with λ_{max} at 516 nm.[14] In the infrared, the overtone 2ν(V=O) of $\equiv SiOVOCl_2$ at 2068 cm^{-1} disappears while new vibrations appear in the regions 3100-2800 and 1600-1300 cm^{-1} due to arylimido ligands.

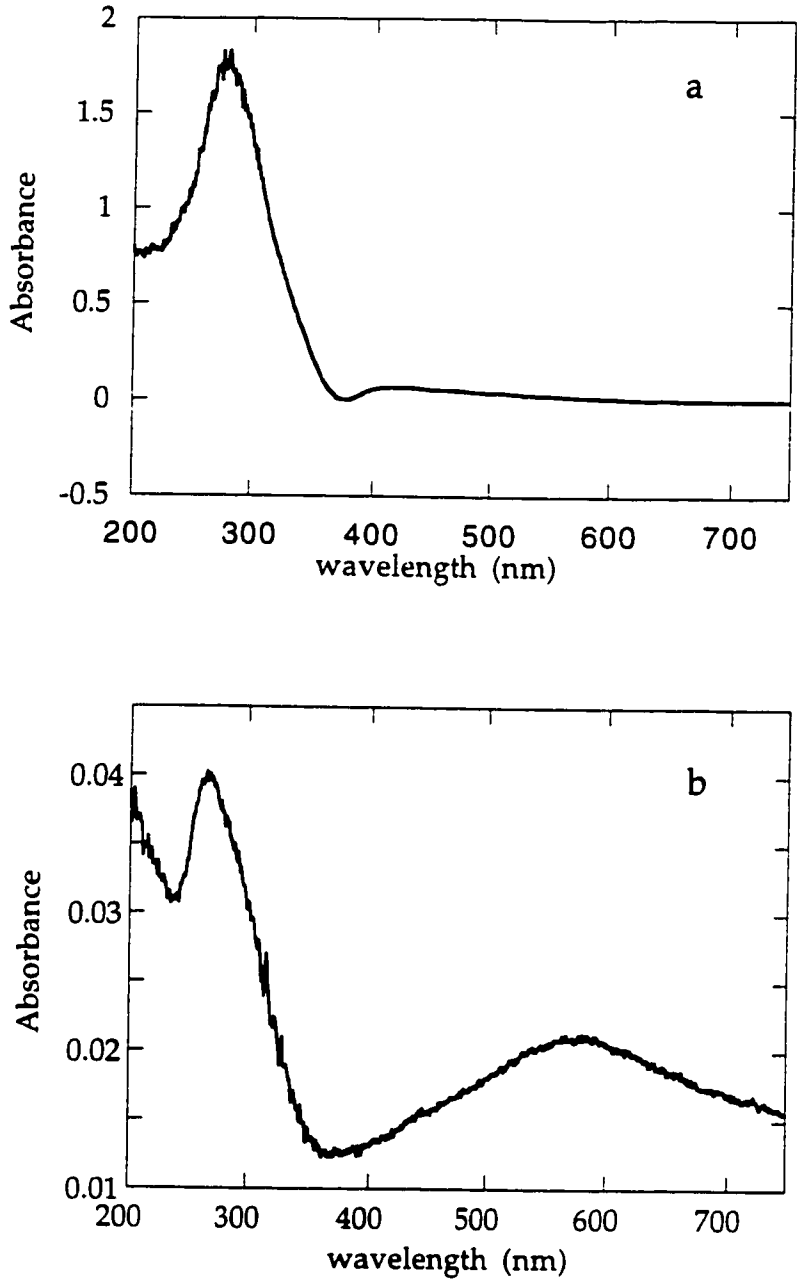

Figure 4.8 Diffuse reflectance UV-visible spectra of (a) ≡SiOVOCl$_2$ in vacuum; (b) after reaction with 1 equivalent *p*-tolylisocyanate followed by evacuation.

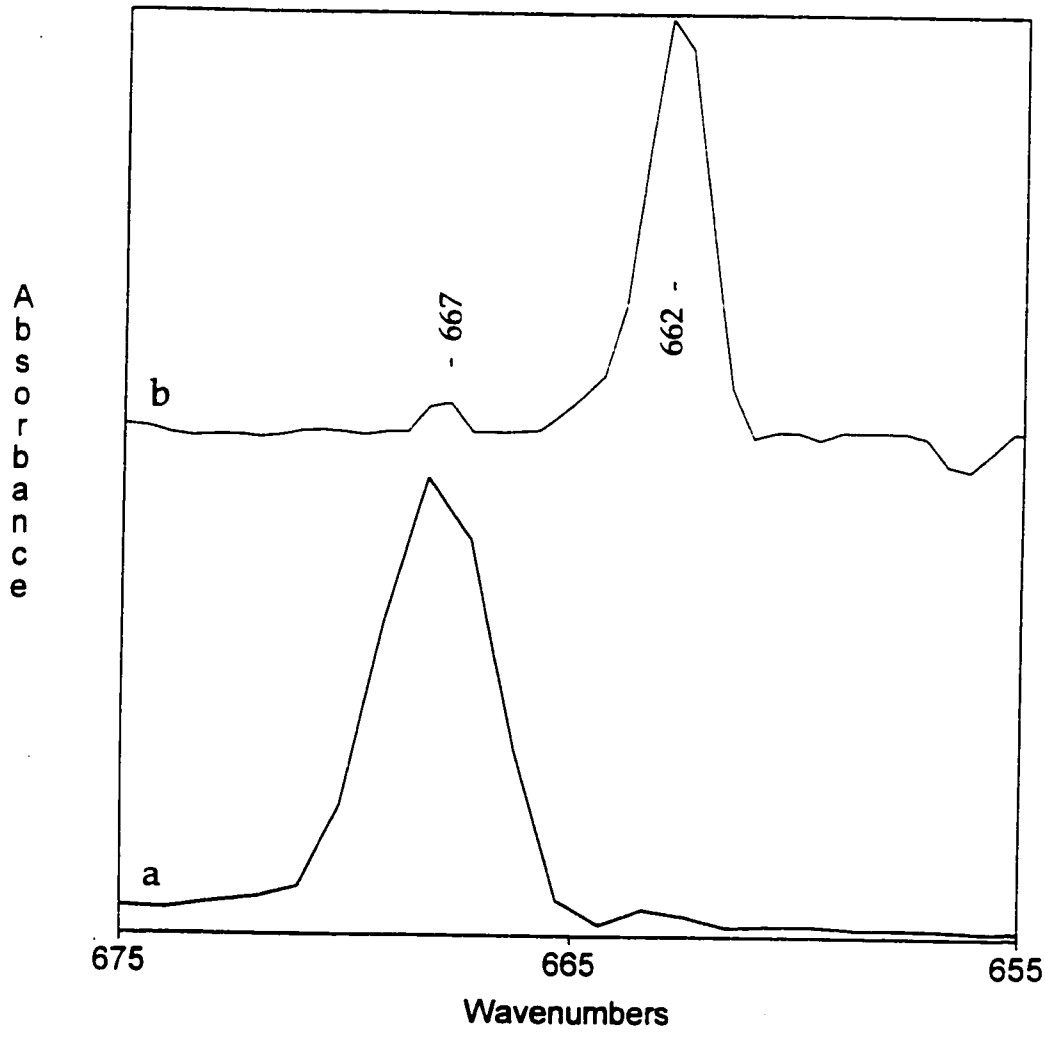

Figure 4.9 Gas phase infrared spectra of CO_2 in the deformation region during the reaction of ArNCO with (a) $\equiv SiOVOCl_2$; (b) $\equiv SiOV^{18}OCl_2$.

The isotopic composition of the CO_2 product is readily determined from its gas phase IR spectrum. In the reaction of ArNCO with $\equiv SiOVOCl_2$, $C^{16}O_2$ is the exclusive product, with a single sharp band at 667 cm^{-1}, Figure 4.9a. Reaction of ArNCO with $\equiv SiOV^{18}OCl_2$ leads to the formation of $C^{16}O^{18}O$, Figure 4.9b, for which the deformation mode is shifted to 662 cm^{-1}. A small band at 667 cm^{-1} is attributed to $C^{16}O_2$ derived from ca. 5% of $\equiv SiOV^{16}OCl_2$ due to incomplete labelling of the molecular precursor $V^{18}OCl_3$. There is no evidence for $C^{18}O_2$ (δ 658 cm^{-1}). The reaction of ArNCO with $\equiv Si^{18}OVOCl_2$ gives only $C^{16}O_2$. We conclude that CO_2 is formed in a concerted reaction without exchange of oxygen between terminal and basal positions at vanadium, or between isocyanates. A probable transition state for the reaction is shown in eq. 4.6.

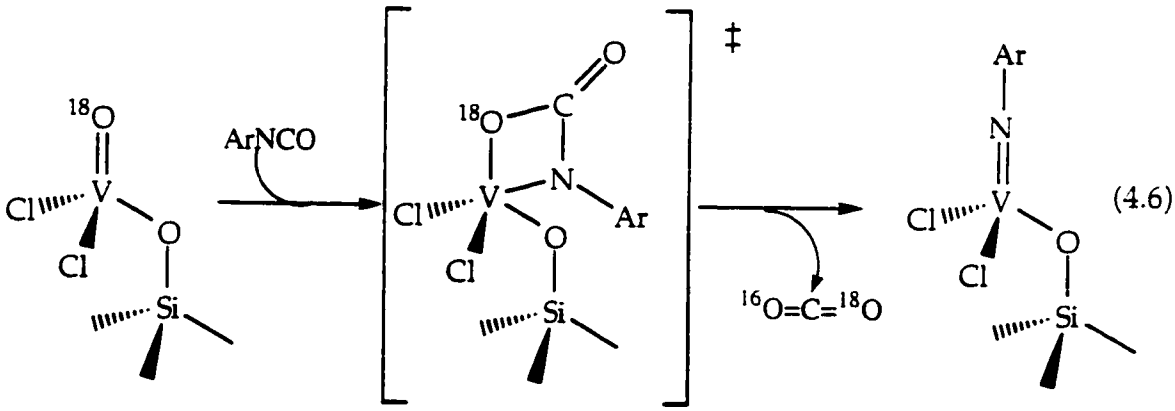

The addition of a second equivalent of ArNCO results in the partial reappearance of the 2ν(V=O) overtone at 2068 cm^{-1} as ≡$SiOVOCl_2$ is partially reformed, eq. 4.7.

$$\equiv SiOV(NAr)Cl_2 + ArNCO \rightarrow \equiv SiOVOCl_2 + [ArNCNAr] \qquad (4.7)$$

Attempts to extract and characterize the carbodiimide have thus far been unsuccessful.

The formation of CO_2 is catalytic at room temperature in the presence of excess ArNCO, as expected from the sum of eqs 4.6 and 4.8. These reactions are analogous to the catalytic condensation of isocyanates to carbodiimides by similar molecular vanadium(V) complexes, although $V(C_6H_4Me)Cl_3$ itself was reported to be inactive.[15]

4.3.2 Photochemical reaction with CO

There is no reaction between ≡$SiOVOCl_2$ and CO at room temperature in the absence of UV light. UV irradiation of ≡$SiOVOCl_2$ in the presence of CO leads to a color change from white to purple, and CO_2 is produced. For experiments involving UV irradiation all manipulations were done in quartz reactors. The diffuse reflectance UV-visible spectrum after reaction shows a broad band at ca. 450 nm, Figure 4.10, assigned to one or more d-d transitions of a reduced vanadium surface species.

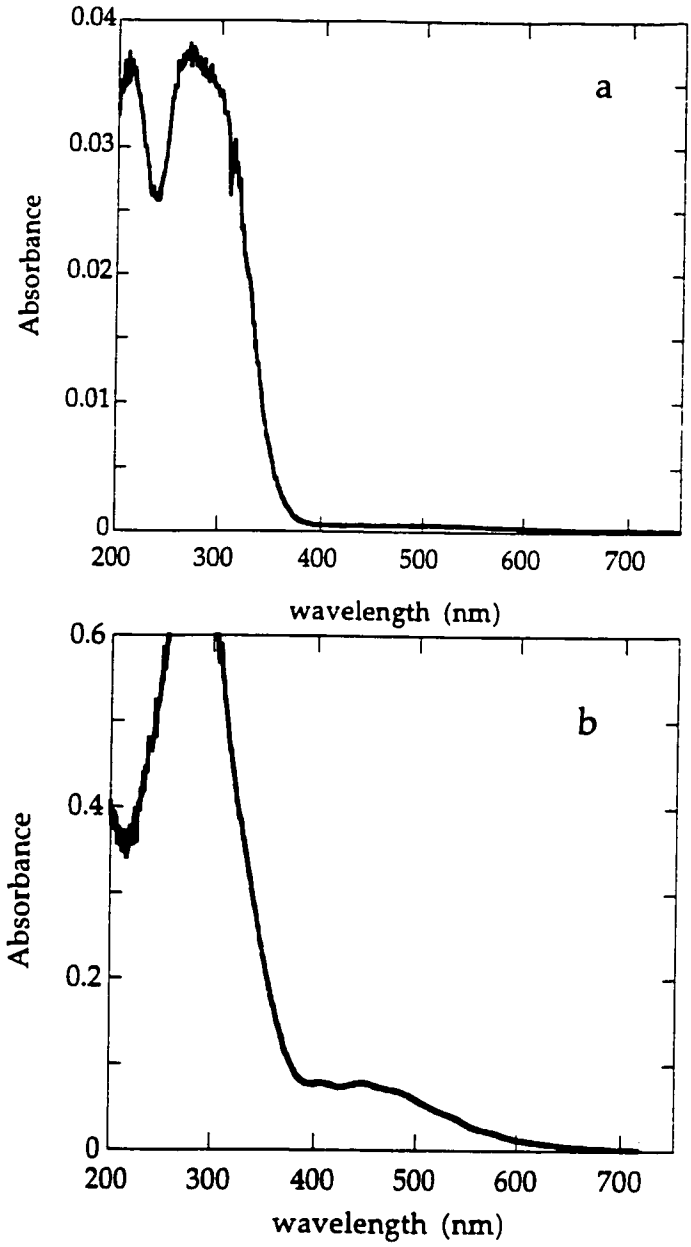

Figure 4.10 Diffuse reflectance UV-visible spectra of (a) $\equiv SiOVOCl_2$ in vacuum; (b) after 120 minutes of irradiation with broad band UV light in the presence of 5 Torr CO.

The 2ν(V=O) overtone in the infrared spectrum disappears. The CO_2 product is singly labelled as $C^{16}O^{18}O$ (ca. 95%) when $\equiv SiOV^{18}OCl_2$ (95% ^{18}O-enriched) is the reactant; with $\equiv Si^{18}OVOCl_2$ (85% ^{18}O-enriched), only $C^{16}O_2$ is produced. When $\equiv SiOV^{18}OCl_2$ oxidizes $C^{18}O$, $C^{18}O_2$ is produced, (deformation mode at 658 cm^{-1}) with a small amount of $C^{16}O^{18}O$ from incomplete labelling of the catalyst and the substrate. These results imply that one oxygen atom of the CO_2 product is derived from CO, while the other originates in the terminal oxo ligand of the vanadium surface complex. There is no evidence for exchange between surface oxygen atoms.

The mechanism of oxidation of CO over silica-supported vanadia catalysts has been proposed to be atom transfer from a photo-activated surface species, $[(\equiv SiO)_3V^{IV}(O^{\cdot-})]^{\cdot}$.[16] Charge transfer from oxygen to vanadium was suggested to render the oxo ligand more nucleophilic. Recently, it was suggested that photon absorption occurs at the HOMO located on the basal Si-O-V group.[17] Regardless of the nature of the excited state, it is clear from our results that oxygen transfer in these systems occur exclusively from the terminal oxo position.

Similar types of photochemical oxidations were attempted for NO and SO_2. To our surprise we found no evidence for the oxidation of these molecules by $\equiv SiOVOCl_2$.

4.3.2.1 Photocatalytic oxidation of CO

The photooxidation of CO by $\equiv SiOVOCl_2$ becomes catalytic in the presence of either O_2 or N_2O. When $\equiv SiOVOCl_2$ was reduced by CO, then reoxidized by $^{18}O_2$ in the presence of $C^{18}O$, $C^{18}O_2$ was formed as the major product (85% doubly labelled, with 15% $C^{16}O^{18}O$ from incomplete labelling of both reactants). When $\equiv Si^{18}OVOCl_2$ was used to catalyze the oxidation of CO by N_2O, $C^{16}O_2$ was the only isotopomer detected. We propose that reoxidation of reduced vanadium replaces oxygen exclusively in the terminal position. Possible mechanisms are shown in eqs. 4.8-4.11. By IR the 2ν(V=O) vibration disappears upon reduction with CO and reappears at the same position upon reoxidation, Figure 4.11.

$$\equiv SiOVOCl_2 + CO \rightarrow \equiv SiOVCl_2 + CO_2 \qquad (4.8)$$

$$\equiv SiOVCl_2 + N_2O \rightarrow \equiv SiOVOCl_2 + N_2 \qquad (4.9)$$

or

$$\equiv SiOVCl_2 + O_2 \rightarrow \equiv SiOV(O_2)Cl_2 \qquad (4.10)$$

$$\equiv SiOV(O_2)Cl_2 + CO \rightarrow \equiv SiOVOCl_2 + CO_2 \qquad (4.11)$$

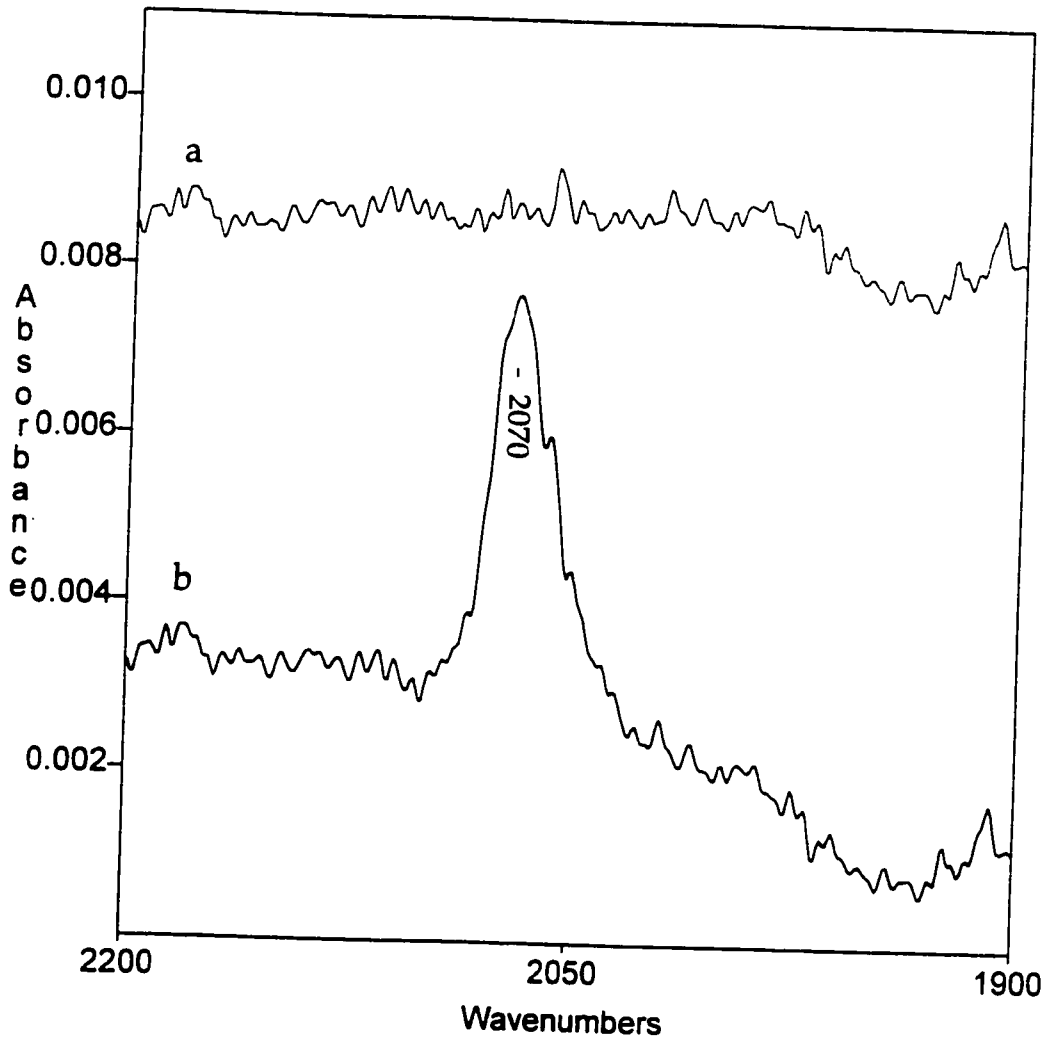

Figure 4.11 Difference infrared spectra of the 2ν(V=O) region of a self-supporting disk of ≡SiOVOCl$_2$ (a) after photo reduction with CO; (b) after reoxidation with N_2O

4.4 Reaction of ≡SiOVO(O^{i}Pr)$_2$ with ^{t}BuOOH

Displacement of alcohol (^{i}PrOH) from ≡SiOVO(O^{i}Pr)$_2$ by *tert*-butylhydroperoxide at room temperature was observed by IR and GC. The exchange reaction is summarized in eq. 4.12:

$$\equiv SiOVO(O^iPr)_2 + xs\ ^tBuOOH \rightarrow \equiv SiOVO(OO^tBu)_n(O^iPr)_{2-n} + n\ ^iPrOH \qquad (4.12)$$

When the reaction with ^{t}BuOOH was performed with deuterium-labelled ≡SiOVO(O^{i}Pr)$_2$, a decrease of 93% in the intensity of the ν(C-D) vibrations, indicating almost full substitution of the isopropoxo ligands by ^{t}butylperoxo ligands, was observed by IR, while ν(C-H) vibrations assigned to the *tert*-butylperoxo ligands appeared. The greater acidity of alkylhydroperoxides (pK_a ca. 12) relative to the alcohols (pK_a ca. 17)[18] drives the elimination of the alcohol. Due to the greater acidity of the alkylhydroperoxides compared to alcohols it was thought that they might cleave the SiO-V linkage. Even though the ν(SiO-V) mode at ca. 960 cm^{-1} is masked by an intense methyl mode of the ^{t}Bu groups at 958 cm^{-1}, we are confident that this is not the case. The pK_a of silica silanols is much lower, ca. 7, than that of the ^{t}butylhydroperoxide and there is no reappearance of ≡SiOH. A weak band at 861 cm^{-1} is assigned to the ν(O-O) vibration, by comparison to the spectrum an authentic ^{t}butylperoxovanadium complex, with ν(O-O) at 880 cm^{-1}.[19]

^{51}V NMR spectroscopy of the product after reaction of ≡SiOVO(O^iPr)$_2$ with the ^{t}butylhydroperoxide showed an upfield shift of ca. 40 ppm from -650 ppm to -690 ppm, Figure 4.12, characteristic of other vanadium(V) peroxo complexes, such as $[VO(O_2)_2(H_2O)]^-$ with δ -691 ppm.[20] Furthermore, the ^{13}C CP-MAS NMR showed the presence of ^{t}Bu groups. The peak at 25 ppm is assigned to the methyl groups while a broad peak at 80 ppm is assigned to the quaternary carbon, and the third peak at 22 ppm is assigned to the methyl groups of residual isopropoxo ligands, Figure 4.13. Based on these results and the structures of analogous complexes in solution we propose the following structure for the surface species.

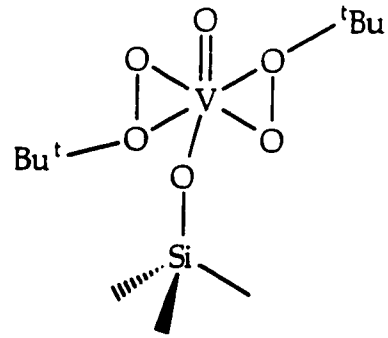

4.4.1 Reaction with Cyclohexene

When the silica-supported ^{t}butylperoxovanadium complex was exposed to cyclohexene vapor at room temperature, there was no reaction.

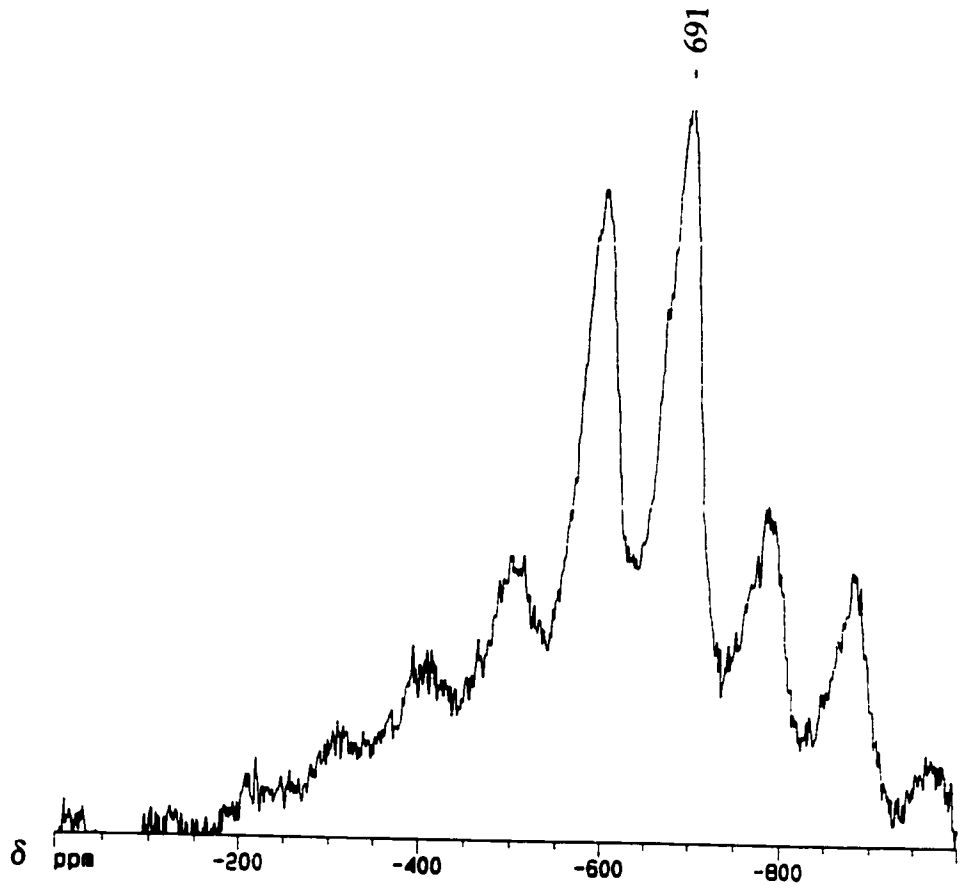

Figure 4.12 ^{51}V MAS NMR spectrum of ≡SiOVO(O^iPr)$_2$ after treatment with ^{t}BuOOH, spin rate 4000 Hz

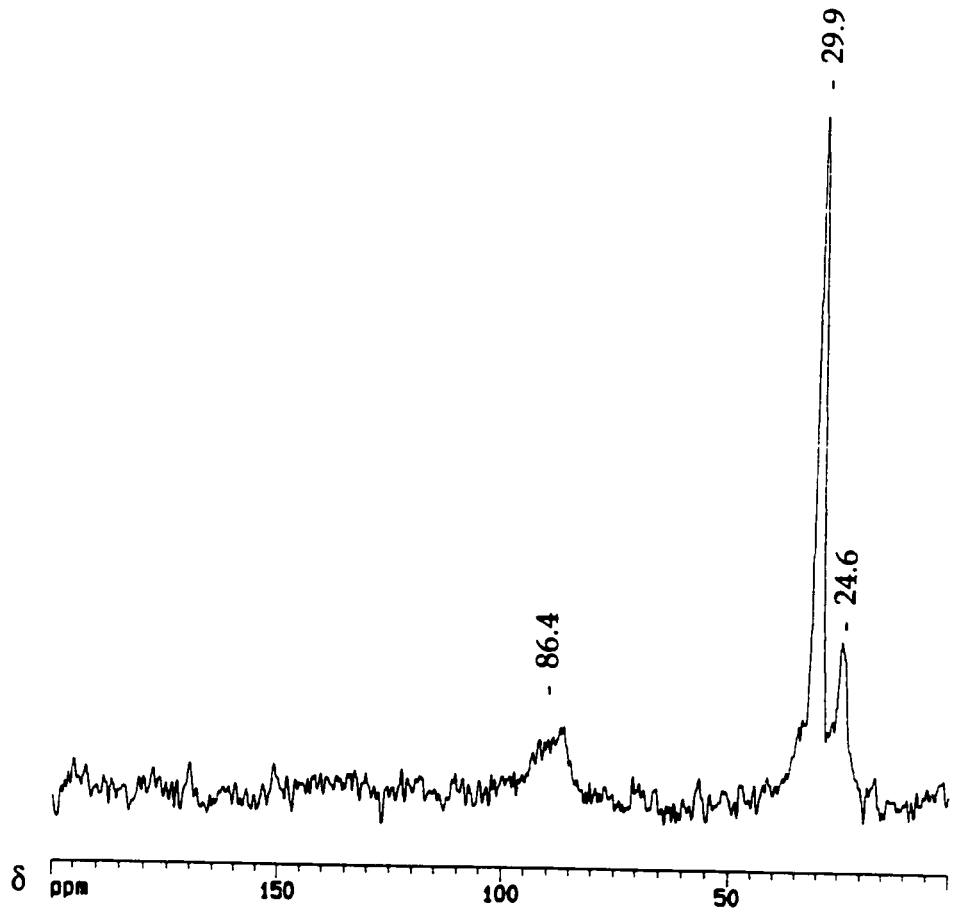

Figure 4.13 ^{13}C CP-MAS NMR spectrum of ≡SiOVO(O^iPr)$_2$ after treatment with ^{t}BuOOH, spin rate 4000 Hz

However if both cyclohexene and ^{t}butylhydroperoxide are present in excess, the silica-supported vanadium complex catalyses the conversion of cyclohexene to cyclohexene oxide. Exposure of ≡SiOVO(O^iPr)$_2$ simultaneously to cyclohexene and ^{t}butylhydroperoxide led to the immediate formation of cyclohexene oxide as the only volatile oxidation product detected by GC. Scheme 4.4 shows a possible mechanism for this reaction.

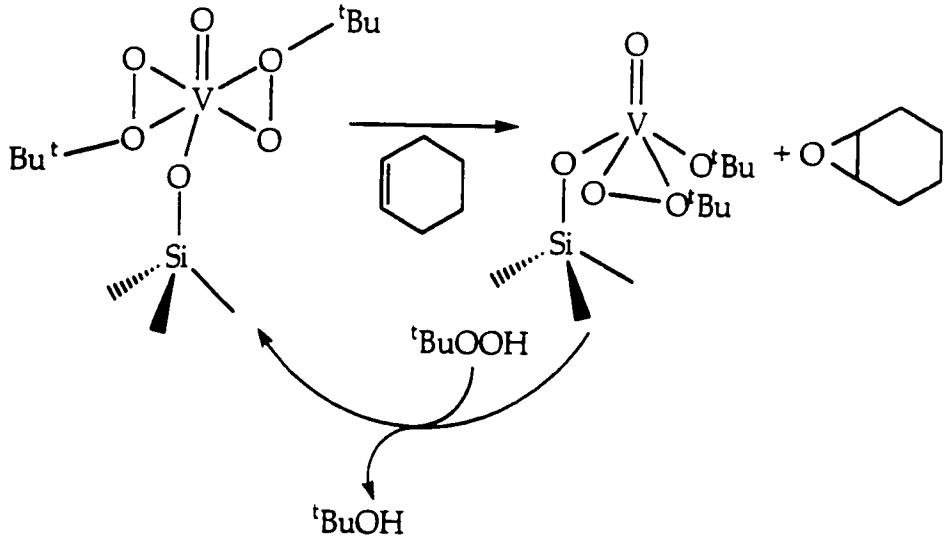

Scheme 4.4 Proposed catalytic cycle for the epoxidation of cyclohexene

Unexpectedly, after prolonged reaction (several hours), new IR modes were observed on the silica surface, Figure 4.14a, and cyclohexene oxide was no longer detectable in the gas phase by GC. The new vibrations at 2940-2860 cm^{-1} and 1450-1360 cm^{-1} are characteristic of $\nu(CH_2)$ and $\delta(CH_2)$ modes, respectively, and there is another new band in the carbonyl region at 1735 cm^{-1}. The bands assigned to ^{t}Bu groups decreased in intensity and the band at 861 cm^{-1} assigned

to the ν(O-O) mode of a ^{t}butylperoxovanadium species disappeared. Further addition of cyclohexene and/or ^{t}BuOOH caused no change in the IR spectra and no more cyclohexene oxide was formed.

The deactivation mechanism of the supported epoxidation catalyst may involve polymerization of the epoxide. The polymer formed blocks the surface, making it impossible for the supported vanadium complex to further catalyze the epoxidation of cyclohexene, and the cyclohexene oxide originally formed is consumed.

Various types of acids initiate the polymerization of epoxides.[21] Mechanisms are frequently complicated and not well understood; some, in fact, are believed to react to form metal alkoxides that cause polymerization to occur via an anionic coordination mechanism. Coordination catalysts yield the highest molecular weight polymers for the polymerization of epoxides. A possible mechanism may involve propagation by coordination of a monomer to the transition metal followed by anionic attack of the alkoxide on the ring, Scheme 4.5.

To test the polymerization hypothesis, $\equiv SiOVO(O^iPr)_2$ was exposed to an excess of cyclohexene oxide at room temperature. A similar IR spectra resulted, shown in Figure 4.14b. Several attempts to extract the polymer for analysis were unsuccesful.

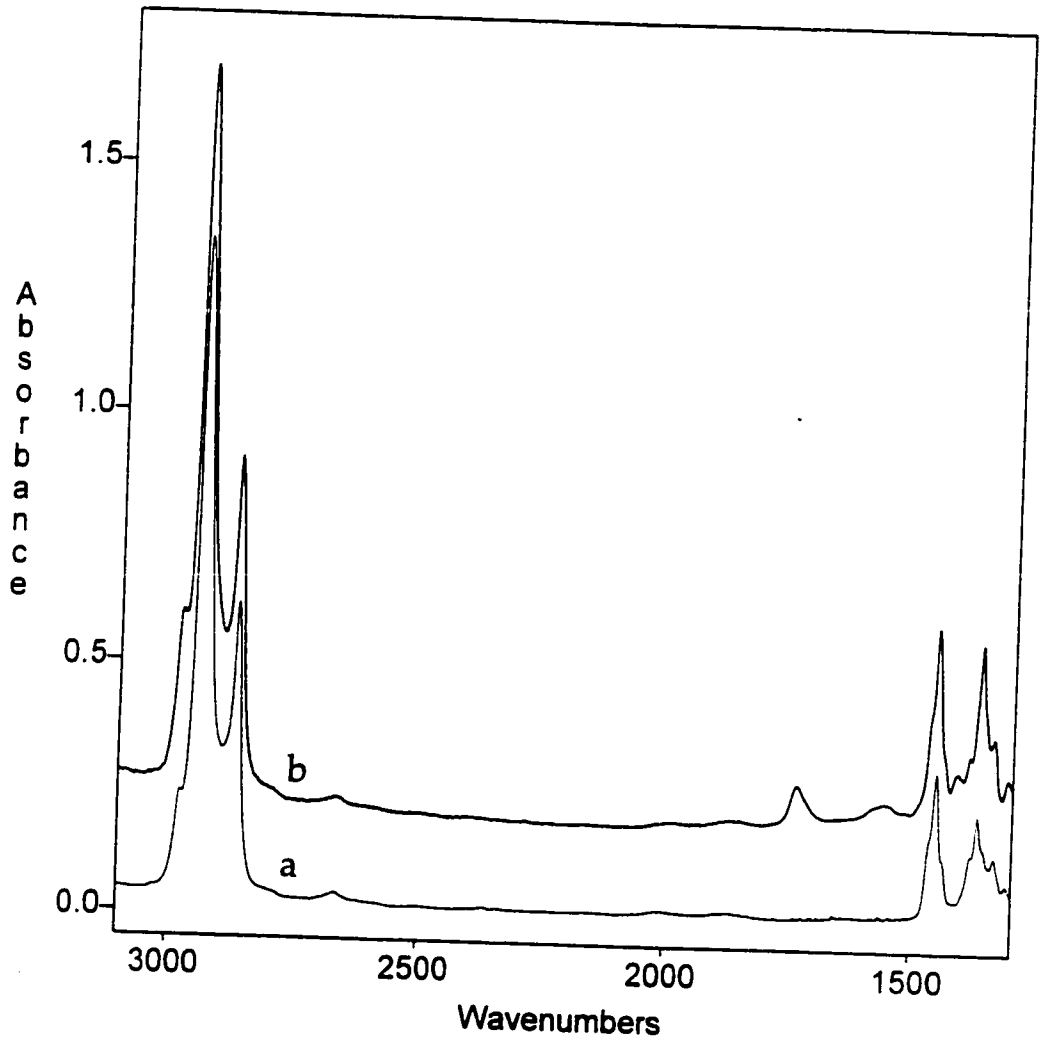

Figure 4.14 Difference infrared spectra of (a) ≡SiOVO(OO^tBu)$_2$ after reaction with cyclohexene; (b) ≡SiOVO(O^iPr)$_2$ after reaction with cyclohexene oxide.

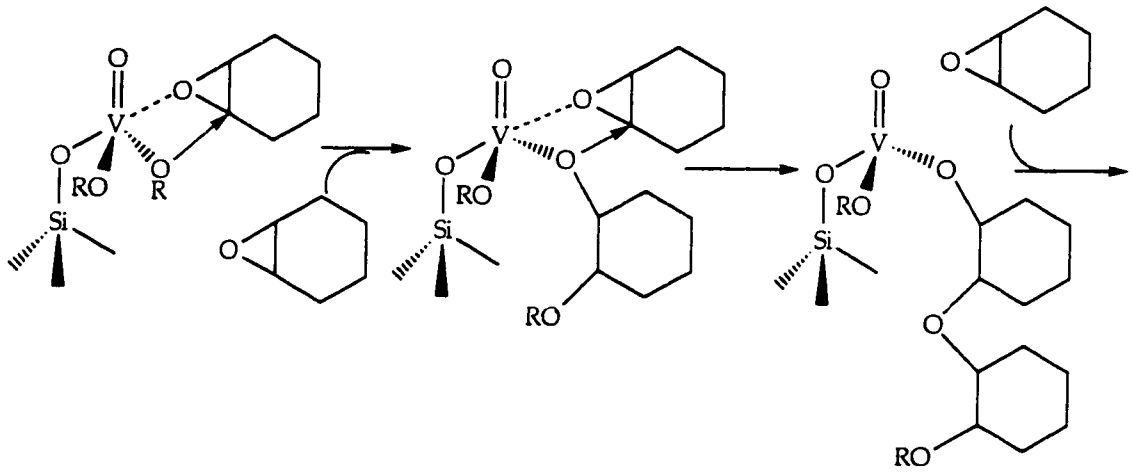

Scheme 4.5 Possible mechanism for the polymerization of cyclohexene oxide catalyzed by a silica-supported vanadium(V) complex

4.5 Conclusions

In this chapter, we have demonstrated how the silica-supported vanadium complexes retain some of the reactivity of molecular analogues and how our method of preparation of supported catalysts can be exploited in the study of reaction mechanisms. We have demonstrated that oxygen transfer reactions involve only the terminal vanadium oxygen bond and not lattice oxygens. We have also prepared the first characterized surface alkylperoxovanadium complex, which catalyses the epoxidation of cyclohexene. We discovered a potentially important deactivation mechanism for vanadium-based epoxidation catalysts.

4.6 References

(1) Sheldon, R. A. In *Aspects of Homogeneous Catalysis*; Dordrecht: Reidel, 1981; Vol. 4, pp 2-70.

(2) Su, C.-C.; Reed, J.; Gould, E. *Inorg. Chem.* **1973**, *12*, 337-342.

(3) Mimoun, H.; Mignard, M.; Brechot, P.; Saussine, L. *J. Am. Chem. Soc.* **1986**, *108*, 3711-3718.

(4) Oyama, S. T. *Res. Chem. Intermed.* **1991**, *15*, 165-182.

(5) Funk, H.; Weiss, W.; Zeising, M. *Z. Anorg. Allg. Chem.* **1958**, *296*, 36-45.

(6) Mittal, R. K.; Mehrotra, R. C. *Z. Anorg. Allg. Chem.* **1964**, *332*, 189-196.

(7) Schwartz, M. A.; Holton, R. A.; Scott, S. W. *J. Am. Chem. Soc.* **1969**, *91*, 2800.

(8) Pauling, H.; Andrews, D. A.; Hindley, N. C. *Helv. Chim. Acta* **1976**, *59*, 1233-1243.

(9) Charbardes, P.; Kuntz, E.; Varagnat, J. *Tetrahedron* **1977**, *33*, 1775-1783.

(10) Erman, N. B.; Aoultchenko, I. S.; Kheifitz, L. A.; Doulova, V. G.; Novikov, Y. N.; Volpine, M. E. *Tetrahedron Lett.* **1976**, 2981-2984.

(11) Nugent, W. A.; Mayer, J. M. *Metal Ligand Multiple Bonds*; Wiley: New York, 1988.

(12) Scott, S. L.; Basset, J. M. *J. Am. Chem. Soc.* **1994**, *116*, 12069-12070.

(13) Vidal, V.; Théolier, A.; Thivolle-Cazat, J.; Basset, J. M.; Corker, J. *J. Am. Chem. Soc.* **1996**, *118*, 4595-4602.

(14) Devore, D.; Lichtenhan, J.; Takusagawa, F.; Maatta, E. *J. Am. Chem. Soc.* **1987**, *109*, 7408-7416.

(15) Birdwhistell, K. R.; Boucher, T.; Ensminger, M.; Harris, S.; Johnson, M.; Toporek, S. *Organomet.* **1993**, *12*, 1023-1025.

(16) Iwamoto, M.; Hirata, J.; Matsukami, K.; Kagawa, S. *J. Phys. Chem.* **1983**, *1983*, 903-905.

(17) Tran, K.; Hanning-Lee, M.; Biswas, A.; Steigman, A. E.; Scott, G. *J. Am. Chem. Soc.* **1995**, *117*, 2618-2626.

(18) Richardson, W. H. *The Chemistry of Peroxides*; Wiley: New York, 1983.

(19) Mimoun, H.; Chaumette, P.; Mignard, M.; Saussine, L. *Nouv. J. Chim.* **1983**, *7*, 467-475.

(20) Conte, V.; DiFuria, F.; Moro, S. *J. Mol. Cat. A: Chem.* **1995**, *104*, 159-168.

(21) Penczek, S.; Kubisa, P. *Adv. Polym. Sci.* **1980**, *37*, 1-8.

Chapter 5

Preparation of V-Ti Mixed Oxide Overlayers on Silica

5.1 Introduction

Heterometallic oxides find wide application in materials science (for example, glasses and ceramics) and heterogeneous catalysis, due to the unique properties conferred by synergy between different metal sites. Mixed oxides are usually prepared by classical co-impregnation or by sol-gel hydrolysis. Both methods suffer from an inability to control the precise composition and homogeneity of the precipitated oxide. A possible solution is the use of heterometallic alkoxide complexes as precursors to well-defined mixed oxides.[1] However, well-characterized bimetallic alkoxide complexes containing two transition metals are rare. Their potential in OMCVD processes has therefore yet to be developed.

One particularly important heterometallic oxide is the ternary V-Ti-Si catalyst. This material is made by wetness impregnation of high surface area silica with titania, followed by deposition from solution of vanadium oxide. It is reported to be more active and selective than any of the possible bimetallic combinations (i.e., V-Si, Ti-Si or V-Ti) for the oxidation of *o*-xylene to phthalic anhydride,[2] and in the selective catalytic reduction of NO_x,[3] for which it is used in a commercial process.[4] Anatase-like Ti overlayers on silica are thought to be much more active than rutile-like phases in V-Ti-Si selective oxidation catalysts, since the rutile phase has been associated with unselective oxidation.[5]

Unfortunately, the usual calcination/dehydration treatments for oxide catalysts prepared by hydrolytic routes are performed in the same temperature range as the anatase-rutile transition, which has therefore been suggested as a major deactivation mechanism for the catalyst.[6]

The nature of the interfacial oxide-oxide interactions in the ternary catalyst is not known, however, the vanadium active sites were suggested to be dispersed as pseudo-tetrahedral monomers, anchored to the titania overlayer via three oxygen bridges.[7] This model resembles the proposed active site on bimetallic V-Si oxide catalysts,[8] as described in chapter 1.

Recently, thermal condensation of metal halides with metal alkoxides has been reported as a novel low temperature non-hydrolytic sol-gel route to transition metal oxides and mixed oxides, eq 5.1.[9]

$$MX_n + M(OR)_n \rightarrow 2\,MO_{n/2} + n\,RX \qquad (5.1)$$

We have synthesized and characterized a series of fully dispersed homogeneous surface complexes, chapters 2 and 3, by grafting VOX_3 onto partially dehydroxylated silica followed by ligand metathesis.[10,11] In the course of our investigation of their reactivity, we discovered a stoichiometric CVD reaction which leads to a heterobinuclear V-Ti alkoxide complex attached to silica. Its composition makes it an interesting model for the ternary catalyst, as it may

represent an intermediate in the hydrolysis-polycondensation reactions which lead to V-Ti-Si.

The gas-solid reaction of excess VOX_3 with the surface hydroxyl groups of silica-500 is reproducible, and produces a material which contains 2.2 wt% V, or 0.40 mmol V/g, and no residual hydroxyl groups, as described in chapter 3. The surface reaction was formulated, based on IR and ^{51}V NMR, as well as isotope labelling studies, as the formation of the chemisorbed complex, $\equiv SiOVOX_2$, eqs 3.2 and 3.3.

5.2 Reaction of $\equiv SiOVOCl_2$ with $TiCl_4$

Upon exposure of $\equiv SiOVOCl_2$ to $TiCl_4$ vapor at room temperature, $VOCl_3$ was observed in the gas phase ($VOCl_3$ is readily identified by its characteristic gas phase IR spectrum, with intense absorptions at 1043 (V=O) and 508 (V-Cl) cm^{-1}). In the infrared spectrum, bands characteristic of $\equiv SiOVOCl_2$, i.e., the overtone 2ν(V=O) at 2070 cm^{-1}, and ν(V-O-Si) at 960 cm^{-1}, Figure 5.1a, disappeared completely, while a new intense band appeared at 920 cm^{-1}, Figure 5.1b. In addition, the band at 505 cm^{-1}, assigned to ν(V-Cl), shifted slightly to 510 cm^{-1}, Figure 5.2. The final spectrum, stable under dynamic vacuum, is identical with that obtained by the direct reaction of $TiCl_4$ with the surface hydroxyl groups of unmodified silica-500.[12] The 510 cm^{-1} band is associated with Ti-Cl vibrations. The assignment of the 920 cm^{-1} band to the Si-O vibration of a polarized Si-O-Ti

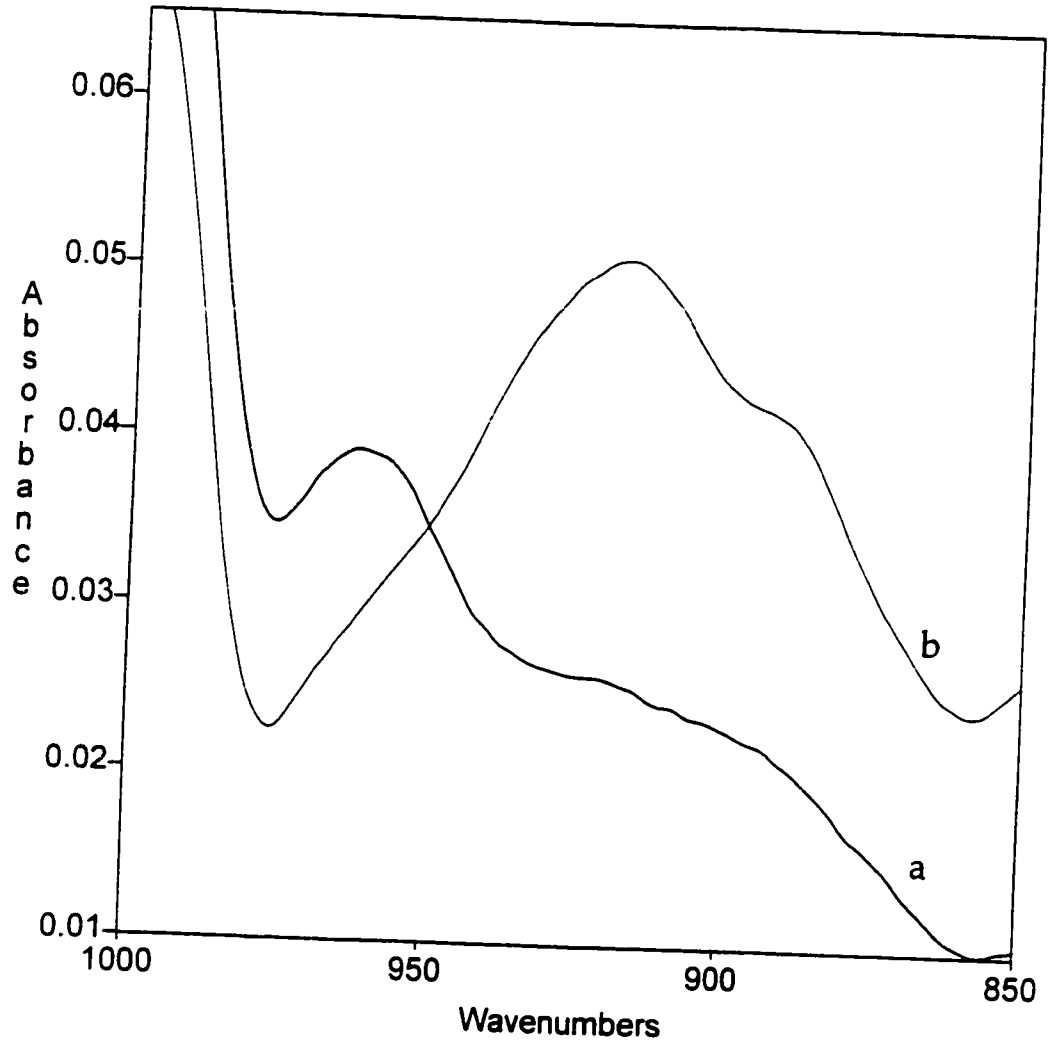

Figure 5.1 Difference *in situ* infrared spectra of thin silica films of (a) ≡$SiOVOCl_2$ and (b) ≡$SiOTiCl_3$ formed by reaction of ≡$SiOVOCl_2$ with $TiCl_4$.

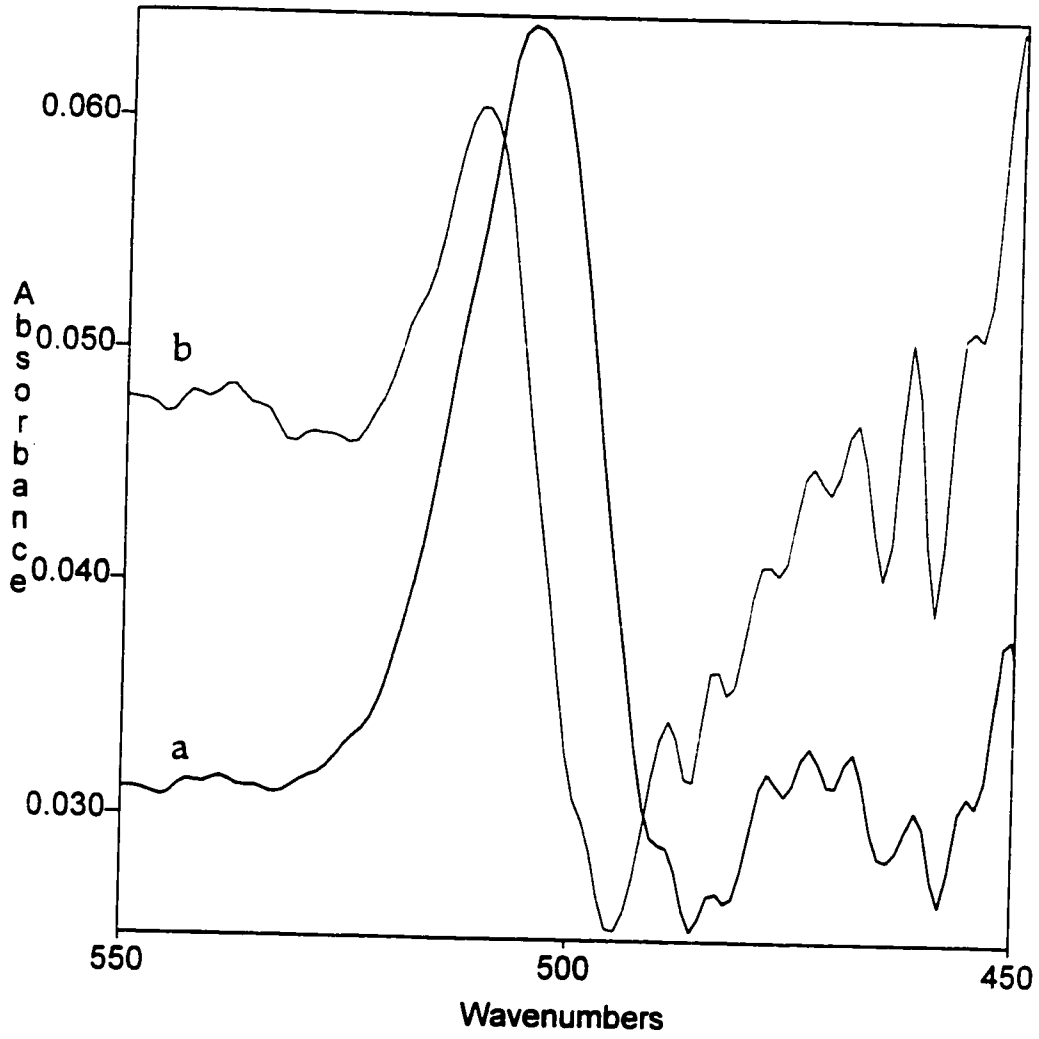

Figure 5.2 Difference *in situ* infrared spectra of thin silica films of (a) ≡$SiOVOCl_2$ and (b) ≡$SiOTiCl_3$ formed by reaction of ≡$SiOVOCl_2$ with $TiCl_4$.

unit is less well-established,[13] but it is always present in Ti-substituted silicas and zeolites.

Elemental analysis of the colorless product, after complete desorption of volatiles, gave <0.1 wt.% V and 2.1 wt.% Ti, i.e., the amount (in moles) of chemisorbed Ti is equal to the initial amount of V present. We conclude that an exchange reaction has occurred, as shown in eq 5.2:

$$\equiv SiOVOCl_2 + TiCl_4 \rightarrow \equiv SiOTiCl_3 + VOCl_3 \qquad (5.2)$$

The possible formation of $VOCl_3$ by reaction of $\equiv SiOVOCl_2$ with adventitious HCl was verified separately and does not occur under these conditions, nor do $VOCl_2(OR)$ complexes react with HCl in solution.[14] The exchange reaction shown in eq 5.2 is not expected to regenerate any surface hydroxyl groups, nor are any observed by *in situ* IR.

5.3 Reaction of $\equiv SiOVOCl_2$ with $Ti(O^iPr)_4$

When $\equiv SiOVOCl_2$ was exposed to $Ti(O^iPr)_4$ vapor at room temperature, no hydroxyl groups reappeared but the IR spectrum of the product showed vibrations characteristic of 2-propoxide groups: 2880-2980 cm^{-1} (ν(C-H)), 1325-1465 cm^{-1} ($\delta(CH_3)$ and δ(OCH)) and 865 cm^{-1}, Figure 5.3. The bands of $\equiv SiOVOCl_2$ at 2070 and 505 cm^{-1} completely disappeared, Figure 5.4, while the band at 960

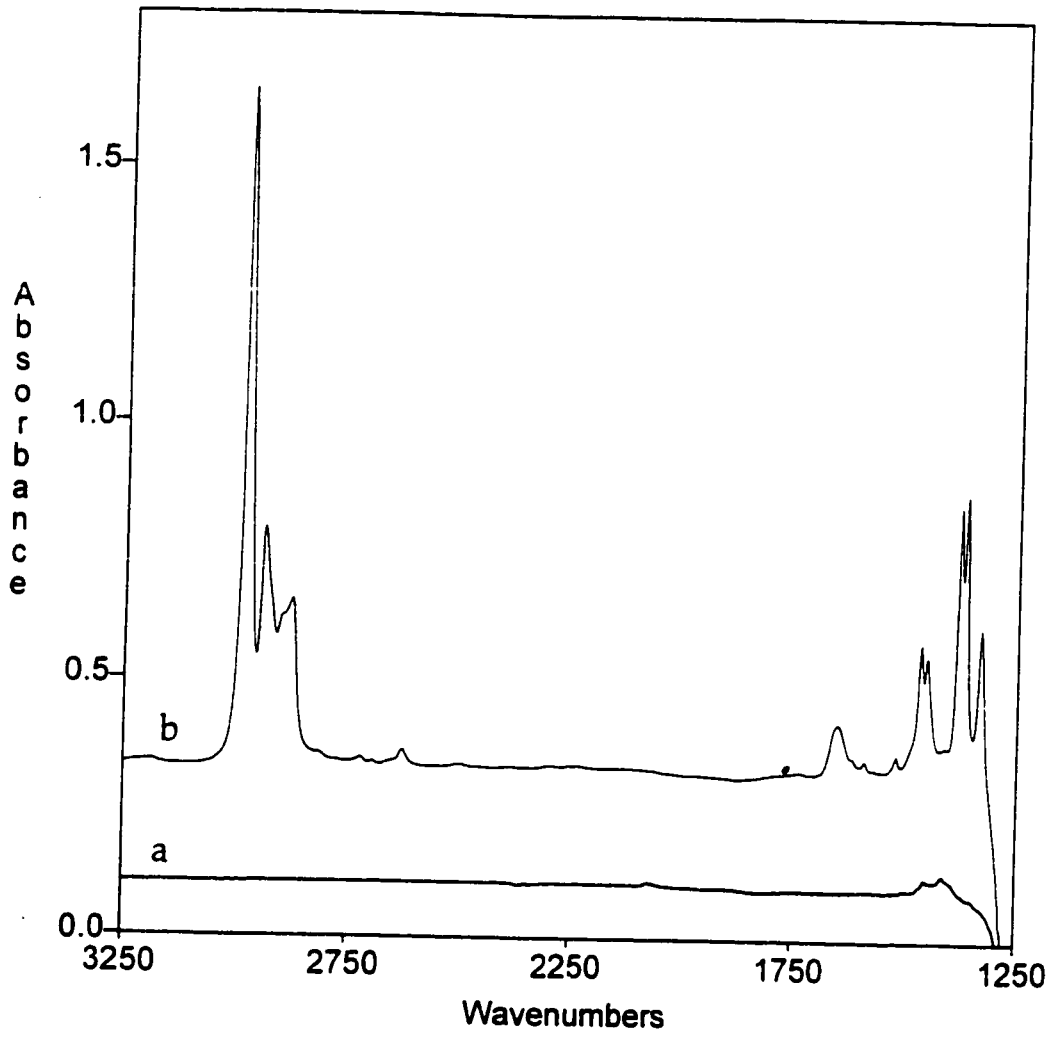

Figure 5.3 Difference infrared spectra of a self-supporting disk of (a) ≡SiOVOCl$_2$ (b) ≡SiOTi(O^{i}Pr)(O)$_2$VO(O^{i}Pr) formed by reaction of ≡SiOVOCl$_2$ with Ti(O^{i}Pr)$_4$.

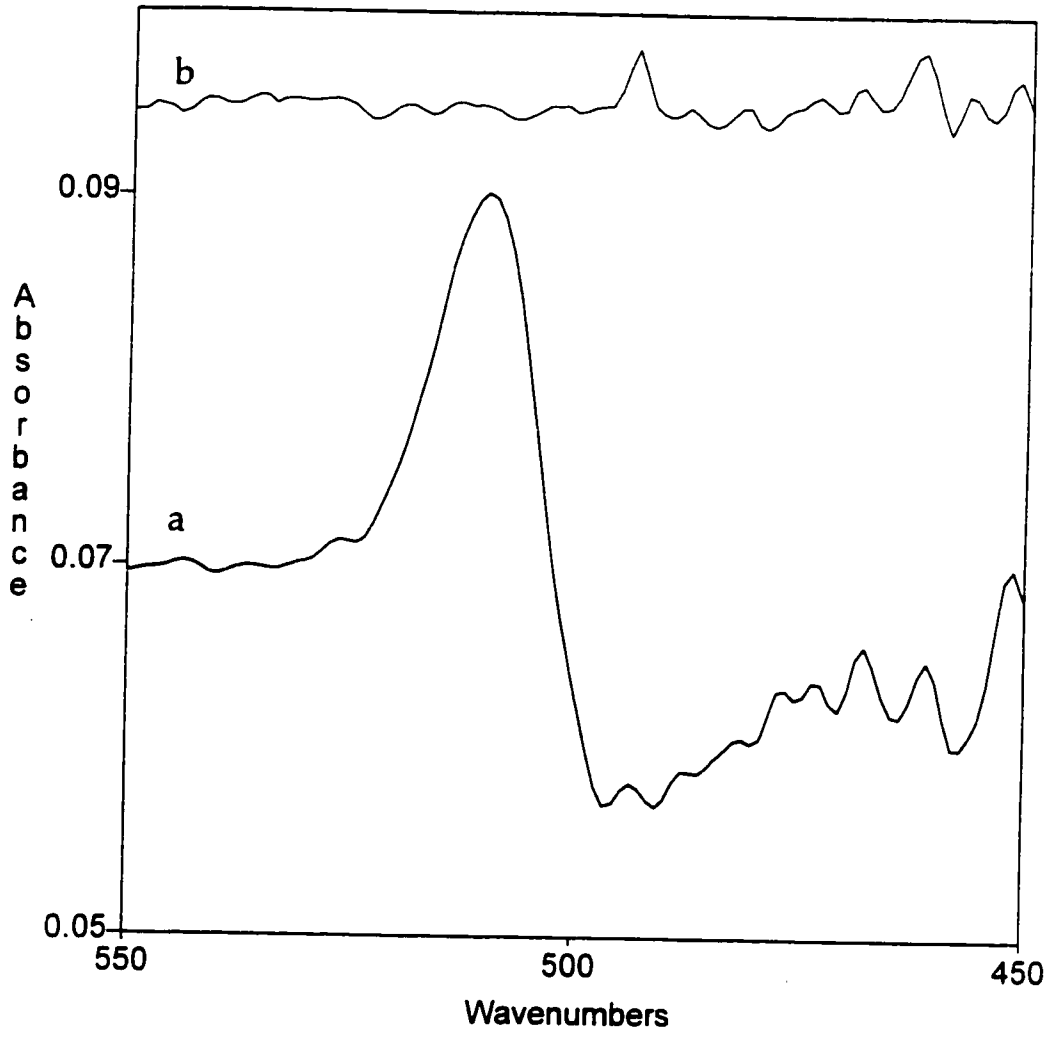

Figure 5.4 Difference infrared spectra of a thin silica film of (a) ≡$SiOVOCl_2$ (b) ≡$SiOTi(O^iPr)(O)_2VO(O^iPr)$ formed by reaction of ≡$SiOVOCl_2$ with $Ti(O^iPr)_4$.

shifted slightly to 945 cm^{-1}, Figure 5.5. The gas phase contained 2-propyl chloride, 2-propanol and propene, but no HCl. Elemental analysis of the product **I** after prolonged desorption of volatiles under dynamic vacuum revealed the presence of V and Ti in a constant molar ratio V/Ti of 0.98 ± 0.07, Table 5.1. The number of isopropyl groups present was determined to be 2.1 ± 0.2 per V, by integration of the ν(C-H) region of the IR spectrum (the intensity of the silica overtone at 1860 cm^{-1} was used as an internal reference). Calcination of the material at 700°C in 400 Torr O_2 caused complete loss of surface hydrocarbyl groups with formation of H_2O and 7 ± 1 mol CO_2/mol V, i.e., roughly 2 isopropyl groups per V. No HCl was detected by IR, even under these harsh conditions. To account for these observations, we propose the reaction shown in eq 5.3.

$$\equiv SiOVOCl_2 + Ti(O^iPr)_4 \rightarrow \underset{\mathbf{I}}{\equiv SiOTi(O)_3V(O^iPr)_2} + \{^iPrCl + {}^iPrOH + CH_3CH{=}CH_2\} \qquad (5.3)$$

The ^{51}V MAS NMR spectrum of **I** consists of a weak resonance at -517 ppm, Figure 5.6b, which is much decreased in intensity compared to the spectrum of the same amount of $\equiv SiOVOCl_2$, -295 ppm, Figure 5.6a, obtained with the same experimental parameters and data analysis.

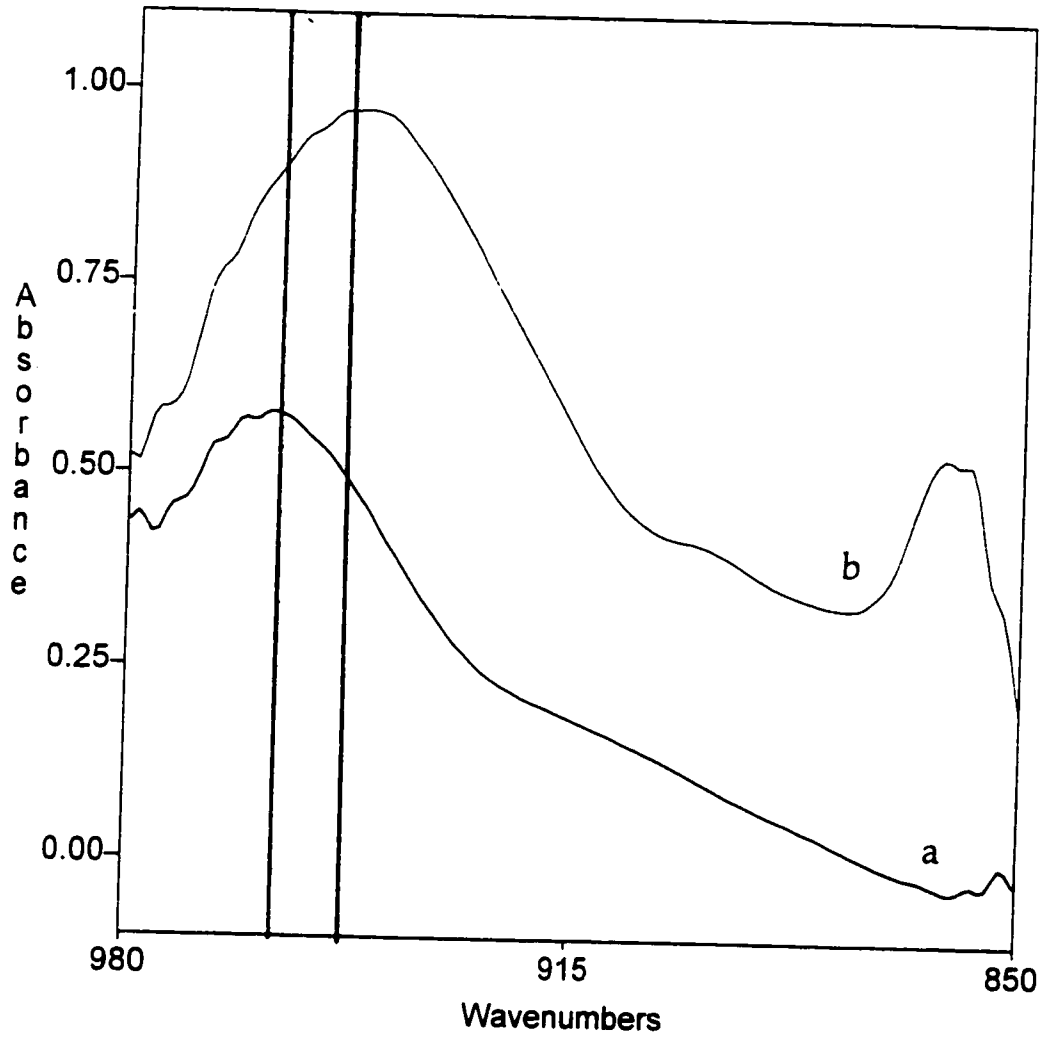

Figure 5.5 Difference infrared spectra of a thin silica film of (a) ≡$SiOVOCl_2$ (b) ≡$SiOTi(O^iPr)(O)_2VO(O^iPr)$ formed by reaction of ≡$SiOVOCl_2$ with $Ti(O^iPr)_4$.

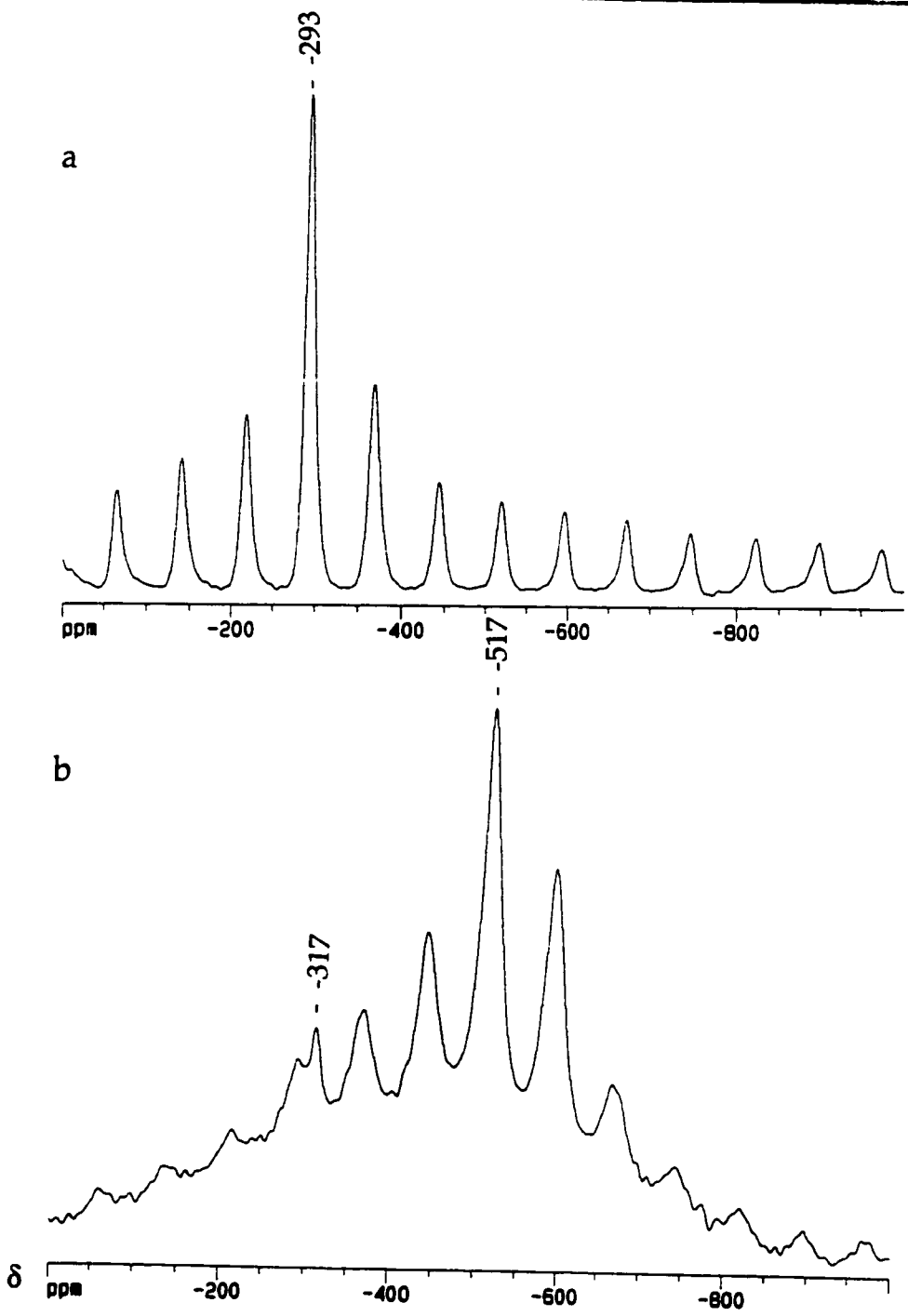

Figure 5.6 ^{51}V MAS NMR (a) $\equiv SiOVOCl_2$ (b) $\equiv SiOTi(O)_3V(O^iPr)_2$ obtained by the reaction of $\equiv SiOVOCl_2$ with $Ti(O^iPr)_4$, spin rates 4000 Hz

Table 5.1. Composition of heterobimetallic surface complexes

Reactants	wt% V	wt% Ti	V/Ti	volatile products
$SiOVOCl_2$ + $TiCl_4$	0.08	2.10	0.03	$VOCl_3$
$SiOVOCl_2$ + $Ti(O^iPr)_4$	1.85	1.82	1.01	$CH_3CHClCH_3$,
	1.81	1.75	1.03	$CH_3CH{=}CH_2$,
	2.06	2.07	0.99	$CH_3CH(OH)CH_3$
	1.75	1.74	1.01	
	1.86	1.96	0.91	
	1.79	1.59	1.06	
average			1.00 ± 0.03	
$SiOVOCl_2$ + $Ti(O^iPr)_4$	1.47	1.60	0.88	$VOCl_2(O^iPr)$,
(large excess)	1.33	1.61	0.83	$VOCl(O^iPr)_2$,
				$CH_3CHClCH_3$,
				$CH_3CH{=}CH_2$,
				$CH_3CH(OH)CH_3$
$SiOVO(O^iPr)_2$ + $Ti(O^iPr)_4$	1.81	1.69	1.03	$CH_3CH{=}CH_2$,
	1.61	1.49	1.03	$CH_3CH(OH)CH_3$
	1.94	1.69	1.09	
	1.95	1.85	1.05	
	1.88	1.79	1.05	
	1.91	1.89	1.01	
average			1.04 ± 0.03	

When ≡SiOVOCl$_2$ is exposed to enough Ti(O^{i}Pr)$_4$ to wet the silica, a small amount (< 25%) of the surface vanadium is converted to the physisorbed forms VOCl$_2$(O^{i}Pr) and VO(O^{i}Pr)$_2$Cl. These complexes were identified in the ^{51}V NMR spectra by their narrow line widths and characteristic chemical shifts at -317 and -505 ppm,[15] respectively. A small band at -317 ppm can be seen in Figure 5.6b. The formation of VO(O^{i}Pr)$_2$Cl was observed in another NMR experiment, where the resonance at -505 ppm dominates the spectrum even when the sample is not spinning, indicating a highly mobile (not chemisorbed) species, Figure 5.7. After prolonged desorption of volatiles, the metals analyses of these samples show reduced (< 2%) vanadium content, Table 5.1.

5.4 Homogeneous reaction of VOCl$_3$ with Ti(O^{i}Pr)$_4$

To verify whether a complex analogous to **I** is formed in solution, VOCl$_3$ and Ti(O^{i}Pr)$_4$ were mixed in a NMR tube. The ^{51}V NMR spectrum of a roughly equimolar mixture of VOCl$_3$ with Ti(O^{i}Pr)$_4$ contains two sharp resonances at -306 and -502 ppm assigned to VOCl$_2$(O^{i}Pr) and VOCl(O^{i}Pr)$_2$ respectively.[15] When the amount of Ti(O^{i}Pr)$_4$ was increased relative to VOCl$_3$, the band at -306 disappeared while the band at -502 ppm increased in intensity. The results show no evidence for a complex analogous to **I**, however they do indicate that ligand exchange is occuring, eq 5.4.

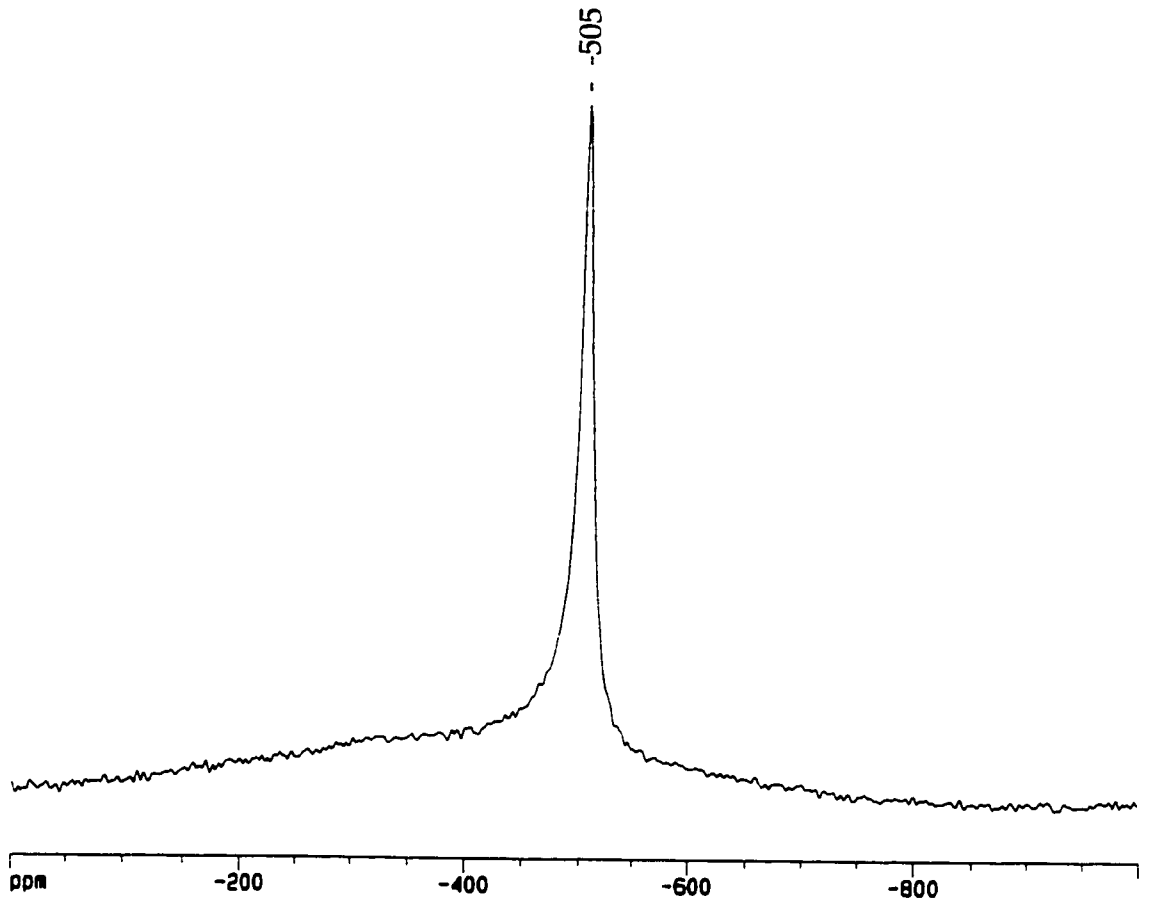

Figure 5.7 ^{51}V of physisorbed $VO(O^iPr)_2Cl$ on silica, produced by reaction of $\equiv SiOVOCl_2$ with a large excess of $Ti(O^iPr)_4$. The spectrum was recorded without spinning.

$$VOCl_3 + Ti(O^iPr)_4 \rightarrow VOCl_2(O^iPr) + VOCl(O^iPr)_2 + Ti(O^iPr)_{4-x}Cl_x \quad (5.4)$$

5.5 Reaction of ≡SiOVO(O^{i}Pr)$_2$ with Ti(O^{i}Pr)$_4$

Since **I** apparantly contains no chloride, we attempted to prepare it independently by reaction of ≡SiOVO(O^{i}Pr)$_2$ with Ti(O^{i}Pr)$_4$. When ≡SiOVO(O^{i}Pr)$_2$ (containing no residual ≡SiOH) was exposed to Ti(O^{i}Pr)$_4$ vapor at room temperature, no change in intensity was observed in the hydrocarbon regions of the IR spectrum (implying no retention of additional 2-propyl groups on the surface). However, the band at 960 cm^{-1} belonging to the ν(Si-O-V) mode of ≡SiOVO(O^{i}Pr)$_2$ shifted to 945 cm^{-1}, which is consistent with the formation of **I**. Elemental analysis of the product revealed the presence of V and Ti, once again in a molar ratio of 1.1 ± 0.1 V/Ti. The gas phase contained a mixture of 2-propene and 2-propanol.

To our surprise, we failed to prepare **I** by the (more logical) reversed order sequential CVD process, SiO_2 + Ti(O^{i}Pr)$_4$ + VO(O^{i}Pr)$_3$. Although Ti(O^{i}Pr)$_4$ reacts with unmodified silica to form a chemisorbed Ti complex,[16] we observed no subsequent reaction with VO(O^{i}Pr)$_3$. However, at that time the nature of the interaction of Ti(O^{i}Pr)$_4$ with silica was not known. Since then A. O. Bouh investigated the reaction of Ti(O^{i}Pr)$_4$ with silica. A brief summary of his findings follows.[17]

When $Ti(O^iPr)_4$ is adsorbed on silica at room temperature, a chemical reaction takes place in which chemisorbed titanium species are formed with concurrent formation of volatile organic products. The organic products were identified by GC as 2-propanol and propylene. Furthermore, the amount of titanium chemisorbed on silica was measured to be (3.91 ± 0.04) wt. % and (3.87 ± 0.03) wt. % on silica-200 and -500 respectively. The similarity of these two results was unexpected, given that the number of surface hydroxyls on silica-500 is roughly half that on silica-200. The amount of titanium corresponds to 1.0 Ti/≡SiOH on silica-200 and 2.0 Ti/≡SiOH on silica-500. Upon calcination of the silica-supported titanium complexes at 700°C in 300 Torr O_2, 6.1 and 7.6 CO_2/Ti were formed for silica-200 and -500, respectively. These results are consistent with the reaction stoichiometries shown below:

on silica-200

$$2 \equiv SiOH + 2\ Ti(O^iPr)_4 \rightarrow [(\equiv SiO)Ti(O^iPr)_2]_2O + 3\ ^iPrOH + C_3H_6 \qquad (5.5)$$

on silica-500

$$\equiv SiOH + 2\ Ti(O^iPr)_4 \rightarrow (\equiv SiO)Ti_2(O^iPr)_5(O) + 2\ ^iPrOH + C_3H_6 \qquad (5.6)$$

When $Ti(O^iPr)_4$ is grafted onto silica, it spontaneously undergoes a condensation reaction similar to the one we proposed for its reaction with silica-supported vanadium complexes, resulting in bimolecular silica-supported

titanium complexes. This hypothesis is the basis for the rest of our work on supported mixed vanadium/titanium complexes which will be discussed later. Bouh et. al. indirectly prepared mononuclear silica-supported titanium alkoxo complexes by the reaction of $Ti(NEt_2)_4$ with silica, followed by ligand exchange with excess ROH. The reaction of mononuclear titanium alkoxo complexes with $Ti(O^iPr)_4$ resulted in the same dinuclear species, as characterized by NMR, IR and elemental analysis, as the direct reaction of $Ti(O^iPr)_4$ with silica. Therefore we attempted to prepare the mixed supported vanadium/titanium complex by a similar route.

5.6 Preparation of V/Ti complex by direct sequential CVD method

The reaction of $Ti(NEt_2)_4$ with silica-200 or -500 results in a color change of silica from white to yellow and liberation of $HNEt_2$ as the exclusive gas phase product as detected my IR and GC. The nature of the surface reactions was described by A. O. Bouh et. al.,[17] eq. 5.7 and 5.8.

on silica-500

$$\equiv SiOH + Ti(NEt_2)_4 \rightarrow \equiv SiOTi(NEt_2)_3 + HNEt_2 \qquad (5.7)$$

on silica-200

$$2 \equiv SiOH + Ti(NEt_2)_4 \rightarrow (\equiv SiO)_2Ti(NEt_2)_2 + 2\, HNEt_2 \qquad (5.8)$$

The reactions of both supported complexes with excess alcohol results in an immediate color change from yellow to white and displacement of the amido ligands as $HNEt_2$, equations 5.9 and 5.10.

$$\equiv SiOTi(NEt_2)_3 + 3\ ROH \rightarrow \equiv SiOTi(OR)_3 + 3\ HNEt_2 \qquad (5.9)$$

$$(\equiv SiO)_2Ti(NEt_2)_2 + 2\ ROH \rightarrow (\equiv SiO)_2Ti(OR)_2 + 2\ HNEt_2 \qquad (5.10)$$

5.6.1 Reaction of $\equiv SiOTi(O^iPr)_3$ with $VO(O^iPr)_3$

Addition of $O{=}V(O^iPr)_3$ to $(\equiv SiO)Ti(O^iPr)_3$ resulted in the formation of 2-propanol and propylene as detected by GC and GC-MS. ^{13}C CP-MAS NMR shows the presence of isopropyl groups and the ^{51}V MAS NMR shows one peak at -660 ppm. Extraction and analysis of the vanadium and titanium as described in Chapter 2 revealed a ratio of V/Ti = 0.96. These results led us to propose that the product of the reaction is the same as that obtained by the reverse CVD method (section 5.2 and 5.3).

5.7 Mechanism of the condensation reaction

The preparation of multicomponent oxides by non-hydrolytic condensation reactions of metal alkoxides has recently been described,[18,19] however, the mechanisms of the reactions are little known.[20] The first step in the formation of 1 from $\equiv SiOVOCl_2$ is likely the reversible coordination of TiX_4,

a strong Lewis acid,[21] to the surface siloxo ligand. The latter becomes a 3e⁻ donor bridging the pair of metal atoms, as in the intermediate **2**.[22] $TiCl_4$ is known to form Lewis acid adducts with ethers[23] and alcohols.[24]

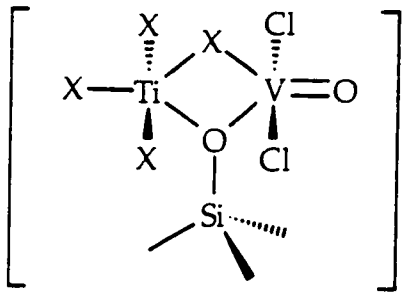

2

When X is Cl, formation of a μ-Cl bridge between Ti and V is followed by cleavage of the heterobimetallic intermediate with liberation of volatile $VOCl_3$ and leaving an SiO-Ti bond to the surface. When X is O^{i}Pr, the major reaction is the formation of the more stable μ-OR bridge,[24] which then yields an oxo bridge by concerted elimination of 2-propyl chloride,[18] eq. 5.11.

$$[VOCl_2(\mu\text{-}OSi)(\mu\text{-}O^iPr)Ti(O^iPr)_3] \rightarrow [\equiv SiOTi(O^iPr)_2(\mu\text{-}O)VOCl(O^iPr)] + {}^iPrCl \quad (5.11)$$

2

Heterolysis of the O-C bond of alkoxide ligands with formation of oxide bridges is promoted by coordination to strong Lewis acids in the synthesis of heterometallic alkoxide complexes.[1] A second such reaction would generate the

product **I**, containing no chloride and two alkoxide ligands per surface complex. The absence of HCl among the volatile reaction products and the lack of reactivity of $\equiv SiOVOCl_2$ towards HCl are evidence for the non-hydrolytic nature of the condensation reaction. When the reactant is $\equiv SiOVO(O^iPr)_2$, we propose that heterolysis of the bridging alkoxide ligand of the heterobimetallic intermediate produces an incipient carbocation which loses a proton to form propene. The proton is captured by another alkoxide ligand to form 2-propanol.

The presence of propene and propanol among the reaction products when the starting material is $\equiv SiOVOCl_2$ suggests that ligand exchange between $\equiv SiOVOCl_2$ and $Ti(O^iPr)_4$ is occurring to produce chemisorbed vanadium alkoxide complexes. Dissociation of **2** to yield volatile $VOCl_x(O^iPr)_{3-x}$ is a minor side reaction which can be minimized by using a small excess of $Ti(O^iPr)_4$ reactant. Facile ligand exchange is well-documented for $TiCl_4/Ti(OR)_4$ mixtures,[25] although not for $VOCl_x(O^iPr)_{3-x}$.[26] The reaction of $\equiv SiOVOX_2$ with a large excess of $Ti(O^iPr)_4$, which liberates chemisorbed vanadium from the surface, implies that ready ligand exchange occurs on the surface between V and Ti. This conclusion is supported by our observation of ligand scrambling in solution, section 5.4.

The exact nature of **I** is not fully known, but a possible structure contains a tetrahedral VO_4 unit sharing a face with octahedral TiO_6:

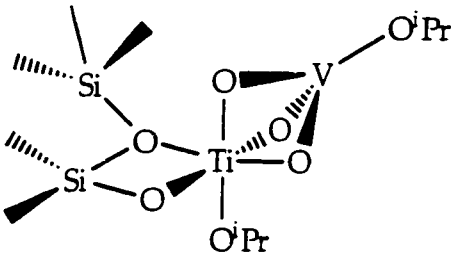

In the proposed structure, the coordination sphere of Ti is completed by 2e$^-$ donation from a surface siloxane bridge site. This model is consistent with all the available spectroscopic and analytical results, including the decrease in intensity of the ^{51}V MAS NMR signal due to the restricted mobility of the V site. The alkoxide ligands of **I** undergo metathesis with other alcohols without destroying its structure, i.e., without disruption of Si-O-Ti or desorption of V from the surface. An alternate structure, which has been proposed for V-Ti-Si active sites,[27] contains pairs of terminal oxo ligands on a VO_2^{2+} unit, which is bound via bridging oxygen atoms to Ti. However, we see no IR evidence for V=O vibrations. Also, **I** fails to react with *p*-tolylisocyanate to form CO_2, in a reaction which is characteristic of the terminal oxo ligands of vanadium, Chapter 4.[28] Coordination of the vanadyl oxygen to the titanium, giving it 6 coordinate geometry, would be consistent with our observations and would explain its reduced reactivity towards isocyanates. It has been demonstrated that coordination of a Lewis acid to the vanadyl has little effect on the ^{51}V NMR chemical shift.[29]

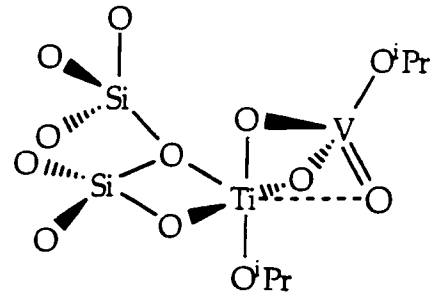

I

The efficiency of formation of mixed metal oxides from molecular precursors has been quantified by their degree of condensation, which is defined as the ratio of the experimental amount of bridging oxygen to the theoretical value for the oxides.[19] For **I**, the degree of condensation is 0.78, and is similar to the best results in non-hydrolytic condensations which yield zirconium titanate.[18] Unlike $\equiv SiOVOX_2$, which is thermally unstable above 70°C and readily decomposes in the presence of water vapor at room temperature, **2** is unreactive towards water at room temperature and can be heated in vacuum to at least 120°C with no observable color changes. We suggest that the greater thermal and hydrolytic stability of the SiO-Ti linkage relative to SiO-V[30] may be responsible for these changes.

5.8 Conclusion

The mixed V-Ti alkoxide complex on silica, **I**, may be a structural model for the active site on dehydrated V-Ti-Si catalysts. The selectivity and activity of these materials have been linked to the high dispersion of V, the absence of

exposed Ti, and the silica support, which contributes high surface area, as well as thermal and mechanical stability.[31] The sequential CVD technique holds promise for the future "design" of well-defined isolated multifunctional active sites in heterometallic oxide catalysts.

5.9 References

(1) Caulton, K. G.; Hubert-Pfalzgraf, L. G. *Chem. Rev.* **1990**, *90*, 969-995.

(2) Dias, C. R.; Portela, M. F.; Galán-Fereres, M.; Bañares, M. A.; Granados, M. L.; Peña, M. A.; Fierro, J. L. G. *Catal. Lett.* **1997**, *43*, 117-121.

(3) Rajadhyaksha, R. A.; Hausinger, G.; Zeilinger, H.; Ramstetter, A.; Schmelz, H.; Knözinger, H. *Appl. Catal.* **1989**, *51*, 67-79.

(4) Groeneveld, M. J.; Boxhoorn, G.; Kuipers, H. P. C. E.; van Grinsven, P. F. A.; Gierman, R.; Zuideveld, P. L. In *Proc. 9th Int. Cong. Catal.*; CIC: Calgary, 1988, pp 1743-1749.

(5) Busca, G. *Langmuir* **1986**, *2*, 577-582.

(6) Oliveri, G.; Ramis, G.; Busca, G.; Escribano, V. S. E. *J. Mater. Chem.* **1993**, *3*, 1239.

(7) Centi, G. *Appl. Catal. A: Gen.* **1996**, *147*, 267-298.

(8) Wachs, I. E. *J. Catal.* **1990**, *124*, 570-573.

(9) Corriu, R. J. P.; Leclercq, D. *Angew. Chem., Int. Ed. Engl.* **1996**, *35*, 1420-1436.

(10) Rice, G. L.; Scott, S. L. *J. Mol. Catal.* **1997**, *A125*, 73-79.

(11) Rice, G. L.; Scott, S. L. *Langmuir* **1997**, *13*, 1545-1551.

(12) Haukka, S.; Lakomaa, E. L.; Root, A. *J. Phys. Chem.* **1993**, *97*, 5085-5094.

(13) Neumann, R.; Levin-Elad, M. *J. Catal.* **1997**, *166*, 206-217.

(14) Crans, D. C.; Chen, H.; Felty, R. A. *J. Am. Chem. Soc.* **1992**, *114*, 4543-4550.

(15) Priebsch, W.; Rehder, D. *Inorg. Chem.* **1985**, *24*, 3058-3062.

(16) Fraile, J. M.; García, J.; Mayoral, J. A.; Proietti, M. G.; Sánchez, M. C. *J. Phys. Chem.* **1996**, *100*, 19484-19488.

(17) Bouh, A. O.; Scott, S. L. *J. Am, Chem. Soc.* **1998**, submitted.

(18) Andrianainarivelo, M.; Corriu, R. J. P.; Leclercq, D.; Mutin, P. H.; Vioux, A. *J. Mater. Chem.* **1997**, *7*, 279-284.

(19) Andrianainarivelo, M.; Corriu, R. J. P.; Leclercq, D.; Mutin, P. H.; Vioux, A. *Chem. Mater.* **1997**, *9*, 1098-1102.

(20) Arnal, P.; Corriu, R. J. P.; Leclercq, D.; Mutin, P. H.; Vioux, A. *Chem. Mater.* **1997**, *9*, 694-698.

(21) Turin, E.; Nielson, R. M.; Merbach, A. E. *Inorg. Chim. Acta* **1987**, *134*, 67-78.

(22) Scott, S.; Basset, J.-M. *J. Mol. Catal.* **1994**, *86*, 5-22.

(23) Hamilton, P. R.; McBeth, R.; Bekebrede, W.; Sisler, H. H. *J. Am. Chem. Soc.* **1953**, *75*, 2881.

(24) Wu, Y.-T.; Ho, Y.-C.; Lin, C. C.; Gau, H.-M. *Inorg. Chem.* **1996**, *35*, 5948-5982.

(25) Weingarten, H.; Wazer, J. R. V. *J. Am. Chem. Soc.* **1965**, *87*, 724-730.

(26) Viet, M. T. P.; Sharma, V.; Wuest, J. D. *Inorg. Chem.* **1991**, *30*, 3026-3032.

(27) Haber, J.; Kozlowska, A.; Kozlowski, R. *J. Catal.* **1986**, *102*, 52-63.

(28) Birdwhistell, K. R.; Boucher, T.; Ensminger, M.; Harris, S.; Johnson, M.; Toporek, S. *Organomet.* **1993**, *12*, 1023-1025.

(29) Feher, F. J.; Blanski, R. L. *Organomet.* **1993**, *12*, 958-963.

(30) Jehng, J. M.; Wachs, I. E. *Catal. Lett.* **1992**, *13*, 9-13.

(31) Reichmann, M. G.; Bell, A. T. *Appl. Catal.* **1987**, *32*, 315-322.

Chapter 6

Silica-supported Organovanadium(IV) Complexes

6.1 Introduction

An area of fundamental importance in polyolefins catalyst research is the link between catalyst structure and catalyst performance. Due to a lack of catalyst structural data, most developmental work has been described as an Edisonian approach.[1] Changes are made in a catalyst formulation based on known chemical reactions, while the reactions taking place in a catalyst preparation are somewhat speculative. The lack of knowledge in relation to the catalyst structure is thought to have greatly hindered new catalyst development.[2]

Industrial alkene polymerization processes employ primarily heterogeneous titanium-based Ziegler-Natta or heterogeneous chromium based catalysts which offer very high productivity.[3] Hence, they, as well as homogeneous metallocene and nonmetallocene single site systems of group IV, are the subject of the majority of research work in this field. Considerably less interest has been directed towards developing vanadium-based catalysts, however this is slowly changing since vanadium catalysts used in the copolymerization of ethylene and propylene yield polymers with a more homogeneous distribution of comonomers along the polymer chain than catalysts based on other transition metals.[2,4]

The organometallic vanadium species used in olefin polymerization are very poorly characterized, particularly when they are used as supported catalysts. These species are generally prepared by impregnating the support with $VOCl_3$[5], VCl_4[6] or even VCl_3, followed by treatment with an aluminum co-catalyst which results in the reduction of higher valent species to vanadium(III) or vanadium(IV) active sites.[1]

Some studies have addressed the question of the structure of the vanadium active sites. Feher and coworkers have studied the interaction of alkylaluminum co-catalysts with a number of inorganic and organometallic vanadium(V) oxo complexes, $O{=}VX_3$ where X = CH_2SiMe_3, O^{i}Pr, Cl, $OSiPh_3$ etc., as well as vanadium-containing silsesquioxanes.[7] The interaction between the co-catalyst and the vanadium was shown by ^{17}O NMR to consist of coordination of the aluminum to the vanadyl oxygen.[8]

6.2 Characterization of surface species

As stated in Chapter 2, the quantity of accessible hydroxyl groups on silica decreases with increasing dehydroxylation temperature. Silica-500 contains 1.2-1.4 OH/nm^2 while silica-200 contains 2.4-2.6 OH/nm^2.[9] However, for the reactions of the vanadium(V) complexes discussed in Chapters 3, 4 and 5, the density of the hydroxyl groups had no bearing on the stoichiometry of the grafting reaction. Nevertheless, it is unwise to assume that this will always be true. For example, it has been reported that the stoichiometry of the reaction CrR_4 with silica is dependent on the density of hydroxyl groups.[10] On

silica-500, CrR_4 reacts with one surface hydroxyl group to form the species $\equiv SiOCrR_3$, while on silica-200 each chromium complex reacts with two surface hydroxyl groups to give $(\equiv SiO)_2CrR_2$. Therefore it was necessary to determine how $V(CH_2SiMe_3)_4$ reacts with silica.

6.2.1 Stoichiometry of grafting

When $V(CH_2SiMe_3)_4$ is sublimed onto silica and allowed to react at room temperature with the surface hydroxyl groups, a chemical reaction takes place resulting in the formation of chemisorbed vanadium species with concomitant color change from white to dark green, and liberation of the protonated ligand TMS (tetramethylsilane), as the only gaseous product detectable by GC, eq. 6.1.

$$n \equiv SiOH + V(CH_2SiMe_3)_4 \rightarrow (\equiv SiO)_nV(CH_2SiMe_3)_{4-n} + n\ SiMe_4 \qquad (6.1)$$

The average value of n was evaluated by comparing the amount of extracted vanadium at the end of the experiment to the amount of TMS liberated in grafting, and in subsequent protonolysis. TMS was quantified by IR spectroscopy, Table 6.1.

Table 6.1 Quantitative analysis of grafting of $V(CH_2SiMe_3)_4$ on silica

Support	mmol[a] V	V/OH	products of grafting mmol[a] RH	RH/V	products of protonolysis mmol[a] RH	RH/V
silica-500	0.37	0.97	0.40	1.05	1.06	2.89
silica-200	0.39	0.49	0.80	2.10	0.74	1.91
	0.37	0.46	0.79	2.13	0.72	1.95
	0.38	0.48	0.74	1.95	0.73	1.92
	0.39	0.49	0.77	1.97	0.76	1.95
	0.40	0.50	0.81	2.03	0.78	1.95
average for silica-200	0.39	0.48	0.78	2.00	0.75	1.92

[a] all values are normalized per gram of silica

Although the values in Table 6.1 are from experiments in which the maximum amount of vanadium was chemisorbed, the ratios RH/V are the same for lower loadings of vanadium. Therefore we conclude that, on silica-500 and silica-200 the following reactions occur exclusively, eq. 6.2 and 6.3.

on silica-200

$$2\ \equiv SiOH + V(CH_2SiMe_3)_4 \rightarrow (\equiv SiO)_2V(CH_2SiMe_3)_2 + 2\ TMS \qquad (6.2)$$

on silica-500

$$\equiv SiOH + V(CH_2SiMe_3)_4 \rightarrow \equiv SiOV(CH_2SiMe_3)_3 + TMS \qquad (6.3)$$

The number of alkyl groups coordinated to each chemisorbed vanadium was confirmed by protonolysis of the silica-supported vanadium species with an excess of HCl, liberating 1.9 TMS/V for silica-200 and 2.9 TMS/V for silica-500, eq. 6.4, 6.5 and Table 6.1.

on silica-200

$$(\equiv SiO)_2V(CH_2SiMe_3)_2 + \text{excess HCl} \rightarrow (\equiv SiO)_2VCl_2 + 2\ TMS \qquad (6.4)$$

on silica-500

$$\equiv SiOV(CH_2SiMe_3)_3 + \text{excess HCl} \rightarrow \equiv SiOVCl_3 + 3\ TMS \qquad (6.5)$$

The products $(\equiv SiO)_2VCl_2$ and $\equiv SiOVCl_3$ were not characterized but were inferred in order to balance the reaction.

6.2.2 Infrared characterization

The progress of the reaction of $V(CH_2SiMe_3)_4$ with silica was followed by infrared spectroscopy. As discussed in Chapter 3, before reaction the spectrum of a self supporting disk of silica-200 contains a sharp band at 3747 cm^{-1}, attributed to non-hydrogen-bonded surface hydroxyl groups, with a

broad low frequency shoulder assigned to hydroxyl groups that are perturbed by hydrogen bonding. Broad bands at 1977, 1868 and 1647 cm^{-1} are the overtones and combinations of intense Si-O fundamental modes originating in the bulk of the silica, and which render the silica virtually opaque below 1200 cm^{-1}, Figure 6.1a. When $V(CH_2SiMe_3)_4$ is sublimed onto a pellet of silica-200, new bands characteristic of alkyl groups appear in the regions 3000-2800 cm^{-1} (CH stretching), 1500-1300 cm^{-1} (methyl and methylene deformations) and 750-680 cm^{-1} (methyl rocking coupled to Si-C stretching), Figure 6.1b. Simultaneously, the band at 3747 cm^{-1} disappears and irreversibly, i.e. it is not regenerated when unreacted $V(CH_2SiMe_3)_4$ is desorbed. The vibrations attributed to alkyl groups decrease only slightly in intensity during desorption. This result confirms that $V(CH_2SiMe_3)_4$ is irreversibly chemisorbed onto the silica surface and that the mechanism of chemisorption is once again reaction with the surface hydroxyl groups.

On silica-500, similar IR spectral changes were recorded during reaction of the surface hydroxyl groups with $V(CH_2SiMe_3)_4$.

6.3 Thermolysis of surface organometallic complexes

When the surface complex on silica-200, $(\equiv SiO)_2V(CH_2SiMe_3)_2$, was heated at ca. 60°C under vacuum for 6 hours, one equivalent of $SiMe_4$ was evolved as the only volatile product as detected by GC, eq. 6.6, while the

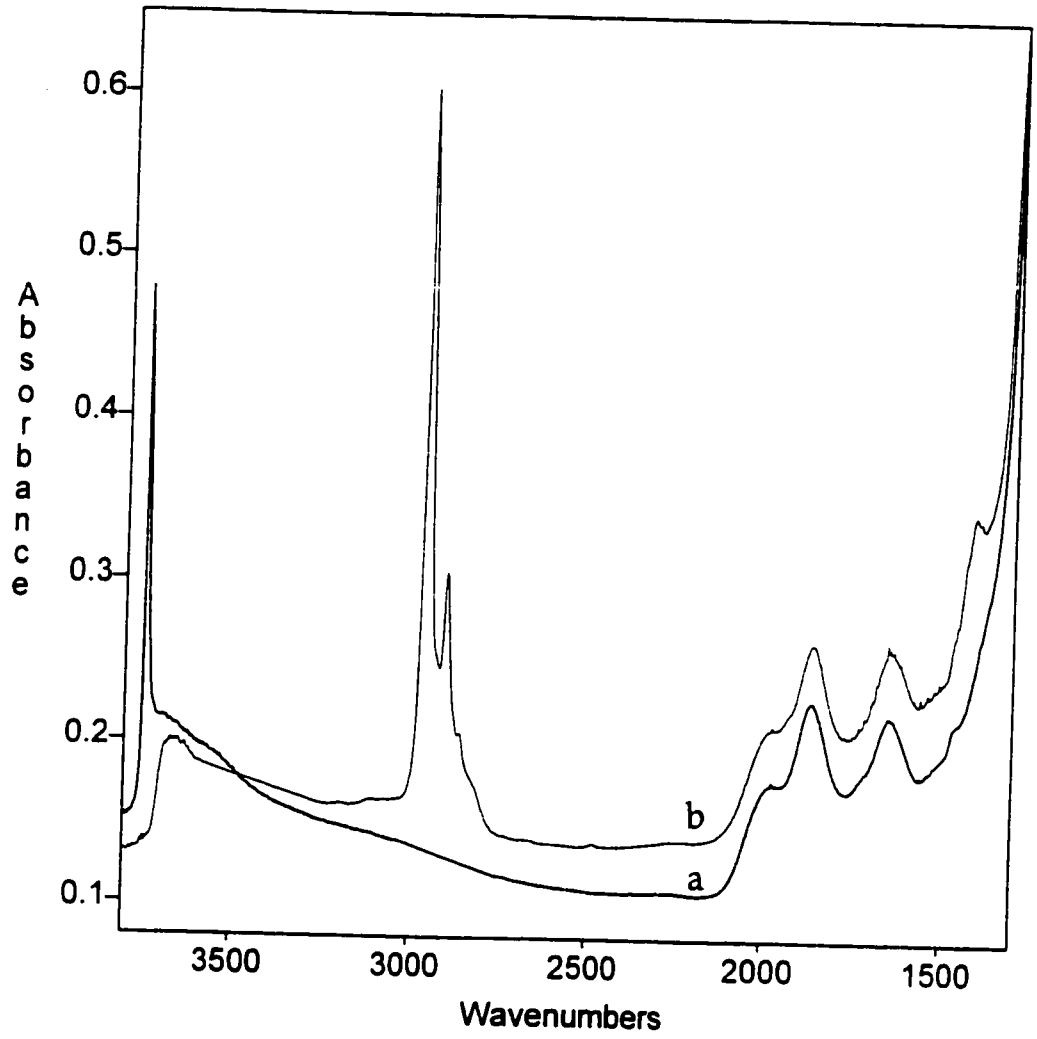

Figure 6.1 Infrared spectra of (a) self-supporting disk of silica-200; (b) after reaction with excess $V(CH_2SiMe_3)_4$.

intensity of the ν(CH) region in the IR spectrum of the modified silica decreased on average by 51% (average of 15 independant experiments), Table 6.2.

$$(\equiv SiO)_2V(CH_2SiMe_3)_2 \rightarrow (\equiv SiO)_2VC_4SiH_{10} + SiMe_4 \qquad (6.6)$$

The nature of the product of the thermolysis will be discussed in more detail later in this chapter.

6.4 Kinetics of thermolysis

Since the thermolysis of $(\equiv SiO)_2V(CH_2SiMe_3)_2$ appears to be a clean stoichiometric reaction, i.e. it results in the liberation of exactly one equivalent of $SiMe_4$, the kinetics of the reaction were investigated. A sample of $(\equiv SiO)_2V(CH_2SiMe_3)_2$ was heated at 58°C in an *in situ* IR cell and the spectrum of the gas phase was recorded periodically, every ten minutes for ten hours. By integration of the ν(CH) region of the gas phase IR spectrum, we were able to monitor the progress of the surface reaction since $SiMe_4$ is the only product of the reaction and it does not adsorb significantly on the silica surface.

Table 6.2 Quantitative analysis of *in vacuo* thermolysis of $(\equiv SiO)_2V(CH_2SiMe_3)_2$

Thermolysis temperature (°C)	**% loss of surface ν(CH) intensity**	**$SiMe_4$/V formed upon thermolysis**
58	52	0.94
60	48	0.92
58	53	1.05
60	50	0.97
57	51	0.95
59	49	0.90
59	46	0.91
58	50	0.99
58	51	0.97
59	49	0.94
57	51	1.00
50	48	0.96
49	49	0.95
70	52	1.05
71	50	0.95
average for all temps.	51 ± 2	0.95 ± 0.10

The result is shown in Figure 6.2. A single exponential (first order) curve fit yielded k(58°C) = 0.0062 ± 0.0002 min^{-1}. Other independent experiments were performed resulting in k(58°C) = 0.0060 ± 0.0002 and 0.0058 ± 0.0002 min^{-1}, illustrating the reproducibility of the rate constant.

The kinetics of the thermolysis reaction of $(\equiv SiO)_2V(CH_2SiMe_3)_2$ were studied at two other temperatures, 50 and 70°C, Figures 6.3a and 6.3b respectively. The rate constants, summarized in Table 6.3, were used to construct an Eyring plot, Figure 6.4. Data was plotted as ln(k/T) versus 1/T. From the Eyring equation, eq. 6.7, we know that a plot of ln(k/T) vs. 1/T yields a curve with slope $-\Delta H^{\ddagger}/R$ and intercept $[\ln(R/Nh) + (\Delta S^{\ddagger}/R)]$.

$$\ln(k/T) = \ln(R/Nh) + \Delta S^{\ddagger}/R - \Delta H^{\ddagger}/RT \qquad (6.7)$$

From the values of the linear fit $\Delta H^{\ddagger}$, (11.0 ± 1.0) kcal/mol, and $\Delta S^{\ddagger}$, (-43 ± 3) cal K^{-1} mol^{-1}, were calculated. The errors in the activation parameters were computed from the following error propagation formulas, eq. 6.8 and 6.9, which were derived from the Eyring equation:[11]

$$(\sigma\Delta H^{\ddagger})^2 = R^2T_{max}^2T_{min}^2/\Delta T^2\{(\sigma T/T)^2[(1 + T_{min}\Delta L/\Delta T)^2 + (1 + T_{max}\Delta L/\Delta T)^2] + 2(\sigma k/k)^2\} \qquad (6.8)$$

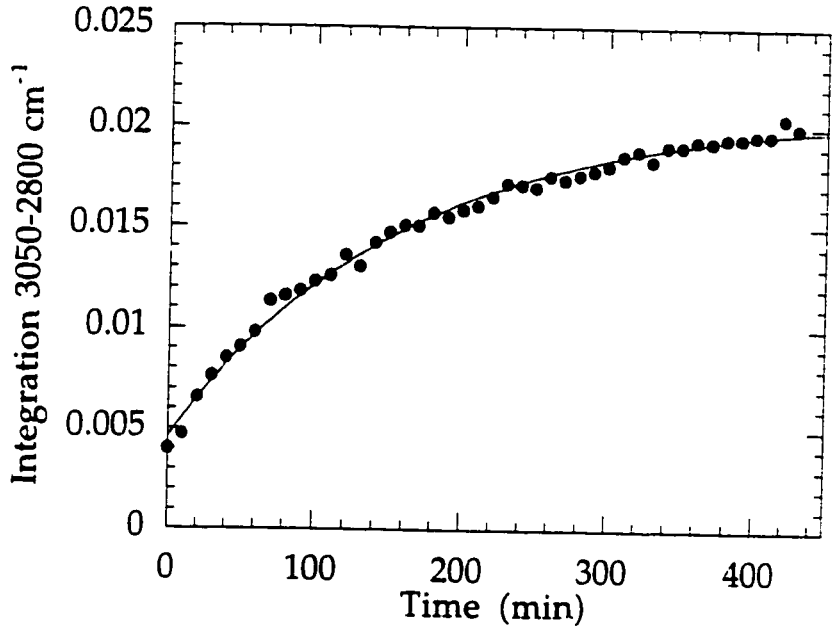

$A_t = A_\infty - (A_\infty - A_0)\exp^{(-kt)}$		
	Value	Error
A_∞	0.020885	0.00021027
A_0	0.0046049	0.00020047
k (min^{-1})	0.0057012	0.00022146
Chisq	5.9324e-06	NA
R	0.99648	NA

Figure 6.2 Time-resolved evolution of $SiMe_4$ from $(\equiv SiO)_2V(CH_2SiMe_3)_2$ at 58°C.

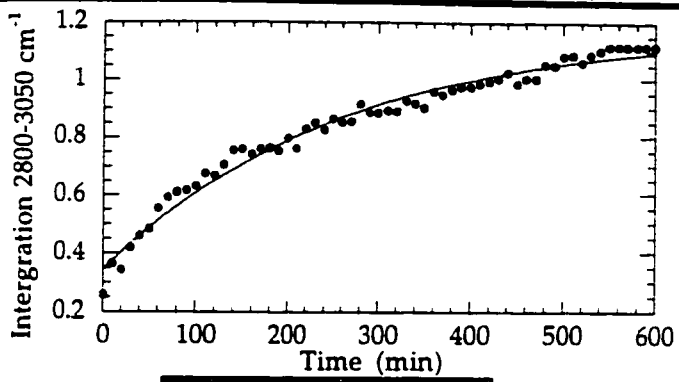

$A_t = A_\infty - (A_\infty - A_0)\exp^{(-kt)}$

	Value	Error
A_∞	1.1816	0.023733
A_0	0.34653	0.014864
k (min^{-1})	0.0037863	0.0002776

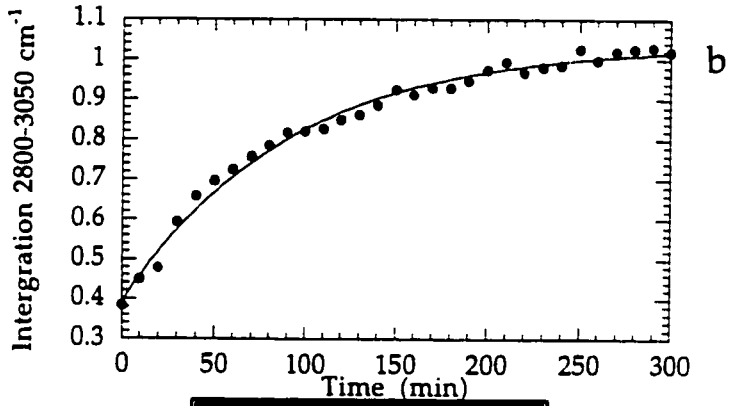

$A_t = A_\infty - (A_\infty - A_0)\exp^{(-kt)}$

	Value	Error
A_∞	1.0385	0.01051
A_0	0.39144	0.012761
k (min^{-1})	0.011157	0.00062658

Figure 6.3 Time resolved evolution of $SiMe_4$ from $(\equiv SiO)_2V(CH_2SiMe_3)_2$ at (a) 50°C; (b) 70°C

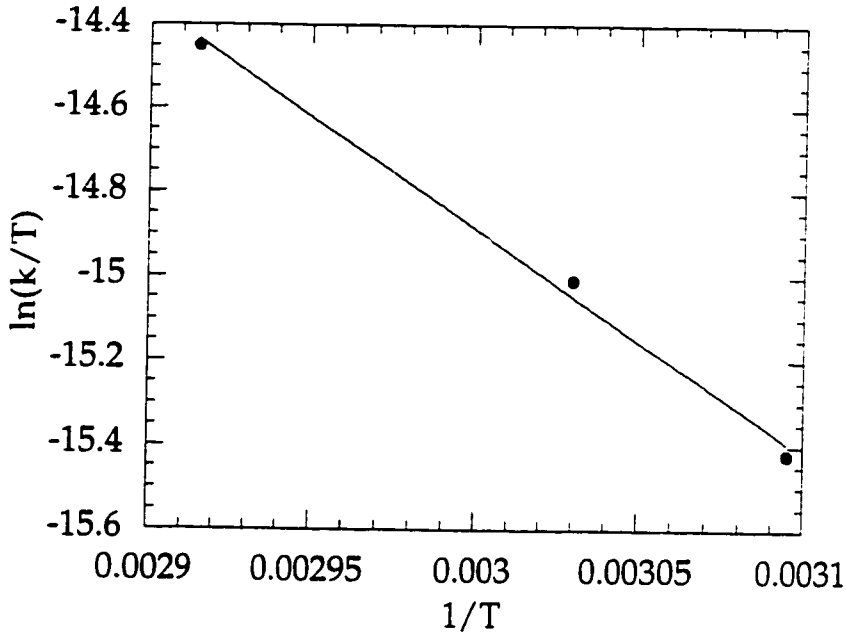

y = m1+m2*m0		
	Value	Error
m1	1.8265	0.75081
m2	-5570.2	249.29
Chisq	0.0010225	NA
R	0.999	NA

Figure 6.4 Eyring plot of the temperature-dependence of rate constants for the thermolysis of $(\equiv SiO)_2V(CH_2SiMe_3)_2$.

$$(\sigma\Delta S^{\ddagger}) = R^2/\Delta T^2\{(\sigma T/T)^2[T_{max}^2(1 + T_{min}\Delta L/\Delta T)^2 + T_{min}^2(1 + T_{max}\Delta L/\Delta T)^2] + (\sigma k/k)^2(T_{max}^2 + T_{min}^2)\} \quad (6.9)$$

where $\Delta T = (T_{max} - T_{min})$ and $\Delta L = [\ln(k_{max}/T_{max}) - \ln(k_{min}/T_{min})]$

Unfortunately kinetics experiments at higher temperatures were not feasible, because the surface product is not stable above 70°C and undergoes further loss of hydrocarbons.

6.5 Magnetic moment

The oxidation state of vanadium being (IV), the surface complex and is paramagnetic. Therefore it was not possible to obtain NMR spectra of $(\equiv SiO)_nV(CH_2SiMe_3)_{4-n}$. It was deemed important, however, to verify that no change in oxidation state occurs during grafting or subsequent thermolysis reactions. A related question of interest concerns the interaction of adjacent grafted vanadium complexes and whether they are truly isolated. These questions can be addressed by measuring the magnetic moment of surface complexes.

The temperature-dependent magnetic susceptibility of the surface complex $(\equiv SiO)_2V(CH_2SiMe_3)_2$ exhibits simple Curie-Weiss behavior above 8 K.

The effective magnetic moment is 1.57 μ_B per metal atom whith Neel temperature of 8 K, Figure 6.5, which is consistent with the formulation of the surface complexes as mononuclear (noninteracting) d^1 surface organometallic fragments. The magnetic moment deviates from simple Curie-Weiss behavior below 6 K indicating weak antiferromagnetic character.

Table 6.3 First-order rate costants for loss of $SiMe_4$ from $(\equiv SiO)_2V(CH_2SiMe_3)_2$

Temperature °C	**Rate constant (k)** min^{-1}
50	0.0038 ± 0.0003
	0.0040 ± 0.0003
58	0.0062 ± 0.0002
	0.0057 ± 0.0002
	0.0060 ± 0.0002
70	0.0112 ± 0.0006
	0.0120 ± 0.0005

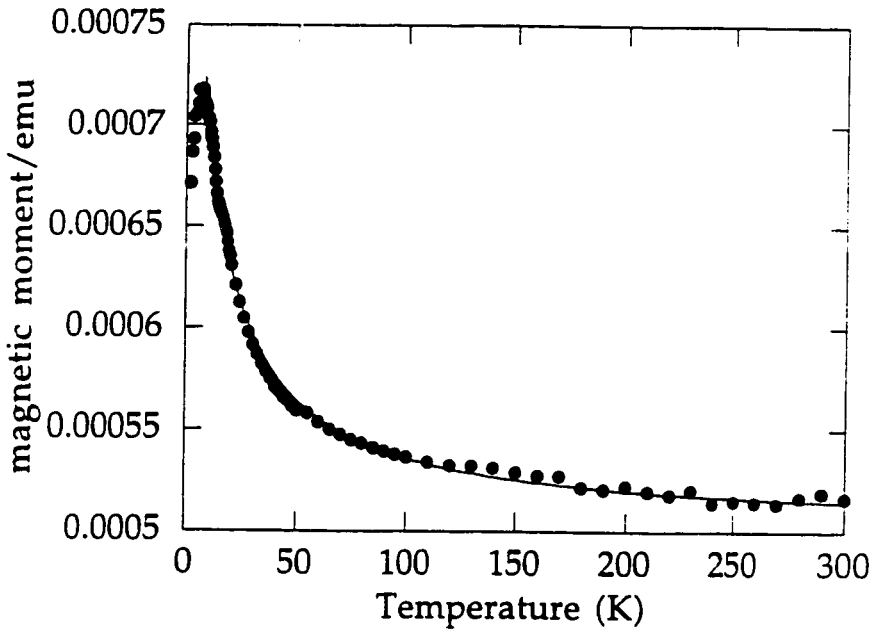

y = m1/(m2+m0)+m3		
	Value	Error
m1	0.003554	0.00010432
m2	8.0511	0.4946
m3	0.00050299	1.1543e-06

Figure 6.5 Temperature-dependent magnetic susceptibility of $(\equiv SiO)_2V(CH_2SiMe_3)_2$.

The product of the thermolysis of $(\equiv SiO)V(CH_2SiMe_3)_2$, eq 6.4, has a magnetic moment of 1.63 μ_B per metal with Neel temperature of 3.6 K, consistent with retention of the surface structure of noninteracting d^1 V(IV) complexes, Figure 6.6. Based upon our observations, first order kinetics, liberation of 1 equivalent of TMS and the retention of the mononuclear d^1 configuration upon thermolysis, we formulate the product of thermolysis as an alkylidene, $(\equiv SiO)_2V{=}CHSiMe_3$.

6.6 Reactivity of supported organometallic fragments

6.6.1 Towards ethylene

At room temperature, there is no reaction between $(\equiv SiO)_2V(CH_2SiMe_3)_2$ and ethylene. However, if $(\equiv SiO)_2V(CH_2SiMe_3)_2$ is heated in the presence of ethylene at ca. 60°C or if ethylene is added directly to the thermolyzed species, an immediate reaction takes place resulting in the consumption of ethylene with simultaneous appearance of bands in the IR characteristic of $(CH_2)_n$, Figure 6.7. The reaction self-terminates after several minutes before consumption of all gas phase C_2H_4. Approximately 40 ethylene molecules were consumed per vanadium, hence the reaction is more aptly described as an oligomerization rather than a polymerization. This behavior has been previously reported for vanadium-based catalysts.[1,4]

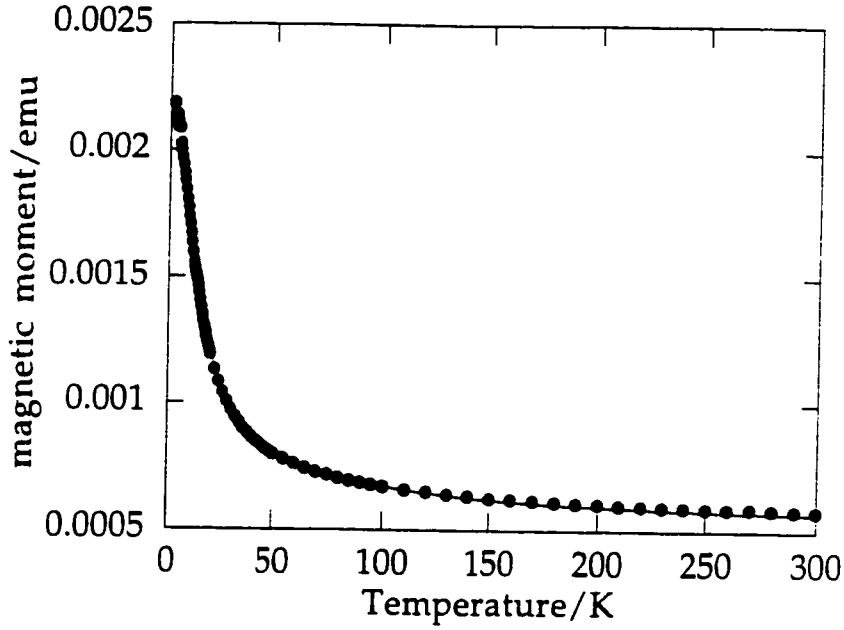

y = m1/(m2+m0)+m3		
	Value	Error
m1	0.016075	0.00033049
m2	3.5741	0.26175
m3	0.00051563	4.7397e-06

Figure 6.6 Temperature-dependent magnetic susceptibility of $(\equiv SiO)_2V{=}CHSiMe_3$.

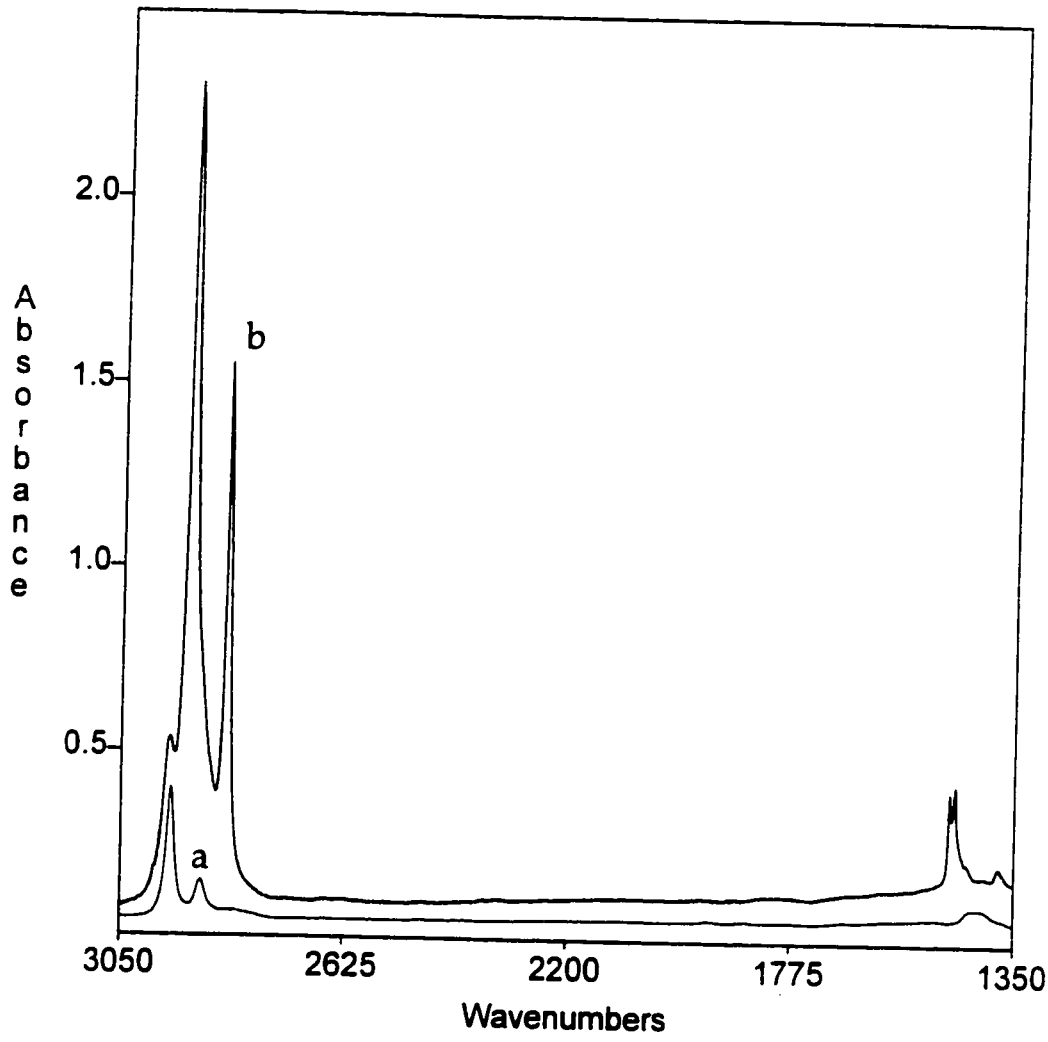

Figure 6.7 Infrared spectra of self-supporting disks of (a) $(SiO)_2V{=}CHSiMe_3$; (b) after reaction with ethylene

Oligomerization is not the only reaction taking place. By GC and GC-MS, traces of α-olefins (1-butene, 1-hexene etc) were detected indicating that metathesis competes with oligomerization.

6.6.2 Towards styrene

As for ethylene, at room temperature there is no reaction between the silica-supported bis(alkyl) complex, $(\equiv SiO)_2V(CH_2SiMe_3)_2$, and styrene. However, if $(\equiv SiO)_2V(CH_2SiMe_3)_2$ is exposed to styrene at the thermolysis temperature, 50-70 °C, or if the thermolyzed species is exposed to styrene at room temperature, trimethylvinylsilane was formed. The initial reaction is formulated as a metathetical exchange, equation 6.10:

$$(\equiv SiO)_2V{=}CHSiMe_3 + PhCH{=}CH_2 \rightarrow (\equiv SiO)_2V{=}CHPh + CH_2{=}CHSiMe_3 \quad (6.10)$$

The surface benzylidene complex react further with styrene to produce oligomers, Figure 6.8.

Discussion

It is often assumed that the hydroxyl groups on the surface of amorphous silica are randomly distributed on the surface,[12] so that their reaction with organometallic complexes, MR_4, should give rise to a variety of different products. It has been reported for silicas dehydroxylated above 450°C

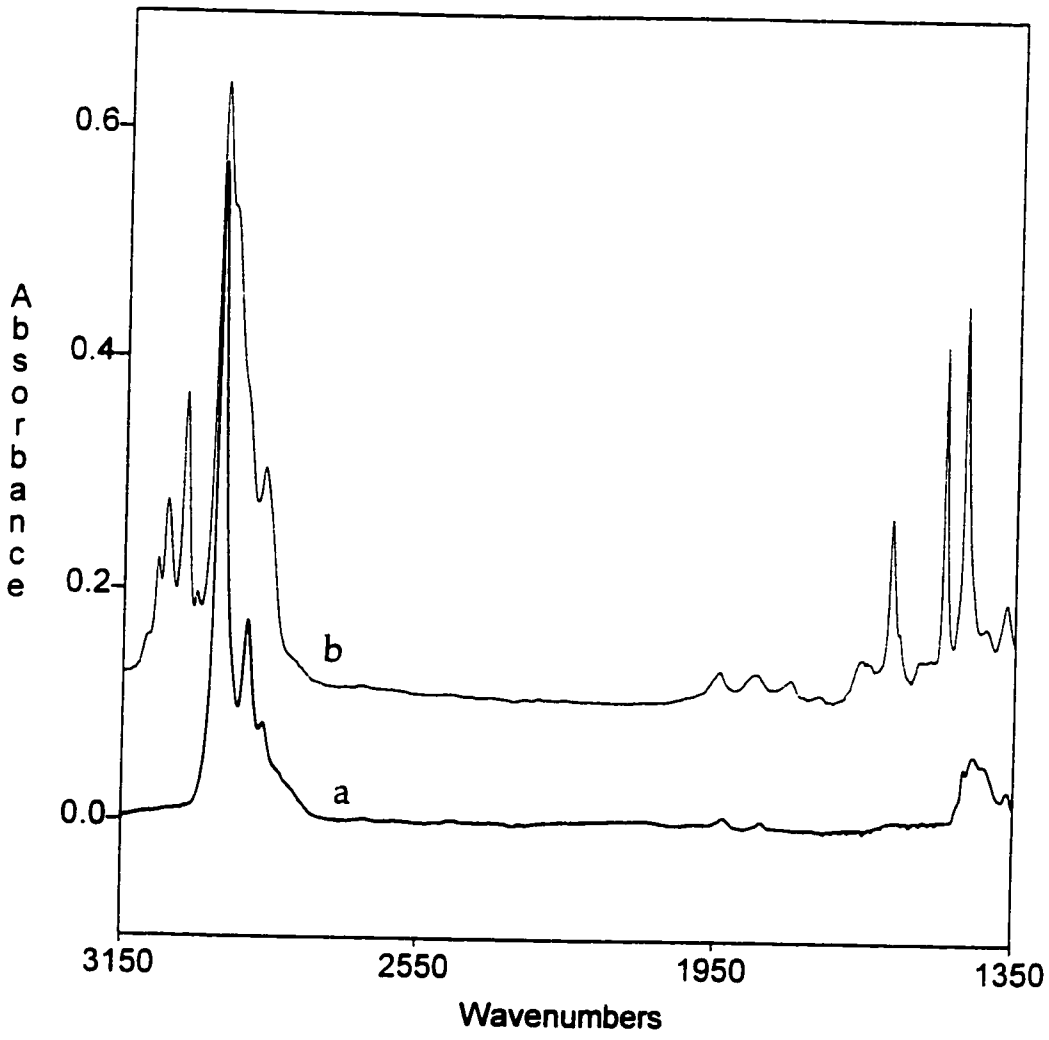

Figure 6.8 Infrared spectra of self-supporting disks of (a) $(SiO)_2V{=}CHSiMe_3$; (b) after reaction with styrene

that the hydroxyl groups are essentially isolated, which leads to a 1:1 reaction resulting in surface organometalllic fragments of the type $(\equiv SiO)MR_3$, reported for several different metals: Ti[13], Zr[14], Hf[15] and Cr.[16] On silica-200, an average grafting stoichiometry of n=2, giving $(\equiv SiO)_2MR_2$ has been reported for Zr[17] and Cr[16] complexes. It has also been suggested that the Group IV complexes are mixtures of mono-, bis- and tris(alkyl) fragments.[13] Here we have confirmed that the average stoichiometry is indeed two for the reaction of $V(CH_2SiMe_3)_4$ with amorphous silica partially dehydroxylated at 200°C and one for silica partially dehydroxylated at 500°C.

The kinetic behavior of the surface organometallic fragment, $(\equiv SiO)_2V(CH_2SiMe_3)_2$, during thermolysis implies that all the surface species are similar, since rates of reactions on surfaces are extremely sensitive to small changes in local structure.[18] Therefore, the reproducibility of the single exponential behavior for the thermolysis reactions is not consistent with the presence of widely different coordination environments at the surface metal atoms.

There are several possible ways that such uniformity in structure might arise. We may consider that the surface hydroxyl groups on partially dehydroxylated silica are not randomly distributed, but that they occur in well-ordered pairs. This possibility was proposed and discussed in Chapter 1 where it was concluded that it is unlikely that an unmodified amorphous

silica possesses the unique kind of paired hydroxyl surface that would be required to produce the uniform surface organometallic complexes discussed.

A second possibility to obtain uniformity in surface structure is by reorganization of the surface during or after grafting.[19] This could be achieved either by migration of surface hydroxyl groups or migration of singly bound surface organometallic fragments $\equiv SiOV(CH_2SiMe_3)_3$. It has been shown that on a silica with surface area of 200 m^2/g that the surface is fully covered by tris(neopentyl)chromium(IV) fragments when the metal content reaches ca. 0.37 mmol Cr/g.[16] On silica-200, this loading is achieved when approximately half of the surface hydroxyls have been consumed. Since full coverage leaves little room for mobility of surface organometallic fragments, it seems more likely that unreacted surface hydroxyls migrate until they are in an optimal position for reaction with a tris(alkyl) fragment. This mechanism is depicted in Scheme 6.1, where the most stable surface environment is suggested to occur when the metal occupies a position in a 6-membered siloxane ring.

Based on the reactions of the thermolyzed species with ethylene and styrene, kinetic studies and characterization of the related chromium system[16], we formulate that the product of thermolysis is an alkylidene species. The formation of alkylidenes by α-H elimination in other Group V complexes, particularly TaR_5, is well known.[20-22] This transformation is, however, unknown for vanadium, for which no homoleptic vanadium(V)

alkyls are known. Vanadium(V) is known to form stable alkylidenes when supported by bulky imido and Cp ligands, **1**,[23] furthermore, α-H elimination is known for the thermolysis of vanadium(III) bisalkyls resulting in vanadium(III) alkylidenes, **2**.[24]

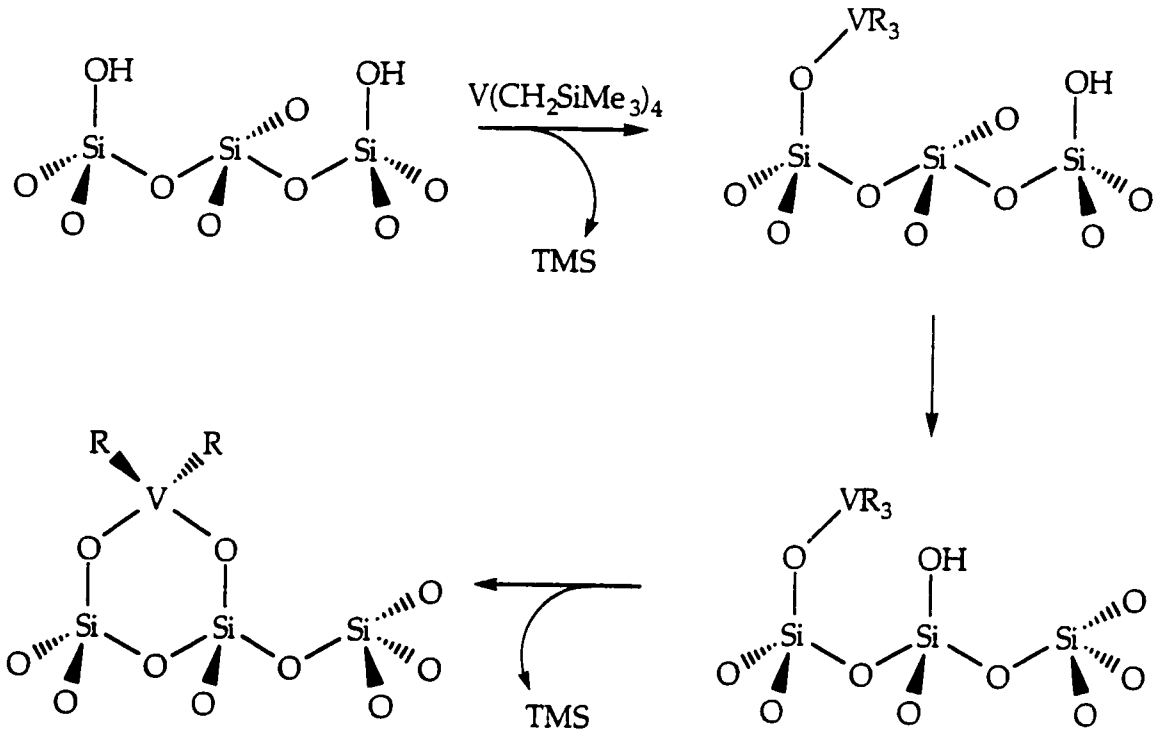

Scheme 6.1 Mechanism for the grafting of VR_4 onto the surface of silica partially dehydroxylated at 200°C

These are examples of a very rare Schrock-type vanadium carbene. Most known vanadium carbene complexes are of the Fischer or electrophilic type where the carbene carbon moiety has Lewis-base character.[25]

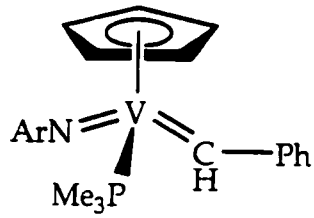

1

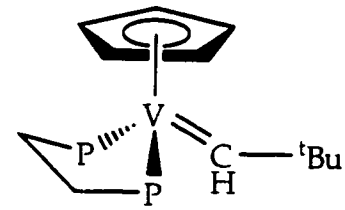

2

We propose that the formation of TMS upon heating arrises from α-H elimination and is probably surface assisted, via coordination of an additional surface oxygen "ligand". Base-assisted alkane elimination has precedent in the formation of a benzylidene complex from $[Cp^*Nb(NR)(CH_2Ph)_2(PMe_3)]$.[26] The alkylidene species may maintain a pseudo-tetrahedral coordination number by interaction with surface siloxane oxygens, eq. 6.11. This coordination is reversible, and an incoming olefin can readily displace the siloxane oxygen. The ability of the silica surface to stabilize coordinatively unsaturated species and then regenerate them to allow substrate binding has been suggested as the reason why a supported olefin hydrogenation catalyst, $Os_3(CO)_{10}(\mu\text{-}H)(\mu\text{-}OSi\equiv)$, has better catalytic properties than molecular $Os_3(CO)_{10}(\mu\text{-}H)(\mu\text{-}OPh)$.[27]

The linear Eyring plot, with a modest value of $\Delta H^{\ddagger}$, (11.0 ± 1.0) kcal/mol, and a large negative $\Delta S^{\ddagger}$, (-43 ± 3) cal $K^{-1}mol^{-1}$, are consistent with other reported values for concerted α-H elimination[28-30] as well as surface assistance in the rate determining step.[26]

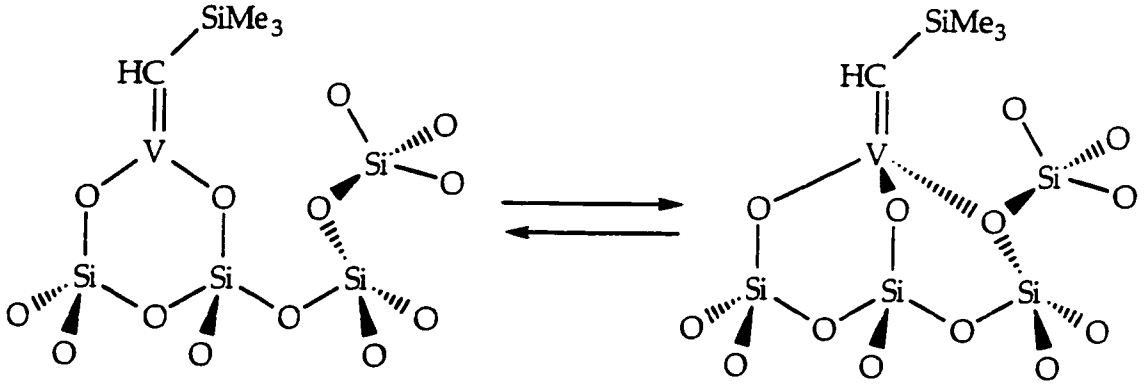

(6.11)

The driving force for alkylidene formation from bis(alkyl) metal complexes is both enthalphic as well as entropic,[31] and the enthalpic term contains contributions from both steric and electronic effects. Two electron-withdrawing siloxy ligands increase the electrophilicity of the metal, favoring the alkylidene over the bis(alkyl) form.[28] At the same time, the second siloxy ligand forces the metal closer to the silica surface compared to the monosubstituted analogue $(\equiv SiO)MR_3$. The consequent increased crowding at the metal center in $(\equiv SiO)_2MR_2$ may cause the M-C_α-Si_β angle to open up, enhancing the rate of α-H elimination. This effect has been noted for $Ta(CH_2EMe_3)_5$ (E is Si or C).[29]

Finally, the ability of the alkylidene species to undergo metathesis with ethylene and styrene and catalyse their polymerization suggests that these single-site catalysts may perform using the Green-Rooney alkylidene mechanism, scheme 6.2.[32] A similar mechanism has been demonstrated for a Ta(V) neopentylidene hydride ethylene polymerization catalysts.[20] The

reversible transformation of a metal alkylidene complex to a metallacycle, as required for metathesis and/or polymerization, was reported to be enthalphically nearly neutral.[31]

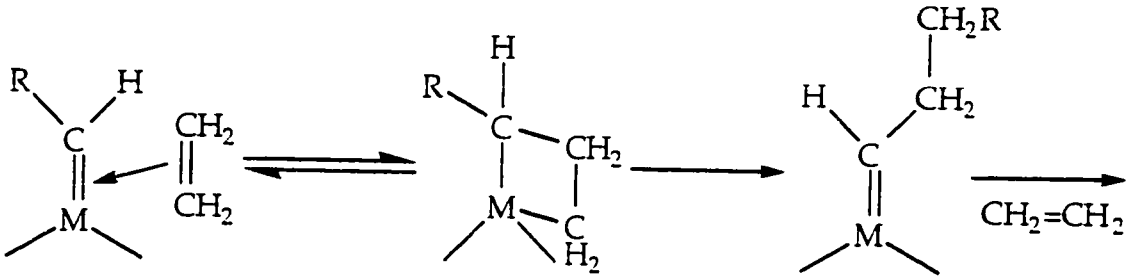

Scheme 6.2 The Green-Rooney alkylidene mechanism for polymerization of olefins.

6.7 Conclusions

Kinetic studies and mass balances demonstrate that the silica-supported bis(trimethylsilylmethyl) vanadium complex is transformed to an alkylidene by thermal α-H elimination in reactions which resemble homogeneous phase chemistry, even though vanadium(IV) alkylidene species are unknown in solution. This unexpected result suggests that, although the unmodified silica surface is amorphous, the surface organometallic complexes are uniform.

6.8 References

(1) McFaddin, D.; Reinking, M. *J. Polym. Sci., Part A: Polym. Chem.* **1995**, *33*, 563-570.

(2) Velikova, M.; Minkova, L.; Damyanov, D.; Rangelov, S. *Eur. Polym. J.* **1997**, *33*, 403-409.

(3) Czaja, K.; Biatek, M. *Macromol. Rapid Commun.* **1996**, *17*, 253-260.

(4) Czaja, K.; Biatek, M. *Macromol. Rapid Commun.* **1998**, *19*, 163-166.

(5) Damyanov, D.; Velikova, M. *Eur. Polym. J.* **1988**, *24*, 661.

(6) Novokshonova, L. A.; Meshkova, I. N. *Polym. Sci.* **1994**, *36*, 1357.

(7) Feher, F. J.; Walzer, J. F.; Blanski, R. L. *J. Am. Chem. Soc.* **1991**, *113*, 3618-3619.

(8) Feher, F. J.; Blanski, R. L. *Organomet.* **1993**, *12*, 958-963.

(9) Morrow, B. A. *Stud. Surf. Sci. Catal.* **1990**, *57*, A161-A224.

(10) Nait Ajjou, J. A.; Scott, S. L. *Organomet.* **1997**, *16*, 86-92.

(11) Morse, P. M.; Spencer, M. D.; Wilson, S. R.; Girolami, G. S. *Organomet.* **1994**, *13*, 1646-1655.

(12) Burneau, A.; Barres, O.; Gallas, J. P.; Lavalley, J. C. *Langmuir* **1990**, *6*, 1364.

(13) Holmes, S. A.; Quignard, F.; Choplin, A.; Teissier, R.; Kervennal, J. *J. Catal.* **1998**, *176*, 173-181.

(14) Quignard, F.; Lecuyer, C.; Bougault, C.; Lefebvre, F.; Choplin, A.; Olivier, D.; Basset, J.-M. *Inorg. Chem.* **1992**, *31*, 928.

(15) D'Ornelas, L.; Reyes, S.; Quignard, F.; Choplin, A.; Basset, J.-M. *Chem. Lett.* **1993**, 1931.

(16) Amor Nait Ajjou, J.; Scott, S. L. *Organomet.* **1997**, *16*, 86-92.

(17) Schwartz, J.; Ward, M. D. *J. Mol. Catal.* **1980**, *8*, 465.

(18) Somorjai, G. A. *Chemistry in Two Dimensions: Surfaces*; Cornell University Press: Ithaca, 1981.

(19) Somorjai, G. A. *J. Mol. Catal. A: Chem.* **1996**, *107*, 39-53.

(20) Turner, H. W.; Schrock, R. R.; Fellman, J. D.; Holmes, S. J. *J. Am. Chem. Soc.* **1983**, *105*, 4942-4950.

(21) Schrock, R. R. *J. Organomet. Chem.* **1976**, *122*, 209-225.

(22) Schrock, R. R. *J. Am. Chem. Soc.* **1978**, *100*, 3359-3370.

(23) Buijink, J.-K. F.; Teuben, J. H.; Kooijman, H.; Spek, A. L. *Organomet.* **1994**, *13*, 2922-2924.

(24) Hessen, B.; Buijink, J.-K. F.; Meetsma, A.; Teuben, J. H.; Helgesson, G.; Hakansson, M.; Jagner, S.; Spek, A. L. *Organomet.* **1993**, *12*, 2268-2276.

(25) Taylor, T. E.; Hall, M. B. *J. Am. Chem. Soc.* **1984**, *106*, 1576.

(26) Cockcroft, J. K.; Gibson, V. C.; Howard, J. A. K.; Poole, A. D.; Siemeling, U.; Wilson, C. *J. Chem. Soc., Chem. Commun.* **1992**, 1668.

(27) Choplin, A.; Besson, B.; D'Ornelas, L.; Sanchez-Delgado, R.; Basset, J.-M. *J. Am. Chem. Soc.* **1988**, *110*, 2783-2787.

(28) Wood, C. D.; McLain, S. J.; Schrock, R. R. *J. Am. Chem. Soc.* **1979**, *101*, 3210-3222.

(29) Li, L.; Hung, M.; Xue, Z. *J. Am. Chem. Soc.* **1995**, *117*, 12746-12750.

(30) Cheon, J.; Rogers, D. M.; Girolami, G. S. *J. Am. Chem. Soc.* **1997**, *119*, 6804-6813.

(31) Luo, L.; Li, L.; Marks, T. J. *J. Am. Chem. Soc.* **1997**, *119*, 8574-8575.

(32) Ivin, K.; Rooney, J. J.; Stewart, C. D.; Green, M. L. H.; Mahtab, R. *J. Chem. Soc., Chem. Commun.* **1978**, 604-606.

Chapter 7

General Conclusions

It is important to emphasize that if we are to fully understand surface reaction mechanisms, we first must fully understand the structures of surface species. Using the concepts of surface organometallic chemistry, we have been able to prepare silica-supported vanadium(IV) and (V) complexes whose uniform structure makes them homogeneous in nature and makes their reactions more amenable to mechanistic studies.

We have demonstrated how the vanadium(V) complexes, $\equiv SiOVOX_2$, retain some of the reactivity of the molecular analogues, and how our method of preparation can be exploited in the study of reaction mechanisms. We hope that our method for preparing the silica-supported vanadium(V) complexes with ^{18}O isotope labels in nonequivalent ligand sites will prove to be especially fruitful. There is no exchange or dilution of the labels either during grafting or during subsequent reactions. We have shown, using ^{18}O labeling, that oxygen transfer reactions of the silica-supported vanadium(V) complexes involve only the terminal oxygen and even under catalytic conditions the lattice oxygens do not take part in the reaction.

Through a non-hydrolytic method we have been able to prepare the first silica-supported mixed vanadium-titanium alkoxide complex. These materials may be structural models for the active sites in dehydrated V-Ti-Si catalysts. The sequential CVD technique employed here holds promise in the

development of well-defined isolated multifunctional active sites in heterometallic oxide catalysis.

We have been able to prepare a silica-supported alkylvanadium(IV) complex, $(\equiv SiO)_2V(CH_2SiMe_3)_2$. We have demonstrated that this complex undergoes clean thermolysis and liberates 1 equivalent of TMS through a first order α-H elimination reaction. Although these transformations are not uncommon for the other group (V) metals, particularly tantalum, as well as for vanadium(III) and (V) complexes supported by imido and Cp ligands to yield alkylidenes, they are unknown for vanadium(IV) alkyls. This result suggests that the surface complexes are homogeneous in nature.

The work presented resulted in a number of publications which are listed here:

Characterization of Silica-supported Vanadium(V) Complexes Derived from Molecular Precursors and Their Ligand Exchange Reactions. Rice, G. L.; Scott, S. L. *Langmuir* **1997**, *13*, 1545-1551.

Site-specific Oxygen-18 Labelling of Silica-supported Vanadium(V) complexes: Implications for Oxidation Catalysis. Rice, G. L.; Scott, S. L. *J. Mol. Catal. A: Chem.* **1997**, *125*, 73-79.

Nonhydrolytic Surface Synthesis of a Heterobimetallic V-Ti Alkoxide Complex on Silica. Rice, G. L.; Scott, S. L. *Chem. Mater.* **1998**, *10*, 620-625.

Kinetics and Mechanisms of Thermally-induced Alkane Elimination from Silica-supported Bis(alkyl)chromium(IV) and -vanadium(IV) complexes. Amor Nait Ajjou, J.; Rice, G. L.; Scott, S. L.; *J. Am. Chem. Soc.* **1998**, *120*, 13436-13443.

Mononuclear and Dinuclear Supported Metal Complexes and their Reactivity in Epoxidation Reactions. Rice, G. L., Bouh, A. O. and Scott, S. L., in preparation.